Photogrammetrie Fernerkundung Geoinformation

Organ der Deutschen Gesellschaft für Photogrammetrie, Fernerkundung und Geoinformation (DGPF) e.V.

Jahrgang 2005, Heft 6

E. Schweizerbart'sche Verlagsbuchhandlung
(Nägele u. Obermiller) Stuttgart 2005

Deutsche Gesellschaft für Photogrammetrie, Fernerkundung
und Geoinformation (DGPF) e.V.
Gegründet 1909

Die *Deutsche Gesellschaft für Photogrammetrie, Fernerkundung und Geoinformation* (DGPF) e.V. unterstützt als Mitglieds- bzw. Trägergesellschaft die folgenden Dachverbände:

International Society for Photogrammetry and Remote Sensing	Deutsche Arbeitsgemeinschaft für Mustererkennung e.V.	GeoUnion Alfred-Wegener-Stiftung

Herausgeber:

Präsident: Prof. Dr.-Ing. Thomas Luhmann, Fachhochschule Oldenburg Ostfriesland Wilhelmshaven, Institut für Angewandte Photogrammetrie und Geoinformatik, Ofener Str. 16, D-26121 Oldenburg, Tel.: +49-441-7708-3172, e-mail: Praesident@dgpf.de, www.dgpf.de
Geschäftsstelle: Dr. Klaus-Ulrich Komp, c/o EFTAS Fernerkundung Technologietransfer GmbH, Ostmarkstraße 92, D-48145 Münster, e-mail: klaus.komp@eftas.com
Published by:
E. Schweizerbart'sche Verlagsbuchhandlung (Nägele u. Obermiller), Johannesstraße 3 A, D-70176 Stuttgart. Tel.: 0711/3514 56-0, Fax: 0711/3514 56-99, e-mail: mail@schweizerbart.de
Internet: http://www.schweizerbart.de
♾ Gedruckt auf alterungsbeständigem Papier nach ISO 9706-1994

ISSN 1432-8364
Hauptschriftleiter: Prof. Dr.-Ing. habil. Klaus Szangolies, Closewitzer Str. 44, D-07743 Jena. e-mail: Klaus.Szangolies@t-online.de
Schriftleiter: Prof. Dr. rer. nat. Carsten Jürgens, Ruhr-Universität Bochum, Geographisches Institut, Gebäude NA 7/133, D-44780 Bochum, e-mail: carsten.juergens@rub.de und Dr.-Ing. Eckhardt Seyfert, Landesvermessung und Geobasisinformation Brandenburg, Heinrich-Mann-Allee 103, D-14473 Potsdam, e-mail: eckhardt.seyfert@lvermap.brandenburg.de
Erscheinungsweise: 7 Hefte pro Jahrgang.
Bezugspreis im Abonnement: € 118,– pro Jahrgang. Mitglieder der DGPF erhalten die Zeitschrift kostenlos.
Anzeigenverwaltung: Dr. E. Nägele, E. Schweizerbart'sche Verlagsbuchhandlung (Nägele u. Obermiller), Johannesstraße 3A, D-70176 Stuttgart, Tel.: 0711/3514 56-0; Fax: 0711/3514 56-99. e-mail: mail@schweizerbart.de, Internet: http://www.schweizerbart.de
Bernhard Harzer Verlag GmbH, Westmarkstraße 59/59a, D-76227 Karlsruhe, Tel.: 0721/944020, Fax: 0721/9440230, e-mail: Info@harzer.de, Internet: www.harzer.de
Printed in Germany by Tutte Druckerei GmbH, D-94121 Salzweg bei Passau

PFG – Jahrgang 2005, Heft 6

Inhaltsverzeichnis

Originalbeiträge zum Thema „High Resolution Mapping from Space"

Berichte und Mitteilungen

Photogrammetrie • Fernerkundung • Geoinformation 6/2005, S. 465–466

Dedicated to GOTTFRIED KONECNY on the occasion of his 75th birthday

High Resolution Mapping from Space

CHRISTIAN HEIPKE, KARSTEN JACOBSEN & MARKUS GERKE, Hannover

Earth imaging from air and space have undergone major changes over the last years. New and significant developments comprise the advent of digital aerial cameras, of high resolution, hyper-spectral satellite imagery, laser scanning and SAR/ InSAR data. Today, all these data are used for the production, refinement, and update of geospatial information. At the same time updating existing geospatial databases has gained more importance, while automation and the worldwide web have had a significant impact on the photogrammetric and remote sensing processing chain.

These developments have formed the background for the ISPRS Hannover Workshop *High Resolution Earth Imaging for Geospatial Information* which was held at the Institute of Photogrammetry and GeoInformation (IPI), University of Hannover between May 17 and 20, 2005 (see also the workshop report by PETER REINARTZ in this issue, page 525). Just as this theme issue, the workshop was dedicated to Prof. GOTTFRIED KONECNY at the occasion of his 75th birthday. GOTTFRIED KONECNY is not only one of the most well known and most respected scientists in photogrammetry and remote sensing on a worldwide scale, to this very day he is also a tireless and very successful advocator of international cooperation and friendship.

This special issue contains updated versions of those workshop papers dealing with high resolution mapping from space. We intentionally left out some excellent articles of aerial sensors and applications in order to sharpen the focus of this issue. In the spirit of GOTTFRIED KONECNY all articles including this editorial are written in English, because only in this way, the material becomes accessible to the international community.

The first paper by MANFRED SCHROEDER gives a short overview of GOTTFRIED KONECNY's achievements in the last 25 years. Starting from the Metric Camera, KONECNY and his institute have been involved in nearly all European space mapping missions. KONECNY is also a great enthusiast of mountains, which is why for his birthday he was presented a remote sensing movie of the Nanga Parbat.

In the second paper, MICHAEL EINEDER describes how the underlying digital terrain model was derived from data of the Shuttle Radar Topography Mission. He presents results from a probability-based iterative algorithm he developed, which is capable of fusing multi-frequency interferograms.

The next paper, written by KARSTEN JACOBSEN, gives an overview of existing and planned space missions for mapping applications. It is pointed out that in the past space technology used to be a technique only for a very limited number of countries, while in the near future there will be approximately a dozen countries operating satellites with a ground sample distance of 2.5 m and below. The consequences of such a major shift are only beginning to show.

The paper by MICHELE CROSETTO et al. reviews the determination of land deformation using differential interferometric synthetic aperture radar (D-InSAR) from space. The authors concisely describe the basic steps and possible applications of D-InSAR when multiple images of the same area are available, followed by some convincing results.

1432-8364/05/2005/0465 $ 0.50

Finally, the paper by TIMOTHÉE BAILLOEUL et al. deals with a novel approach for building refinement from Quickbird images combined with GIS information. Starting at the building location given through the GIS, active contour models (snakes) are initialised to determine the building extent in the images. A coarse DEM can be used to further improve the results.

A few words of thanks at the end: we are very grateful to all IPI staff for their invaluable help in organizing the workshop, to the workshop participants who have made the meeting a success, and to the authors of this special issue for making available their excellent papers, and for keeping a tough timeline. Last not least, we would like to thank the PFG editor-in chief and his team for allowing us to publish this special issue and for all the help they extended to us in the technical preparation.

Anschriften der Autoren:

Prof. Dr. CHRISTIAN HEIPKE
e-mail: heipke@ipi.uni-hannover.de

Dr.-Ing. KARSTEN JACOBSEN
e-mail: jacobsen@ipi.uni-hannover.de

Dipl.-Ing. MARKUS GERKE
e-mail: gerke@ipi.uni-hannover.de
Institut für Photogrammetrie und
GeoInformation (IPI), Universität Hannover
Nienburger Straße 1, D-30167 Hannover

Manuskript eingereicht: Juni 2005
Angenommen: Juli 2005

Photogrammetrie • Fernerkundung • Geoinformation 6/2005, S. 467–476, 2 figs.

25 Years Space Photogrammetry in Germany – a Research Field initiated by GOTTFRIED KONECNY*

MANFRED SCHROEDER, Wessling

Keywords: photogrammetry, Metric Camera, MOMS, SPOT-5, HRSC, SRTM

Abstract: The German photogrammetrists started to show interest in the field of "Space Photogrammetry" at the beginning of the Eighties. The first space experiment especially devoted to photogrammetry was proposed by GOTTFRIED KONECNY; it was the *"Metric Camera Experiment"* based on a conventional aerial survey camera, which was successfully conducted under his supervision in 1983 on the first Spacelab Flight. In cooperation with other colleagues he was also involved in the follow on DLR-missions MOMS-02 on the D2 Space Shuttle Flight in 1993 and in the MOMS-2P/ Priroda Flight on the Russian MIR station from 1996–1999. In these missions the so called along track stereo-imaging principle was applied for the first time in space.

The same imaging principle is also used for the HRSC-camera developed by DLR and presently successfully used in ESA's *"MARS EXPRESS Mission"* for topographic mapping of the Mars surface.

A complete new method – SAR-Interferometry – for deriving digital terrain models from space was used in NASA's *"Shuttle Radar Topography Mission (SRTM)"* in the year 2000. DLR participated in this mission with an own X-band Synthetic Aperture Radar (SAR)-System.

The paper gives a survey on the development of space photogrammetry in Germany and refers to GOTTFRIED KONECNY's contribution to this development. Facts of the above mentioned missions will be presented and their results will be reviewed.

Zusammenfassung: *25 Jahre Weltraum-Photogrammetrie in Deutschland – ein von GOTTFRIED KONECNY initiiertes Forschungsfeld.* Die deutschen Photogrammeter begannen in den 80er Jahren sich für die Weltraumphotogrammetrie zu interessieren. Das erste Weltraumexperiment, das speziell der Photogrammetrie gewidmet war, wurde von GOTTFRIED KONECNY vorgeschlagen. Es handelte sich um das *Metric Camera Experiment* auf der Grundlage einer konventionellen Luftbildkamera, das unter seiner Führung 1983 auf dem ersten Spacelab-Flug erfolgreich durchgeführt wurde. In Zusammenarbeit mit anderen Kollegen war er auch an den folgenden DLR-Missionen MOMS-02 auf dem D2 Space Shuttle Flug 1993 und MOMS-2P/ Priroda auf der russischen MIR Station von 1996–1999 beteiligt. In diesen Missionen wurde die so genannte *along track stereo*-Bilddatenerfassung erstmals vom Weltraum aus angewandt.

Dasselbe Prinzip wird auch in der vom DLR entwickelten HRSC Kamera verwendet, die derzeit erfolgreich in der *ESA Mission MARS EXPRESS* zur topographischen Erfassung der Marsoberfläche eingesetzt wird.

Eine vollständig neuartige Methode – SAR Interferometrie – zur Ableitung digitaler Geländemodelle aus dem Weltraum wurde auf der *Shuttle Radar Topography Mission (SRTM)* der NASA im Jahre 2000 angewandt. Das DLR nahm an der Mission mit einem X-Band Synthetic Aperture Radar (SAR)-System teil.

Dieser Beitrag beschreibt die Entwicklungen der Weltraumphotogrammetrie in Deutschland mit Bezug zu GOTTFRIED KONECNYS Beiträgen auf diesem Gebiet. Die genannten Missionen und ihre Ergebnisse werden kurz vorgestellt.

* Enhanced version of a paper published in the proceedings of the ISPRS Hannover Workshop 2005 "High Resolution Earth Imaging for Geospatial Information", May 17–20, 2005, Institute of Photogrammetry and GeoInformation, University of Hannover.

1432-8364/05/2005/0467 $ 2.50

1 Introduction – The Role of Gottfried Konecny

In the context of this paper the term "Space Photogrammetry" is understood as "surveying and measuring of the three dimensional form of the solid surface of the Earth and of other planets from space images and generating cartographic products, such as DEMs, orthophotos and topographic maps from these image data". Nowadays also the visualisation of the three dimensional landscapes can be regarded as a presentation of topographic information.

Gottfried Konecny was one of the first scientists in the field of surveying and mapping in Germany who recognized that space techniques can be used to cover the worldwide need for topographic mapping at various scales. A first opportunity to realize his ideas was offered to him by ESA's Spacelab Program which foresaw to operate European payloads on the American Space Shuttle Flights. Konecny's proposal for a cartographic space experiment was accepted and flown in November/December 1983 as the so called "Metric Camera Experiment" on the first Spacelab Mission. This was the begin of Space Photogrammetry in Germany.

That this first photogrammetric space experiment could be performed is owed to Konecny's skill to convince scientific advisory boards, the funding governmental authorities and even sceptical colleagues of the advantage of space sensors for mapping tasks. His ability to combine a "technical vision" with a "practical application" was very beneficial to succeed with this photogrammetric experiment proposal in competition to many other proposals from various scientific disciplines.

Beside its scientific goals the Metric Camera Experiment had also the effect that it led to a closer cooperation of the Remote Sensing Community and the "classical" Photogrammetric Community in Germany. In particular the photogrammetric University Institutes started to show stronger interest in space activities. This common understanding for "using space techniques for mapping tasks" had in the medium term the effect, that further photogrammetric space experiments, e. g. MOMS, were decided on and carried out. It is the merit of Gottfried Konecny to have made most of the German photogrammetric institutes "space minded".

Konecny worked after his return from Canada and the USA and since he took over the position of the director of the Institute of Photogrammetry and Surveying at the University of Hannover in the year 1971 always close together with the German Aerospace Research Center (DLR), particular with its former Institute of Optoelectronics – now integrated in the Remote Sensing Technology Institute. In the eighties and the nineties he was a scientific adviser to this institute and in this role he strongly influenced and promoted the MOMS mission as well as the HRSC-Mars mission. He also assisted DLR in an attempt to fly a MOMS-type camera on the French SPOT-5 mission (Fig. 1).

This cooperation between space engineers and photogrammetrists was very fruitful for both sides: technical requirements for advanced sensor technology were defined and innovative methods for digital data evaluation and new mapping techniques were developed. Through this cooperation between photogrammetrists and space engineers the development of "Digital Photogrammetry" in Germany got a strong impulse.

Since more than 5 years high resolution optical sensors deliver image data of a ground resolution of 1 m and better and also sophisticated Interferometric Side Looking Radarsystems (IF-SAR) have been employed in space. Both techniques offer unique possibilities for the generation of topographic products. Especially in the field of IF-SAR DLR has developed a high standard of know how which can be used in future space missions with topographic applications.

For the coordination of the joint interests of photogrammetric University Institutes and the German Aerospace Center/Space Agency with respect to future mapping space missions it would be very helpful if a

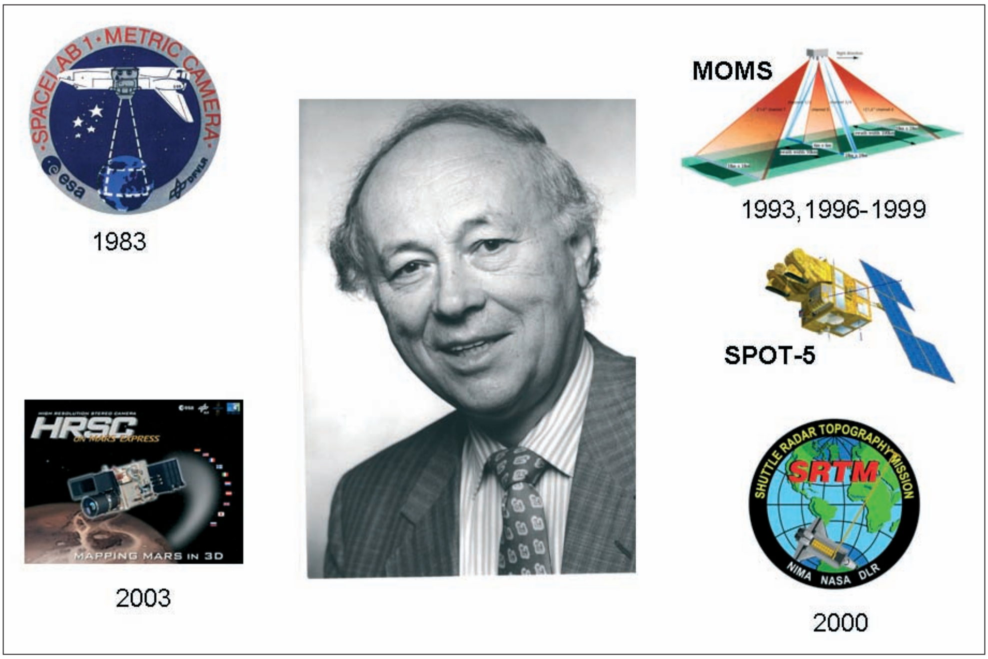

Fig. 1: Gottfried Konecny surrounded by icons representing photogrammetric space missions of the last 25 years in which Germany participated or showed interest in.

young colleague could take over the role of a mediator and adviser which was hold by Gottfried Konecny until the end of the nineties.

2 Metric Camera Experiment

Topographic mapping tasks could not be fulfilled satisfactory with space images of the LANDSAT-type at the end of the seventies. Therefore the surveying community requested high resolution stereoscopic space imagery taken with a calibrated mapping camera. Two photogrammetrists in particular articulated the requirements for "Space Photogrammetry" on behalf of the surveying science community: Gottfried Konecny in Europe and Fred Doyle in the USA. These requirements were favoured by the American plans for a Space Shuttle Program.

A proposal by Gottfried Konecny, to operate within the first European Spacelab Mission on board the 9th Space Shuttle Flight an Aerial Survey Camera was accepted as "Metric Camera Experiment" by the European Space Agency (ESA) in the year 1977. The instrument was a slightly modified Zeiss aerial survey camera with a focal length of 305 mm, which was provided to ESA as multi experiment facility. ESA in turn ensured the experiments flight and selected co-investigators.

The Metric Camera Team was composed of:

- Principal Investigator: G. Konecny, University Hannover,
- Project Engineer: M. Schroeder, DLR, Oberpfaffenhofen,
- Project Manager: A. Langer, DLR, Cologne,
- Industrial Contractor: T. Miski, ERNO, Bremen,
  H.K. Meier, Carl Zeiss, Oberkochen,
- ESA-Project Coordinator: M. Reynolds, ESTEC, Noordwigk.

ESA was assisted in scientific and operational matters by a "Metric Camera Working Group", chaired by G. KONECNY. The other members were: I. DOWMAN (UC, London), G. TOGLIATTI (PT, Milano) & M. DUCHER (IGN, Paris).

After several launch shifts the Spacelab-Flight took place from November 28th to December 8th 1983 (KONECNY 1984, SCHROEDER 1984).

The Metric Camera Experiment was unique in that it was the first calibrated mapping camera in space to take stereoscopic images on the large film format of 23 cm × 23 cm. The camera was operated over nearly all continents (with the exception of Australia) and obtained over 1000 images, of which 550 were on colour infrared film and about 450 on black and white film. All photos were taken with at least 60% overlap in flight direction for stereoscopic evaluation. In total an area of 11 million km^2 was photographed, each photograph covering in area of 190 km × 190 km at a scale of 1 : 820 000.

The objective of the experiment was to test the capability of high resolution stereoscopic space images for compiling and updating topographic and thematic maps. About 50 co-investigators participated in the evaluation of the image data and their final results were presented at a Metric Camera Workshop at DLR, Oberpfaffenhofen in February 1985. The results can be summarized as follows:

- Ground resolution: 10–15 m (pixel equivalent)
- Planimetric accuracy: $\pm$ 10 m
- Height accuracy: $\pm$ 15 m
- Due to the limited ground resolution the maximum map scale that can be derived is 1:100 000.

Since the launch for the Metric Camera Flight, originally planned for the summer months, was slipped to end of November, the lighting conditions over the earth became very unfavourable and the sun elevation never exceeded 30° for all camera operations. NASA therefore promised to refly the camera on the American Earth Observation Mission (EOM 1/2) scheduled for launch in summer 1986. For this flight the camera was equipped with a forward motion compensation and high resolution films to improve the ground resolution considerably. The camera system was already integrated into EOM 1/2 – payload and waiting for launch when the Challenger accident happened in early 1986.

After this accident the schedule of the Space Shuttle Flights was completely revised by NASA and the Metric Camera Experiment was assigned to the ATLAS-mission to be launched in 1989. In this mission the camera would not have been operated in the pressurized Spacelab module but had to be installed in a pressurized container, which was covered by an optical window at the inner wall of the cargo bay of the Shuttle. Operation of the camera in this configuration required a complete redesign of the camera system. The phase-A study for these modifications were just finished when the German Ministry for Research and Technology decided to stop the project because of financial reasons.

KONECNY together with DLR made various attempts to refligh the Metric Camera on other missions, e. g. on the German D-3 mission and on the Russian MIR-station, but got not the support of the Ministry for Research and Technology.

The only calibrated mapping camera which has been flown after the Metric Camera was the American *Large Format Camera*, which was operated on a Space Shuttle Flight in October 1984 on the initiative of FRED DOYLE.

Up to now no further space missions with large format calibrated cameras have been carried out.

International Cooperation

Some few Metric Camera images were not included in the official image catalogue, because they were taken over former east block countries. The reason for taking out these images was that in the mission planning for the Metric Camera it was agreed with NASA and ESA not to take images over east block countries. But the orbit prediction for the mission planning had an uncertainty of approx. 30 s; this had the effect, that during the mission in contradiction to the agreed rules occasionally some pictures were taken over east block countries. To avoid tedious discussions with NASA and ESA these images were simply taken out of the catalogue and kept hidden, but under control in the archive.

One of these officially "not existing" images was the so called *"Rügen-image"* covering parts of the former DDR and of Poland; it was recently published as cover photo of the PFG-magazine, No. 2, 2005. When G. Konecny was president of ISPRS he participated in several meetings in the DDR. At one of these occasions he took the "*Rügen-image*" secretly with him and showed it to Karl-Heinz Marek and Klaus Szangolies. In return they showed him some space images taken from Russian space missions.

To continue this secret information exchange on space images from West and East more formally they agreed to held an ISPRS-workshop in the DDR, to which the Russian colleagues could be invited. Klaus Szangolies organized this workshop entitled *"Use of Space Photographic Data for Mapping of the Earth Surface"* at Leipzig in September 1987. This was a historic event for photogrammetrists, because for the first time high resolution Russian space images were officially shown to colleagues from the West. After this meeting some information channels were opened which could be used to obtain more Russian space images.

3 MOMS – the first Along Track Stereo Camera in Space

MOMS (Modular Optoelectronic Multispectral Stereo Scanner) was a German space borne push broom scanner for high resolution (HR), multispectral (MS) and threefold along-track stereoscopic imaging (Schroeder et al. 2000). The initiative for the development of the camera and its operation in space came from Johannes Bodechtel, University of Munich, and Franz Lanzl, DLR-Institute of Optoelectronics. The stereo-module of the camera consisted of the HR nadir looking lens with a focal length of 660 mm and two inclined lenses with 237 mm focal length. Thus, the Earth's surface was imaged three times from three different directions within approximately 40 seconds only, corresponding to an orbit distance of approximately 300 km. This along-track stereo principle is highly advantageous for image correlation in the data evaluation process, since all three image strips are recorded under more or less the same imaging conditions. The stereo angle of 21.4° results in a base/height ratio of approximately 0.8. The spectral bandwidth of all three channels was 520–760 mm. The multispectral-module consisted of two lenses with 220 mm focal length. Both focal planes contained two linear CCD-arrays each with different spectral filter glasses for imaging in the following four bands: 440–505 nm (blue), 530–575 nm (green), 645–680 nm (red), 770–810 nm (NIR).

The camera, called *MOMS-02*, was first flown during the German Spacelab mission D2 (STS55) in spring 1993. Within 11 days, 48 image strips were taken from a 300 km orbit with 28.5° inclination. Four hundred processed scenes are available. The ground pixel size was 13.5 m for the MS- and the inclined stereo-channels and 4.5 m for the HR-channel. For the first time, the along track stereo principle was successfully used for the generation of high quality digital elevation models (DEM) from space.

After the shuttle mission the camera system was refurbished for a second flight onboard the PRIRODA module of the Russian space station MIR. The camera, renamed *MOMS-2P*, was launched on May 5th, 1996 from Baikonur (Kasakstan) and mounted to the outside wall of PRIRODA on May 30th, 1996. For the MIR orbit altitude of 400 km the ground pixel size was 18 m and 6 m (HR). The inclination of 51,6° allowed for imaging of industrialized as well as developing countries.

The MOMS-2P data were recorded on an onboard tape recorder located inside the PRIRODA module. Due to its limited data rate of 100 Mbit/sec, only subsets of all seven channels could be recorded simultaneously. The swath width for different channel combinations varied between 36 and 100 km.

Full tapes were returned to Earth by Sojus- and Space Shuttle flights. Operation of the camera was terminated August 16, 1999. In March 1997 technical problems occurred with the HR channel. Since that time two nadir looking MS channels and two inclined channels each with 100 km swath width were mainly used for stereos-copic imaging.

In total, approximately 65 million km^2 of earth's land mass were recorded and processed. The processing of the MOMS data was accomplished by a science team of several German university institutes and was coordinated by DLR. The "thematic users" were coordinated by J. BODECHTEL, University Munich, and H. KAUFMANN, Geo Research Center Potsdam, and the "topographic users" were coordinated by F. ACKERMANN and D. FRITSCH, University Stuttgart.

For the task of thematic and stereoscopic data evaluation a digital photogrammetric workstation (DPWS) has been established at DLR in cooperation with photogrammetric university institutes in Munich, Hannover, and Stuttgart.

The contributions of the cooperation partners to the DPWS were as follows:

- Automatic Image Matching: University Stuttgart (F. ACKERMANN) and DLR-Institute of Optoelectronics (M. LEHNER),
- Photogrammetric Bundle Block Adjustment: Technical University Munich (H. EBNER),
- Digital Elevation Models: University Stuttgart (F. ACKERMANN, D. FRITSCH),
- Orthophotos: University Hannover (G. KONECNY, K. JACOBSEN),
- Interactive Digital Stereo Point measurements: University Hannover (G. KONECNY, J. SCHIEWE) and DLR-Institute of Optoelectronics (R. MÜLLER),
- Integration into the XDIBIAS–Image Processing System, DLR-Institute of Optoelectronics (M. SCHROEDER, P. REINARTZ).

Up to now MOMS data covering an area of more than 400.000 km^2 have been processed with the DPWS to DEMs and orthoimages by DLR.

Accuracy analysis using independent ground control led for MOMS-2P/PRIRODA to point accuracies of 8 m in X, Y and Z for test sites in Germany.

With the MOMS missions the "along track" stereo imaging principle was successfully demonstrated and paved the way for similar missions by France, India and Japan.

4 SPOT-5

With the missions Metric Camera and MOMS for more than a decade valuable technical and scientific experience in space photogrammetry were gained in Germany. A logical programmatic consequence would have been to continue on this line with a national operational satellite mission equipped with a high resolution stereo camera system. But in the second half of the nineties there was no chance to get the governmental support for such a mission because most of the Earth Observation's budget was spent for Shuttle Radar missions.

A new glimpse of hope occurred at the horizon when the French Space Agency (CNES) offered to DLR to fly a German Stereo Camera on their SPOT-5 mission. The originators of this idea were F. LANZL on DLR-side and M. Arnaud on CNES-side. A CNES/DLR study team was set up which investigated for more than a year technical aspects of a camera concept, the distribution of data including the data receiving at DLR's Neustrelitz ground station and a business plan.

The study team consisted of: M. ARNAUD, C. FRATTER, A. BAUDOIN (all CNES), PH. MUNIER (Spot Image) and F. LANZL, P. SEIGE, M. SCHROEDER, R. SANDAU, R. PISCHEL (all DLR) with G. KONECNY (University Hannover) as photogrammetric adviser.

As G. KONECNY, who also assisted CNES in defining the SPOT 5 mission, had insider knowledge of both sides his role as catalysator and moderator of these bilateral talks was very helpful and important.

Because of the fixed time schedule for the running SPOT-5 project a decision on the stereo camera had to be made in September 1997. At this time the concentration and merging of the European space industry was under way and the German space agency DARA was integrated into DLR at the same time. Under these circumstances a positive decision on the German side could not be accomplished. One of many reasons was that the German space industry was not willing to spend own money in the development of the stereo camera. The company that came out of the industrial merging process was EADS. But instead by the German branch of this company the camera was finally realized and financed via the French branch of the company as pure French stereo camera on SPOT-5.

For the German side remained the satisfaction that their along track stereo imaging principle was international accepted. SPOT-5 with the high resolution stereo camera (HRS) was finally launched in May 2002. The camera delivers stereoscopic images of 10 m ground resolution and 100 km swath width.

In 2003 CNES and SPOT Image provided original images to the science community in the framework of the ISPRS/CNES HRS-Scientific Assessment program (Baudoin et al. 2004). Results of this program were presented at the ISPRS Istanbul Congress in June 2004. From Germany DLR's Remote Sensing Technology Institute and the Hannover Institute of Photogrammetry and Geo Information participated in this program.

It could be shown that a stereoscopic evaluation of SPOT5-HRS data, only using anciallary data delivered by the image provider and not using ground control points, leads to an absolute accuracy of terrain heights in the order of 5 to 9 m (bias), with a standard deviation of 2 to 4 m for single points and 4 to 7 m for the interpolated DEM in comparison to a reference DEM of superior quality. With only one to two ground control points the bias error could be reduced to 0 to 1 m.

5 HRSC-Mars Express

The development of the *High Resolution Stereo Camera (HRSC)* has its origin at DLR's Institute of Optoelectronics and is based on the technical experience obtained with MEOSS and MOMS. MEOSS stands for Monocular Electro Optical Stereo Scanner and was a compact three line push broom camera using only one single lens. MEOSS was foreseen to fly on an Indian satellite, but due to two launch failures this camera never became operational in space. Like MEOSS the HRSC has only one lens, but different to MEOSS it uses nine CCD-lines in the image plane.

The HRSC was originally planned to fly on the Russian mission MARS 96, but this mission failed shortly after launch due to a failure of the upper stage of the launch vehicle.

A redesigned HRSC, reduced to a mass of only 19.6 kg was accepted by ESA to fly on their mission Mars Express, which was launched in 2003. The camera started to take pictures of the Mars surface on 9 January 2004 (R. Jaumann & U. Köhler 2004).

Of the nine CCD-lines five are used for stereoscopic viewing: one is looking nadir, two are looking forward in different directions and two backward in the same manner; the other four lines are used for multispectral imaging in blue, green, red and infrared.

With a focal length of 175 mm and an orbit altitude at the perihel of 265 km the maximum ground resolution is about 10 m. The objective of the HRSC mission is to produce a topographic image map with a ground resolution of 20 to 40 m of the whole Mars surface of 145 Mio. km^2.

The initiator and coordinator of the HRSC development was Gerhard Neukum. He and his team moved at the beginning of the nineties from the Institute of Optoelectrics in Oberpfaffenhofen to Berlin, where DLR had founded a new Institute of Planetary Research. This institute is now responsible for controlling and operating the camera and for processing of all raw data to scientific image products. G. Neukum, who is now with the Free University of Berlin, is the Principal Investigator of the HRSC-experiment and coordinates all scientific activities. For the mapping tasks the following German photogrammetrists are members of the HRSC science team: J. Albertz, TU-Berlin; M. Buchroithner, TU-Dresden; E. Dorrer and H. Mayer, University Bundeswehr München; H. Ebner and U. Stilla, TU-München; Ch. Heipke, University Hannover; F. Scholten, DLR-Berlin.

6 Shuttle Radar Topography Mission (SRTM)

SRTM used the principle of interferometric synthetic aperture radar (IF-SAR) for DEM generation from orbit altitude (Rabus et al. 2003). For the first time this mission provided a nearly global high-quality DEM with a grid point distance of 1 and 3 arc sec. The SRTM-DEM covers the earth between latitudes 60° N and 57° S, it was acquired with the same sensor in a single mission and was produced with a single technique-synthetic aperture radar (SAR) interferometry. All data were acquired within 11 days because the radar system used was actively scanning the earth's surface independent of darkness or cloud cover. Between 2000 February 11 and 22, two antenna pairs operating in C- and X-bands were simultaneously illuminating and recording radar signals onboard the Shuttle Endeavour. SRTM was jointly performed by NASA, the German Aerospace Center (DLR) and the Italian Space Agency (ASI). The C-band data covering an area of 119 million km^2 were processed by NASA-JPL. DLR was responsible for the X-SAR system, this included the instrument design, the mission planning, calibration, as well as the development and operation of the processing and archiving system. The X-band data that covered approximately 58 million km^2 were processed to DEMs and orthophotos; the processing of all X-band data was completed in 2004 and these data are now available to the users from DLR's remote sensing data archive.

The X-band DEM is provided in geographic coordinates. The horizontal spacing is 1 arc sec; the elevation value is given in meters. WGS84 is used as horizontal and vertical datum. This means that ellipsoidal heights are provided. The DEM accuracy is $\pm$ 16 m absolute und $\pm$ 6 m relative vertical accuracy.

The configuration used for DEM generation is the so-called across-track interferometer. This resembles a stereo arrangement: two SARs fly on (ideally) parallel tracks and view the earth's surface from slightly different directions at the same time. This SAR observation technique is called single pass interferometry. SRTM was the first and till today the only single-pass interferometer in space.

Two single-pass interferometers were built and operated in parallel, the US C-band (5.6 cm) system and a German/Italian X-band (3.1 cm) system X-SAR. The master channels (transmit and receive) of both interferometers were installed in the shuttle cargo bay. The secondary (receive-only) antennas were mounted at the tip of a 60-m long lightweight mast. During lift-off and landing, the mast was stowed away in a 3-m long canister. Once in orbit, the mast was unfolded by a smart mechanical construction.

The X-SAR swath width was in the order of 45 km leading to gaps in the mapping pattern. However, the X-band interferograms and the derived DEMs are of higher quality than those from the C-band. The height accuracy of the X-band data is superior to the C-band data by a factor of approximately 2.

The whole X-band SRTM mission was mainly carried out by DLR. The key persons were

- for instrument development, calibration and operation: W. Keydel, A. Moreira, M. Werner (DLR-Institute of High Frequency Techniques)
- and for processing R. Bamler, M. Eineder (DLR-Remote Sensing Technology Institute) and A. Roth (DLR-German Remote Sensing Data Center).
- The project manager was R. Werninghaus, Project Directorate Space Management – Earth Observation.

Birthday Present – Nanga Parbat

Gottfried Konecny has always had a certain emotional relationship to the mountain Nanga Parbat in Pakistan, which goes probably back to his years of study in Munich. His teacher there was Richard Finsterwalder who produced the first topographic map of the Nanga Parbat.

In montaineous areas the generation of digital terrain models from interferometric SAR-data is somewhat difficult, but M. Eineder, DLR, has improved the interferometric methods for alpine terrain and has derived a high quality digital terrain model of the Nanga Parbat region (M. Eineder 2005).

Over this model a colour image of SPOT was draped and a beautiful perspective view on the Nanga Parbat could be obtained (Fig. 2). Rupert Müller, DLR, produced from this data a flight animation around the mountain, which was showed for the first time at the ISPRS workshop on "High-Resolution Earth Imaging for Geospatial Information" in Hannover, 17–20 May 2005.

The image of Fig. 2 and the flight animation were dedicated to Gottfried Konecny and given to him as present on the occasion of his 75th birthday.

7 Conclusions

What is the future of Space Photogrammetry? Space missions with photogrammetric cameras with large film format for stereoscopic imaging are out since 1984. Instead of them the along track stereo imaging principle introduced by the German MOMS mission was accepted as a reliable method and will be used in various photogrammetric space missions:

Fig. 2: Perspective view on the Nanga Parbat obtained from a digital terrain model derived from SRTM-data, over which a SPOT image was draped. The SPOT image was provided by CNES/SPOT Image.

- SPOT-5/High Resolution Stereo Camera (HRS) was launched in May 2002. But the original stereo data are not available to the photogrammetric users. Spot Image, the data distributor, offers only the derived DEM products.
- ALOS/Prism is a Japanese mission with a three line stereo camera (Prism) with 2.5 m ground resolution and swath width of 35 km. This mission is scheduled for launch in 2005.
- Cartosat 1 is an Indian satellite with a stereo camera with forward and backward look directions. The ground resolution is 2.5 m and the swath width 27 km. The satellite was launched on the 5th of May 2005.

In Germany no dedicated photogrammetric mission with an optical imaging instrument is planned. But there is a good chance that the experience gained with interferometric SAR method during the SRTM mission can be reused in the TanDEM-X mission. This mission foresees two SAR-satellites flying close together in a so called tandem configuration, presently analysed in a phase A study. The objective of the new mission would be to generate a global DEM with approximately 3 m height accuracy. The launch is planned for 2008/09.

To get an optimal benefit from the running and upcoming photogrammetric space missions an international cooperation of the mapping scientists and professionals is necessary. Gottfried Konecny has always in his professional life underlined the need for mapping in all countries and has always shown innovative technologies to accomplish it. With the upcoming space missions we may have the tools to complete the tasks of global mapping in medium to large scales. I am sure that Gottfried Konecny, also after his 75th birthday, will continue to use his many international contacts to establish networks of cooperation to fulfil the task of global mapping.

References

Baudoin, A., Schroeder, M., Valorge, C., Bernard, M. & Rudowski, V., 2004: The HRS-SAP initiative: A Scientific assessment of the High Resolution Stereoscopic instrument on board of SPOT-5 by ISPRS investigators. – International Archives of Photogrammetry 35B, 20th ISPRS Congress Istanbul

Eineder, M., 2005: Alpine Digital Elevation Models from Radar Interferometry – a Generic Approach to Exploit Multiple Imaging Geometries. Proc. ISPRS-Workshop 2005: High Resolution Earth Imaging for Geospatial Information, Hannover, Germany, 17–20 May 2005, on CD-ROM.

Jauman, R. & Köhler, U., 2004: Neue Bilder vom Roten Planeten. – DLR-Nachrichten, Mai 2004/G 12625.

Konecny, G., 1984: The Photogrammetric Camera Experiment in Spacelab 1. BuL 52, Heft 3a.

Rabus, B., Eineder, M., Roth, A. & Bamler, R., 2003: The shuttle radar topography mission – a new class of digital elevation models acquired by Spaceborne radar. – ISPRS Journal of Photogrammetry & Remote Sensing **57**(4): 241–262.

Schroeder, M., 1984: Flight Performance of the Spacelab Metric Camera Experiment. – Proc. IGARSS 84 Symposium, Strasbourg 27–30, ESA SP-215.

Schroeder, M., Kornus, W., Lehner, M., Müller, R., Reinartz, P. & Seige, P., 2000: MOMS – the first along track stereo camera in space – a mission review. – Proc. ASPRS Congress, Washington, May 2000, on CD-ROM, 8pp.

Address of the author:

Hon. Prof. Dr. Manfred Schroeder
Deutsches Zentrum für Luft- und Raumfahrt
Institut für Methodik der Fernerkundung
D-82234 Wessling, Tel.: +49-(0)8153 282790 Fax: +49-(0)8153 281444
e-mail: manfred.schroeder@dlr.de

Manuskript eingereicht: Juni 2005
Angenommen: Juli 2005

Photogrammetrie • Fernerkundung • Geoinformation 6/2005, S. 477–485, 7 figs.

Alpine Digital Elevation Models from Radar Interferometry – A Generic Approach to Exploit Multiple Imaging Geometries*

MICHAEL EINEDER, DLR Oberpfaffenhofen

Keywords: photogrammetry, Synthetic-Aperture-Radar, SAR, InSAR, SAR-Interferometry, Digital Elevation Model, DEM, geocoding

Abstract: The generation of Digital Elevation Models (DEMs) from Synthetic Aperture Radar Interferometry (InSAR) has developed rapidly in the last 10 years. This new method proofed to be operational with the global success of the Shuttle Radar Topography Mission in the year 2000 and with several companies offering regional topographic mapping campaigns based on airborne InSAR today. However, the current radar systems and the current processing methods will deliver robust results only over moderate terrain. When confronted with steep mountains or canyons, the measurement principle poses a number of problems that are quite hard to solve. The reason being the radar viewing geometry that limits the range of observable terrain slopes in one acquisition and the problem to unwrap the ambiguous phase, a measure for the radar look angle. The paper shows examples from the Shuttle Radar Topography Mission in mountainous terrain and demonstrates some specific deficiencies. Then, some processing techniques are sketched that can help to achieve improved results with available data. Finally, techniques for future high resolution InSAR DEM missions are proposed to minimize the artefacts in mountainous terrain and to actively use multi-angle, multi-frequency observations for more robust and more complete DEM reconstruction.

Zusammenfassung: *Erzeugung digitaler Höhenmodelle von gebirgigen Gebieten aus interferometrischen Radardaten – ein allgemeiner Ansatz zur Verschmelzung unterschiedlicher Aufnahmegeometrien.* Die Erzeugung digitaler Höhenmodelle aus interferometrischen Radardaten hat sich in den letzten zehn Jahren zu einem anerkannten Verfahren entwickelt. Im Jahr 2000 wurden große Teile der Erde durch die Shuttle-Radar-Topografie-Mission SRTM aus dem Weltraum kartiert. Im regionalen Bereich bieten heute mehrere Firmen hoch auflösende Höhenmodelle aus interferometrischen Flugzeugradardaten an. Allerdings sind die Ergebnisse dieser Technik bisher nur in moderatem Relief zuverlässig. In steilem Gebirge oder bei tiefen Canyons leidet das Verfahren unter systeminhärenten Nachteilen. Die Gründe liegen zum einen in der Schrägsichtgeometrie des Radars, welche die abbildbare Geländeneigung begrenzt, und zum anderen im Abrollen der mehrdeutigen interferometrischen Phase, einem Maß für den Blickwinkel des Radars. Der Artikel zeigt Beispiele der Shuttle-Radar-Topografie-Mission in gebirgigem Gelände und erläutert die Abbildungsprobleme dort. Weiterhin werden neuere Verarbeitungstechniken vorgestellt, welche zu besseren Rekonstruktionsergebnissen führen können. Außerdem wird erläutert, wie zukünftige interferometrische DEM-Missionen verschiedene Aufnahmewinkel und verschiedene Radarwellenlängen nutzen können, um auch unter schwierigen Bedingungen qualitativ hochwertige und lückenlose Höhenmodelle zu erzeugen.

* Enhanced version of a paper published in the proceedings of the ISPRS Hannover Workshop 2005 "High Resolution Earth Imaging for Geospatial Information", May 17–20, 2005, Institute of Photogrammetry and GeoInformation, University of Hannover.

1432-8364/05/2005/0477 $ 2.25

1 Introduction

Radar interferometry exploits the highly accurate distance measurement contained in the phase of each pixel of two complex synthetic aperture radar (SAR) images to triangulate the topographic height of a scattering facet on ground. The achievable horizontal resolution is determined by the capabilities of the SAR system, in the order of 5 to 30 meters for space based SAR systems and in the order of 0.1 to 1 meter for airborne systems. The vertical accuracy depends on the wavelength which is between 3 and 25 centimeters for common microwave SARs, on the thermal noise of the SAR system and, most important, on the baseline, i. e. the effective distance between the two antennas. Limited by the named technical parameters, vertical DEM accuracies between 0.1 meters for airborne systems to 5–20 meters for space borne systems are currently achieved. An important InSAR DEM mission was the Shuttle Radar Topography Mission (SRTM), which mapped the Earth with a resolution of 30 meters and an accuracy in the order of 6 meters (90%) between 57° southern and 60° northern latitude.

Compared to optical stereo systems the interferometric SAR technique is robust in many ways: The system carries its own microwave illumination and can penetrate clouds with negligible attenuation. There is no scene contrast needed as for non-coherent optical systems because the distance information is inherent in the phase of each single pixel.

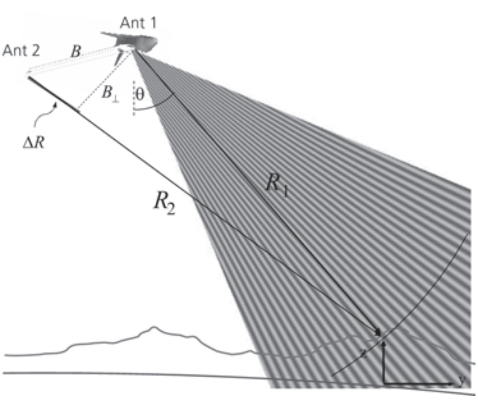

Fig. 1: Imaging geometry and phase field in the zero Doppler plane of a single pass interferometer like SRTM.

Fig. 1 shows the imaging geometry of a side looking single-pass SAR interferometer. A microwave pulse with wavelength λ is transmitted from antenna 1 to the earth surface. The echoes from different distances are recorded by antenna 1 and antenna 2. Both are separated by the baseline B with an effective component $B_\perp$ orthogonal to the line of sight. The radar echoes are sampled with a frequency between 10 MHz and 150 MHz resulting in a spatial resolution between 15 meter and 1 meter. Due to coherent demodulation of the received echo each sample carries also a phase information which is a sensitive measure for the delay time and hence, the distances R_1 and R_2:

$$\phi_1 = -2\pi \frac{2 R_1}{\lambda} \quad \text{and}$$

$$\phi_2 = -2\pi \frac{R_1 + R_2}{\lambda} \tag{1}$$

The interferometric phase difference

$$\phi = \phi_1 - \phi_2 = \frac{2\pi}{\lambda} \Delta R \tag{2}$$

is a measure for the range difference with sub-wavelength accuracy and hence, also for the elevation angle θ

$$\frac{\partial \theta}{\partial \phi} = \frac{\lambda}{B_\perp 2\pi} \tag{3}$$

But because ϕ_1 and ϕ_2 can only be determined in the interval $[-\pi, \pi]$, also the difference ϕ is only an ambiguous measure for θ. In other words, one interferometric phase value ϕ may be caused by different elevation angles θ separated by approximately

$$\Delta\theta = \frac{\lambda}{B_\perp}$$

At one echo sample with a distance R_1 this corresponds to ambiguous height values separated by

$$\Delta z = \frac{\lambda R \sin\theta}{B_\perp} \tag{4}$$

For SRTM X-SAR conditions ($\lambda = 3.1\,\text{cm}$, $R = 400\,\text{km}$, $B_\perp = 60\,\text{m}$, $\theta = 54^\circ$) Δz is about 167 meters.

While the InSAR technique is robust and simple, some specific properties currently limit its applicability to flat and moderately rough terrain: Earth observation SARs are imaging with an incidence angle between 20° and 60° from nadir. This leads to shadowing effects at mountain backsides and to multiple reflections (layover) from slopes that are tilted towards the radar steeper than the incidence angle. Shadow and layover effects do not only distort certain parts of the imaged surface, they interfere with another property of InSAR: the ambiguous measurement of the range by exploiting the phase. The phase of a SAR pixel changes several hundred cycles between adjacent pixels and offers the high accuracy that allows to work with relatively small baselines and work independent of scene contrast as a shift in pixel geometry is not required between the "stereo" observations. On the other hand, only the fractional part can be exploited since the absolute cycle number is unknown. This limits SAR interferometry to applications where the differential phase change between two neighbouring pixels in two images is less than half a cycle. Larger height changes, e. g. caused by steep topography, are estimated by integrating smaller changes, a computation step called *phase unwrapping*. The phase unwrapping process is so far only solved reliably for moderate topography. Errors in phase unwrapping propagate as large errors (multiple phase cycles) into large areas of the scene.

Radar layover and shadow complicate phase unwrapping extremely and cause InSAR DEMs in alpine topography generally not to be very reliable.

Phase unwrapping errors are generally detected by processing DEMs from independent passes and then comparing the results. Phase unwrapping errors lead to large vertical and horizontal shifts which are easy to detect. If no errors are present, the DEMs can be averaged, reducing the relative vertical error caused by thermal sensor noise or signal decorrelation due to temporal changes.

If however, phase unwrapping errors are detected, robust methods to improve the results by using multiple observations are scarce. The majority of approaches published so far help only to combine SAR acquisitions of almost identical viewing geometry. Only then are the geometric distortions in the acquisitions less than one pixel and the phase values can be compared in the image geometry. If different incidence angles from different orbital tracks are mixed or even different aspect angles as viewed from ascending and descending orbits, then the three dimensional geometric distortions are so different that the images can not be co-registered for further joint processing. To co-register them requires the three dimensional geometry that should finally be derived – a circular problem.

A solution for this problem has been derived, tested and published in (Eineder & Adam 2005). It will be shortly summarized in this paper.

2 SRTM X-SAR Data in Mountainous Terrain

Fig. 2 shows the intensity image of the STRM X-SAR over Nanga Parbat mountain (8125 m) in the Himalayas. Clearly visible are the large shadow areas where no radar echo is received and hence, no height can be reconstructed from the interferometric phase. For ease of interpretation the image has been geocoded to UTM projection. The interferometric phase of the Nanga Parbat area is shown in Fig. 3, as well geocoded to UTM. It can be clearly seen that many fringes are missing and hence the phase unwrapping and DEM reconstruction are not very reliable. Even if there is no signal present in the shadow areas, the three dimensional shadow line can be reconstructed by exploitation of the well known geometry of SAR shadow and its relationship to the interferometric phase (Eineder & Suchandt 2003).

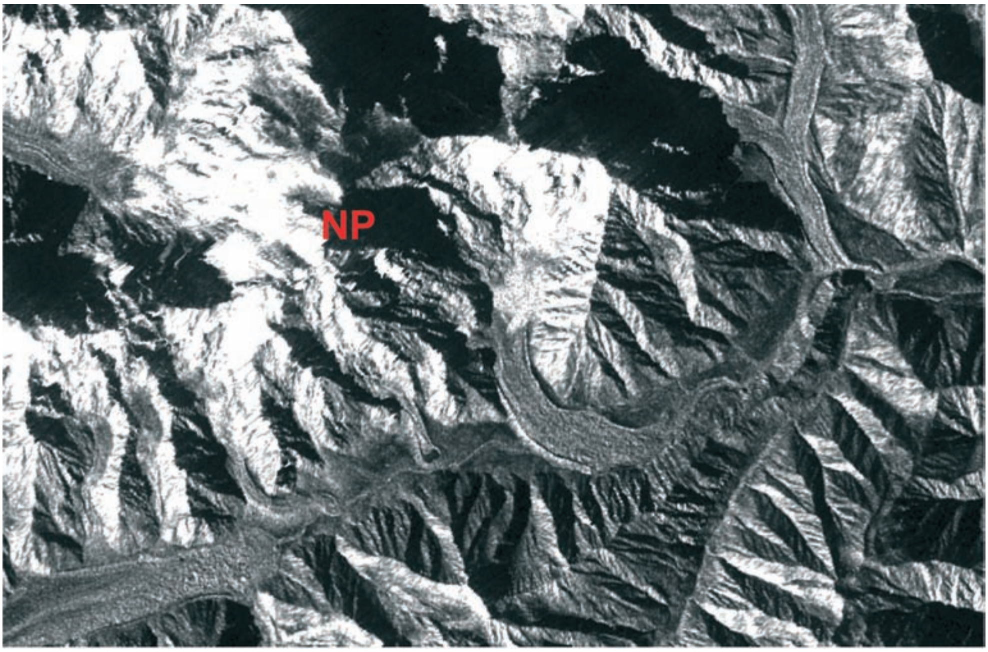

Fig. 2: Geocoded SRTM X-SAR intensity image of Nanga Parbat (NP) area with large regions in radar shadow. The image covers an area of 23 km × 15 km.

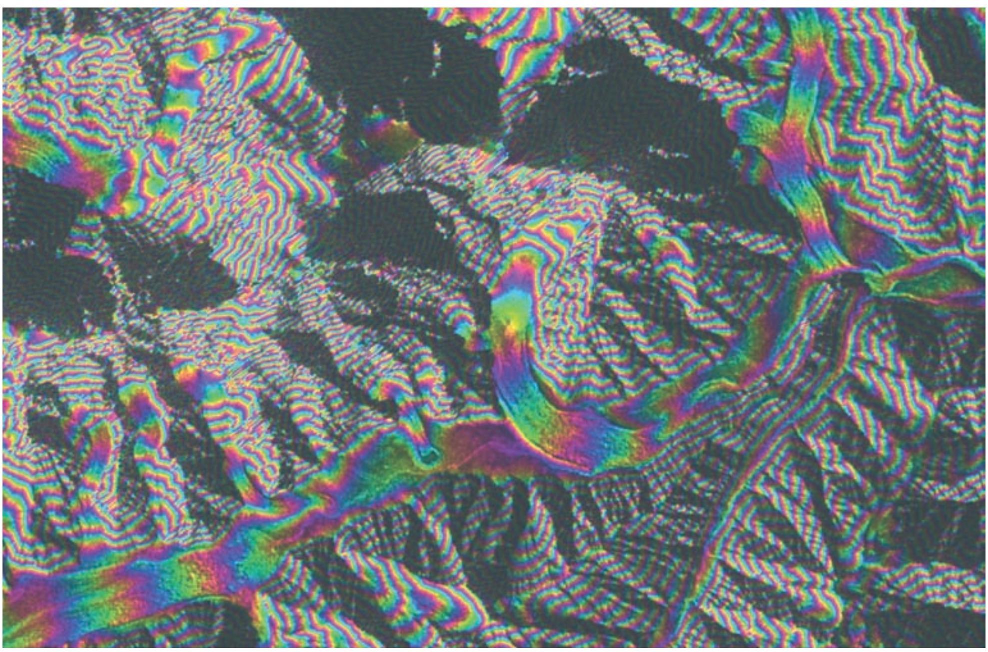

Fig. 3: Geocoded SRTM X-SAR interferometric phase image of Nanga Parbat (NP). The phase is shown in cyclic false colors, the luminance taken from the SAR intensity. One fringe corresponds to app. 175 meters elevation difference.

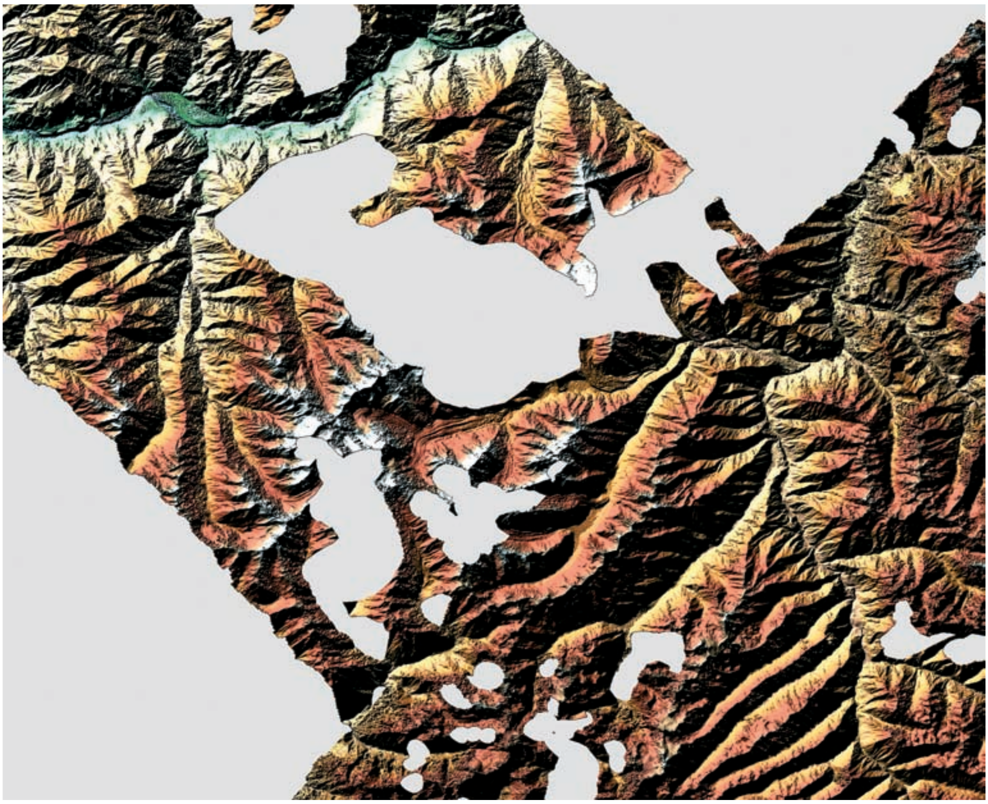

Fig. 4: SRTM X-SAR DEM of larger area round Nanga Parbat (ca. 70 km × 50 km). Not covered areas and problematic areas have been masked by DLR.

However, even if this method succeeded in several experiments it was not used for operational SRTM DEM production at DLR because of the limited experience that was available with it. Furthermore, the method would help with phase unwrapping but would not provide true heights in the shadow area neither could it help to cure the problem of layover. Therefore, as shown in Fig. 4, larger areas of the SRTM-X band DEMs have been masked because of the risk of wrong heights due to phase unwrapping errors. The C-Band DEMs of SRTM have been produced at NASA/JPL with different phase unwrapping algorithms and with double (ascending and descending) coverage. Fig. 5 shows the corresponding area and it can be seen that also there areas are left "white" because of shadow and phase unwrapping problems.

Having two radar systems (X and C band) and two passes (ascending and descending) one might argue that it should be possible to process the data jointly and make phase unwrapping more stable. However, SAR systems were so far mostly limited to one frequency and hence algorithms to unwrap multi frequency interferograms are little developed. An increasing number of publications on this subject can be noticed in the recent years. So far, the existing algorithms are restricted to the case that both radar systems were at almost the same position and the viewing geometry almost identical. A general approach to fuse interferograms of completely different observation geometries was missing because the geometric distortions of the different geometries need to be corrected prior to fusion. But to correct the distortions would require the DEM that

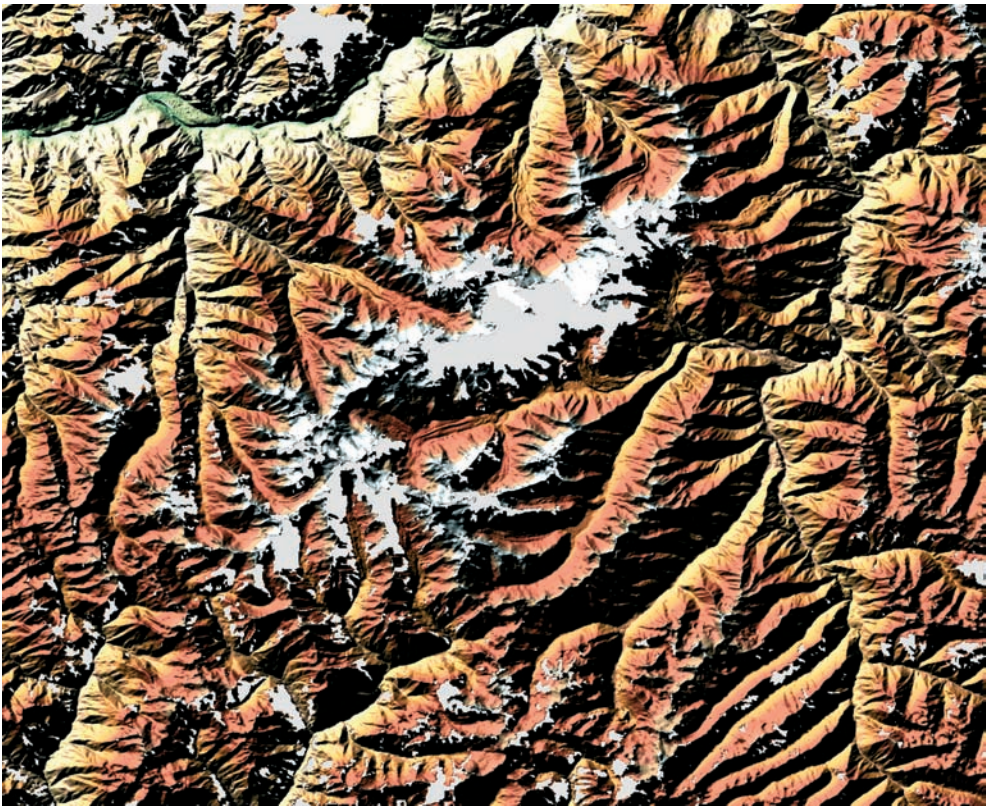

Fig. 5: SRTM C-band DEM of larger area round Nanga Parbat (ca. 70 km × 50 km). Problematic areas have been masked by NASA.

should be the output of the process. A reflexive problem?

3 A Multi Geometry Fusion Approach

Efficient algorithms and the power of today's computers allowed a first demonstration that the problem is solvable (Eineder & Adam 2005). The key ideas of this method are as follows:

- since a projection of one radar imaging geometry into another one is not possible without having a DEM, the whole reconstruction is best performed in the DEM geometry and not in the radar slant range geometry as commonly done,
- given the three dimensional position of an estimated point on an assumed DEM surface, the slant range coordinates and the expected interferometric phase of this estimate can be determined easily and efficiently (Eineder 2003a),
- no phase unwrapping is performed on the single interferograms,
- instead phase unwrapping is performed by maximization of the probability that all interferometric observations match this estimate,
- the maximization process is slow due to an iteration in the vertical direction for each DEM pixel. It can easily be accelerated and stabilized if a priori knowledge, e. g. in the form of available DEMs is included.

As shown in (Eineder & Adam 2005) and in Fig. 6 the renouncement of phase unwrapping requires a minimum number of observations before the algorithm stabilizes on the correct height.

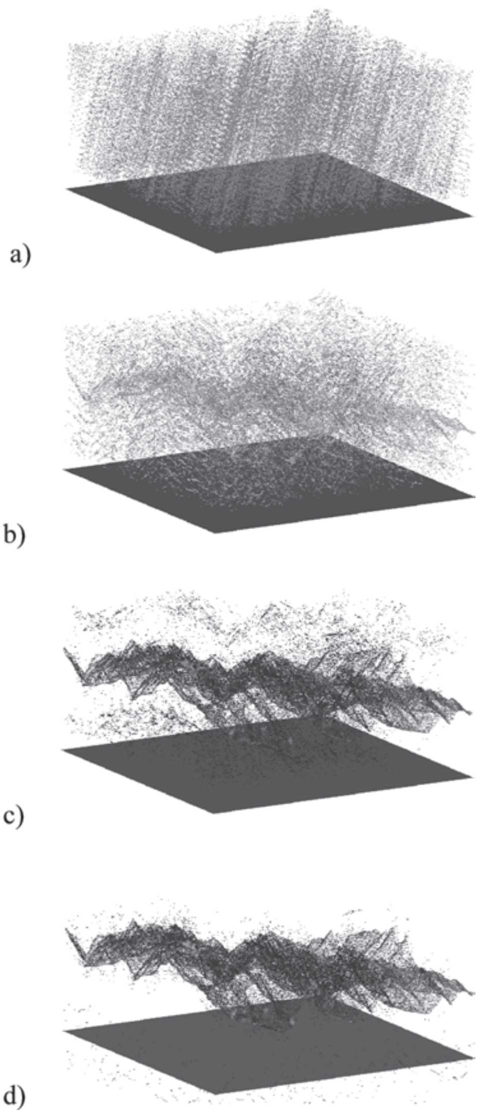

Fig. 6: Digital Elevation Model of Sterzing, Italy, reconstructed from multi-geometry SRTM data using a maximum likelihood approach. Size: 30 km × 15 km. Top to Bottom: improving convergence with increasing number of observations: a) descending X-band; b) descending X-band and ascending C-band; c) X-band and C-band, both in ascending and descending; d) X-band and C-band, both in ascending and descending plus 1 km GLOBE DEM as reference.

Since this generic approach models the radar imaging process and its error sources, it is very well suited for future expansions. For example, neighbourhood relationships that are completely ignored in the current version could be incorporated. Fig. 6 shows how a DEM solution reconstructed from different numbers of interferograms stabilizes with increasing number of observations.

4 Optimization for future missions

In the recent years several InSAR missions for DEMs with improved accuracy have been proposed, such as the interferometric cartwheel (Massonnet et al. 2000) by CNES, an L band satellite constellation by ESA (Zink 2003) and recently TanDEM-X, a constellation of two X-band satellites in formation flight (Moreira et al. 2004).

Due to their flexible baseline geometry and the multiple incidence angles, such missions are well suited to be optimized to map alpine areas without gaps and with correct phase unwrapping. As shown in (Eineder 2003b), shadow and layover effects can not be completely avoided but minimized at an incidence angle of 45° or, reduced to a larger extent by combining observations with different viewing geometries.

Fig. 7 shows such a combination for extremely rugged mountainous terrain. Shadow and layover have been simulated with the help of a 10 meter resolution DEM for the viewing geometry of TerraSAR-X (Buckreuss et al. 2003), a German X-band satellite to be launched in summer 2006. There is a total number of 13 possible observations in the 11 day repeat orbit. From those, two observations in the nominal right looking mode have been selected that minimize the area of layover and shadow to 3 %, if they are combined.

Further optimizations with respect to height reconstruction can be performed by varying the baseline. Large baselines are desirable to achieve a small height error of the DEM. On the other hand, the danger of phase unwrapping errors grows with the

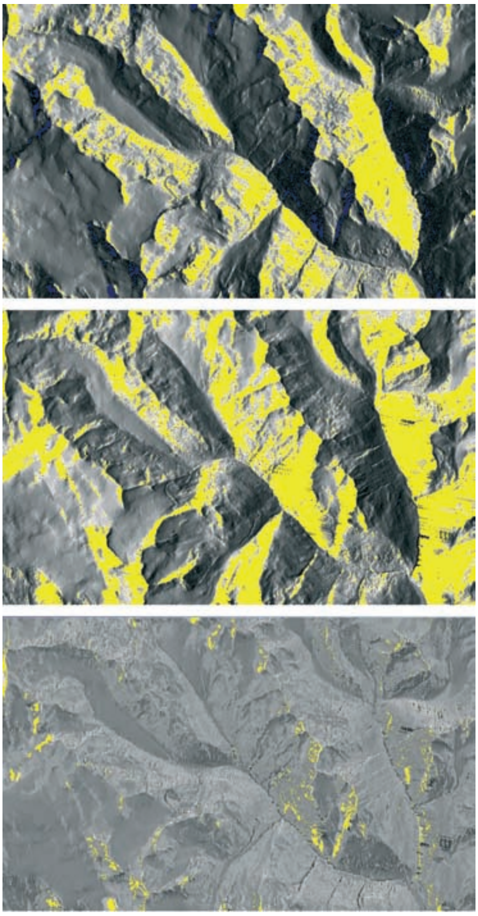

Fig. 7: Simulated shadow and layover areas (yellow) in the steep Ötztal mountains (Austria) for 41° incidence angle descending (top), 30° incidence angle ascending (mid) and a combination of both (middle).

length of the baseline. It is the strong belief of the author, that for rugged terrain phase unwrapping can only be solved reliably if multi-geometry, multi-baseline or multi-wavelength observations are performed and are jointly processed.

For example, small baseline interferograms that are easier to unwrap can be used to derive the phase constant of larger baseline interferograms. Small baselines can be achieved by reducing the difference between the orbits of the two satellites. They can also be synthesized by taking the phase difference from two interferograms with larger but similar baselines. Given a fixed baseline, a different effective baseline can also be reached by changing the incidence angle significantly. But then the image geometries will no more be compatible and methods as described in chapter 3 must be used. Another approach to achieve multiple wavelengths is to use the wavelength dispersion within the range bandwidth for phase unwrapping (BAMLER & EINEDER 2005, VENEZIANI et al. 2004).

5 Summary

While InSAR DEMs are operational over moderate and hilly topography they are not yet reliable in rugged terrain. In order to minimize shadow and layover effects, the viewing geometry must be optimized for single observation to approximately 45°. Multiple observations are required to achieve complete coverage, but then incidence angle combinations different from 45° with either different incidence angles or different aspect angles must be selected. Beneath optimization of the viewing geometry new reconstruction methods based on multiple observations will have to be used in the future. All those options may soon be available with future missions like, e. g. TerraSAR-X in a tandem (MOREIRA et al. 2004). A configuration which allows precise orbit control, multi mode SAR imaging, large bandwidth and high resolution.

6 References

BAMLER, R. & EINEDER, M., 2005: Accuracy of Differential Shift Estimation by Correlation and Split-Bandwidth Interferometry for Wideband and Delta-k SAR Systems. – IEEE Geoscience and Remote Sensing Letters, Vol. 2 (2): 151–155.

BUCKREUSS, S., BALZER, W., MÜHLBAUER, P., WERNINGHAUS, R. & PITZ, W., 2003: The TerraSAR-X Satellite Project. – IGARSS 2003, Toulouse, 21.–25.07. 2003, IEEE, IGARSS 2003.

EINEDER, M. & ADAM, N., 2005: A maximum likelihood estimator to simultaneously unwrap, geocode and fuse SAR interferograms from different viewing geometries into one digital elevation model. – IEEE Transactions on Geoscience and Remote Sensing, Vol. 43 (1): 24–36.

Eineder, M. & Suchandt, S., 2003: Recovering Radar Shadow to Improve Interferometric Phase Unwrapping and DEM Reconstruction. – IEEE Transactions on Geoscience and Remote Sensing, Vol. 41 (12): 2959–2962.

Eineder, M., 2003a: Efficient Simulation of SAR Interferograms of Large Areas and of Rugged Terrain. – IEEE Transactions on Geoscience and Remote Sensing, Vol. 41 (6): 1415–1427.

Eineder, M., 2003b: Problems and Solutions for InSAR Digital Elevation Model Generation of Mountainous Terrain. – ESA FRINGE workshop 2003, ESA, Frascati.

Massonnet, D., Thouvenot, E., Ramongassie, S. & Phalippou, L., 2000: A wheel of passive radar microsats for upgrading existing SAR projects. – IGARSS 2000, Honolulu.

Moreira, A., Krieger, G., Hajnsek, I., Hounam, D., Werner, M., Riegger, S. & Settelmeyer, E., 2004: TanDEM-X: A TerraSAR-X Add-On Satellite for Single-Pass SAR Interferometry. – IGARSS 2004, Anchorage, Alaska.

Veneziani, N., Giacovazzo, V.M. & Bovenga, F., 2004: Height Retrieval by Using a Pseudo-Differential Approach in SAR Interferometry – Preliminary Results with Actual SAR Data. – IGARSS 2004, Anchorage.

Zink, M., 2003: The TERRASAR-L Interferometric Mission Objectives. – ESA FRINGE workshop 2003, ESA, Frascati.

Address of the author:

Dr. rer. nat. Michael Eineder
Deutsches Zentrum für Luft- und Raumfahrt
DLR, D-82234 Wessling, Oberpfaffenhofen
Tel.: +49 8153 281396, Fax: +49 8153 281444
e-mail: Michael.Eineder@dlr.de

Manuskript eingereicht: Juni 2005
Angenommen: Juli 2005

VAKAT

Photogrammetrie • Fernerkundung • Geoinformation 6/2005, S. 487–496, 4 figs., 4 tabs.

High Resolution Satellite Imaging Systems – an Overview*

KARSTEN JACOBSEN, Hannover

Keywords: photogrammetry, remote sensing, Satellite, optical sensors, SAR

Abstract: More and more high and very high resolution optical space sensors are available. Not in every case the systems are well known and the images are distributed over popular distributing channels or are accessible for any user. Several imaging satellites are announced for the near future. In the following, mainly the characteristics of systems usable for topographic mapping are shown, limiting it to sensors with a ground sampling distance (GSD) of approximately 15 m and better.

Not only the GSD of the imaging system is important, also the type of imaging with a transfer delay and integration sensor (TDI) or by reducing the angular speed with a permanent rotation of the satellite during imaging should be mentioned, like the accuracy of the attitude control and determination unit. The radiometric and spectral resolution has to be taken into account. For operational use the swath width, viewing flexibility and imaging capacity has to be respected. Stereo combinations taken from neighboured paths are affected by changes in the object space, atmospheric conditions or different length of shadows. With Cartosat-1 we do have a stereo systems like the existing, but restricted SPOT 5 HRS sensor, generating a stereoscopic coverage within some seconds by viewing forward and afterward in the orbit direction.

Synthetic Aperture Radar (SAR) sensors with up to 1m GSD are announced for the near future, allowing an imaging independent upon cloud coverage. Of course the information contents of SAR-images are not the same like for optical images with the same GSD, but nevertheless we are coming into the range of interest for mapping applications.

Zusammenfassung: *Hoch auflösende bildgebende Satellitensysteme – ein Überblick*. Immer mehr hoch auflösende optische Weltraumsensoren sind verfügbar. Nicht in jedem Fall sind die Systeme gut bekannt und die Bilder über etablierte Vertreiber zu beziehen. Einige Systeme sind für die nahe Zukunft angekündigt. Im Folgenden werden die Charakteristika der Systeme vorgestellt, die für topographische Datenerfassung nutzbar sind, womit die Bodenauflösung auf 15 m oder besser beschränkt ist.

Nicht nur die Bodenauflösung ist von Bedeutung, auch die Art der Vorwärtsbewegungskompensation durch Time Delay Integration (TDI) oder mittels Verringerung der Winkelgeschwindigkeit des Satelliten durch permanente Rotation während der Aufnahme, ebenso wie die Genauigkeit der äußeren Orientierung. Die radiometrische und die spektrale Auflösung sind wichtig wie auch die Streifenbreite und die Flexibilität der Bilderfassung. Die hoch auflösenden optischen Satelliten können die Blickrichtung sehr schnell ändern und ermöglichen damit eine stereoskopische Aufnahme in ein und demselben Orbit, allerdings auf Kosten der Anzahl Szenen, die in dem Orbit aufgenommen werden können. Auf der anderen Seite werden Stereoaufnahmen aus verschiedenen Orbits durch Änderungen des Objekts, der Atmosphäre sowie der Schattenlängen beeinträchtigt.

Synthetische Apertur Radar (SAR) Sensoren mit bis zu 1 m Bodenauflösung, die eine Bilderfassung unabhängig von der Wolkenbedeckung zulassen, sind für die nahe Zukunft angekündigt. Natürlich ist der Informationsgehalt von SAR Bilddaten nicht derselbe, wie der einer optischen Aufnahme gleicher Bodenauflösung, trotzdem kommen wir damit in für topographische Anwendungen sehr interessante Bereiche.

* Enhanced version of a paper published in the proceedings of the ISPRS Hannover Workshop 2005 "High Resolution Earth Imaging for Geospatial Information", May 17–20, 2005, Institute of Photogrammetry and GeoInformation, University of Hannover.

1432-8364/05/2005/0487 $ 2.50

1 Introduction

With the higher resolution and unrestricted access to images taken by satellites, a competition between aerial images and space data exists, starting for a map scale 1: 5000. Based on experiences, optical images should have approximately a ground sampling distance (GSD) of 0.05 mm up to 0.1 mm in the map scale corresponding to a map scale of 1: 20 000 up to 1:10 000 for a GSD of 1 m. GSD is the distance of the centre of neighboured pixels projected on the ground. Because of over- or under-sampling, the GSD is not identical to the projected size of a pixel, but for the user, the GSD appears as pixel size on the ground. An over- or under-sampling is only influencing the image contrast, which also may be caused by the atmosphere.

Mapping today is a data acquisition for geoinformation systems (GIS). In a GIS the positions are available with their national coordinates, so by simple theory a GIS is independent upon the map scale, but the information contents corresponds to a publishing scale. In no case the full information is available in a GIS, for a large presentation scale the generalisation starts with the size of building extensions which are included, while for small scales the full effect of generalisation is required. So for large presentation scales more details have to be identified in the images while for smaller scales a larger GSD may be sufficient. If the GSD exceeds 5 m, not all details, usually shown in the corresponding publishing scale can be identified.

Not only optical images have to be taken into account, in the near future high resolution synthetic aperture radar (SAR) images will be available. Radar has the advantage of penetrating clouds, so a mapping is possible also in rain-forest areas.

Within few years there will be an alternative between the satellite images and aerial images coming from high altitude long endurance (HALE) unmanned aerial vehicles (UAV) with an operating altitude in the range of 20 km.

Not from all systems images are accessible, they may not be classified, but sometimes no distribution system exists and it is difficult to order images.

2 Details of Imaging Sensors

2.1 *View Direction*

The first imaging satellites have had a fixed view direction in relation to the orbit. Only by panoramic cameras, scanning from one side to the other, the swath width was enlarged. For a stereoscopic coverage a combination of cameras with different longitudinal view directions was used, like for the CORONA 4 serious and later MOMS, ASTER, SPOT 5 HRS and Cartosat-1. With SPOT by a steer able mirror the change of the view direction across the orbit came. IRS-1C and -1D have the possibility to rotate the whole panchromatic camera in relation to the satellite. This requires fuel and so it has not been used very often. IKONOS launched in 1999 was the first civilian reconnaissance satellite with flexible view direction. Such satellites are equipped with high torque reaction wheels for all axes. If these reaction wheels are slowed down or accelerated, a moment will go to the satellite and it is rotating. No fuel is required for this, only electric energy coming from the solar paddles.

2.2 *TDI-sensors*

The optical space sensors are located in a flying altitude corresponding to a speed of approximately 7 km/sec for the nadir point. So for a GSD of 1 m only 1.4 msec exposure time is available, this is a not sufficient integration time for the generation of an acceptable image quality, by this reason, some of the very high resolution space sensors are equipped with time delay and integration (TDI) sensors. The TDI-sensors used in space are CCD-arrays with a small dimension in flight direction. The charge generated by the energy reflected from the ground is shifted with the speed of the image motion to the next CCD-element and more charge can be added to the charge collected by the first CCD-element. So a larger charge can

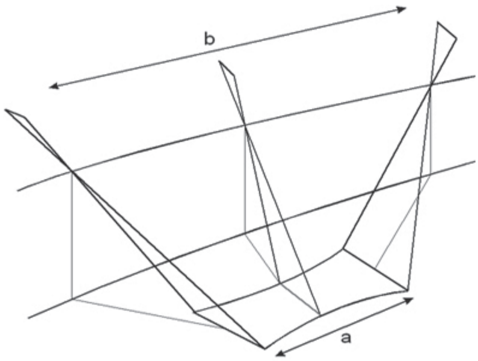

Fig. 1: Enlargement of integration time with factor b/a by continuous change of view direction.

be summed up over several CCD-elements. There are some limits for inclined view directions and vibrations, so in most cases the energy is summed up over 13 CCD-elements. IKONOS, QuickBird and OrbView-3 are equipped with TDI-sensors while EROS-A and the Indian TES do not have it. They have to enlarge the integration time by a permanent rotation of the satellite during imaging (see Fig. 1). Also QuickBird is using this because the sensor originally was planned for the same flying altitude like IKONOS, but with the allowance of a smaller GSD, the flying height was reduced, resulting in a smaller pixel size. The sampling rate of 6900 lines/sec could not be enlarged and this has to be compensated by the change of the view direction during imaging, but with a quite smaller factor like for EROS-A and TES.

2.3 *CCD-configuration*

Most of the sensors do not have just one CCD-line but a combination of shorter CCD-lines or small CCD-arrays. The CCD-lines are shifted against each other – see Fig. 2.

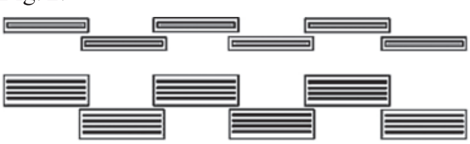

Fig. 2: Arrangement of CCD-lines in focal plane, above: panchromatic, below: multi-spectral.

The merging of sub-images achieved by the panchromatic CCD-lines belongs to the inner orientation and the user will not see something about it. Usually the matching accuracy of the corresponding sub-images is in the lower sub-pixel range so that the geometry of the mosaiced image does not show any influence. This may be different for the larger offset of the colour CCD-lines. Not moving objects are fused without any problems during the pan-sharpening process. By theory only in extreme mountainous areas unimportant effects can be seen. This is different for moving objects – the time delay of the colour against the panchromatic image is causing different locations of the intensity and the colour. The different colour bands are following the intensity. This effect is unimportant for mapping because only not moving objects are used.

2.4 *Staggered CCD-lines*

The ground resolution can be improved by staggered CCD-lines (Fig. 3). They do include 2 CCD-lines shifted half a pixel against each other, so more details can be seen in the generated images. Because of the over-sampling, the information content is not corresponding to the linear double information. For SPOT 5 the physical pixel size projected to the ground is 5m, while based on staggered CCD-lines the supermode has 2.5 m GSD. By theory this corresponds to the information contents of an image with 3 m GSD.

2.5 *Multi Spectral Information*

Sensors usable for topographic mapping are sensitive for the visible and near infrared (NIR) spectral range. The blue range with a wavelength of 420–520 nm is not used by all sensors because of the higher atmosphe-

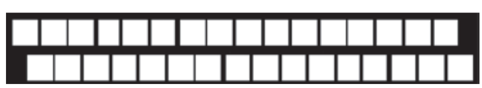

Fig. 3: Staggered CCD-lines.

ric scatter effect, reducing the contrast. In most cases the multispectral information is collected with a larger GSD like the panchromatic. With the so called pan-sharpening, the lower resolution multispectral information can be merged with the higher resolution panchromatic to a higher resolution colour image. This pan-sharpening is using the character of the human eye which is more sensitive to grey values like for colour. A linear relation of 4 between panchromatic and colour GSD is common.

The panchromatic range does not correspond to the original definition – the visible spectral range. Often the blue range is cut of and the NIR is added to the spectral range of approximately 500 to 900 nm.

2.6 *Imaging Problems*

Modern CCD-sensors used in space do have a radiometric resolution up to 11 bit, corresponding to 2048 different grey values. Usually there is not a good distribution of grey values over the whole histogram, so the important part can be optimised for the presentation with the 8 bit grey values of a computer screen. The higher radiometric resolution includes the advantage of an optimal use of the grey values also in extreme cases like bright roofs just beside shadow part. Also for 11 bit-sensors, there are some limits. If the sun light will be reflected by a glass roof directly to the sensor, an oversaturation will occur and the generated electrons will flow to the neighboured CCD-elements and the read-out will be influenced over short time. The oversaturation (Fig. 4) is not causing problems, but the human operator should know about it to avoid a misinterpretation of the objects.

2.7 *Direct Sensor Orientation*

The satellites are equipped with a positioning system like GPS, gyroscopes and star sensors. So without control points the geolocation can be determined. For example IKONOS can determine the imaged positions with a standard deviation of approximately 4m. Often more problems do exist with not well known national datum.

3 Imaging Satellites

Imaging satellites at first have been used for military reconnaissance. So 20 month after the launch of SPUTNIK in October 1957 the US tests with the CORONA system started in 1959. For reconnaissance the USA used film up to 1963 while the Soviet Union and later Russia made the last satellite photo flight in 2000. The historical images have been declassified by the USA in 1995; also Russia is selling now the old images.

For civilian or dual use (use for military and civilian applications) the digital imaging

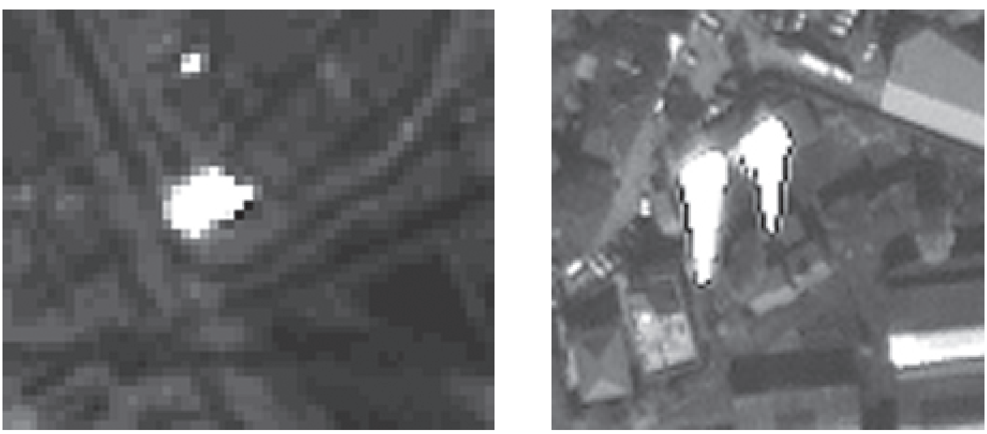

Fig. 4: Oversaturation; left: ASTER, right: IKONOS.

from space started with Landsat 1 in 1972, but the GSD was not sufficient for mapping purposes. This changed with the French SPOT satellite, at first launched in 1986. With the stereoscopic possibilities and 10 m GSD this system was used for the generation and updating of topographic maps up to a scale 1:50 000 but not with the same information contents of traditional maps in this scale. This has been improved with the Indian IRS-1C in 1995 having a GSD of 5.7 m. The next big step came with the very high resolution IKONOS in 1999. Today there is a large variety of imaging sensors in space including not so expensive small satellite systems operated by a growing number of countries.

With the synthetic aperture radar (SAR) imaging radar systems are available which are independent upon the cloud coverage.

Tab. 1: Larger optical space sensors.
MS = multispectral fore = view forward in orbit direction
aft = backward in orbit direction

System	launch	GSD [m] pan/MS	swath [km]	remarks
SPOT 1 France SPOT 2 SPOT 3 SPOT 4	1986 1990 1993 1998	10/20	60	+/−27° across orbit
SPOT 5 France	2002	5/10 2.5 HRS 5*10	60 120	+/−27° staggered 23° fore 23° after
JERS-1 Japan	1992	OPS 18	75	+ SAR
MOMS 02 Germany	1993	4.5/13.5	37/78	nadir + 21.5° fore + 21.5° after
MOMS-2P Germany	1996	6/18	48/100	like MOMS 02
IRS-1C + 1D India	1995 1997	5.7/23	70/142	+/−26° across
IRS P6 India Resourcesat	2003	5.7 MS	23/70	+/−26° across
KOMPSAT-1 South Korea	1999	6.6 pan	17	+/−45° across
CBERS-1 + 2 China + Brazil	1999 2003	20	113	+/−31° across
Terra USA / ASTER Japan	1999	15, 30, 90 all MS	60	nadir + 24° aft
IKONOS-2 USA SpaceImage	1999	0.82/3.24	11	free view direction, TDI
EROS A1 Israel Imagesat	2000	1.8 pan	12.6	free view direction
TES India	2001	1 pan	15	free view direction
QuickBird-2 USA DigitalGlobe	2002	0.62/2.48	17	free view direction, TDI
OrbView-2 USA OrbImage	2003	1/4	8	free view dir., TDI
FORMOSAT-2 Taiwan	2004	2/8	24	free view dir., TDI
IRS-P5 Cartosat-1 India	2005	2.5 pan	30	−5°, +26° in orbit

Because of the speckle and quite different imaging conditions, the SAR images cannot be compared directly with optical images having the same GSD. So up to now only in tropical rainforest areas SAR has been used for the generation of topographic maps but this may change with the coming very high resolution SAR satellites.

Especially in the beginning several space missions failed. So from the 10 launches of CORONA KH-1 only one was successful while for the CORONA KH-4A only 3 of 52 missions failed. The highest ground resolution was possible with panoramic cameras like the CORONA serious without KH-5 and the similar Russian KVR-1000. Also for military reconnaissance a stereoscopic coverage was important, so the most often used CORONA 4-serious was equipped with 2 convergent mounted cameras. The Soviet Union preferred frame cameras for getting the 3rd dimension – they used for example the KVR-1000 in combination with the TK-350.

Space images got a growing market share in photogrammetry. They have been established as a completion and partially as replacement of aerial images. They can be used in remote locations and "no-fly"-zones. In several countries aerial images are classified and a commercialisation is complicate or impossible. Because of the availability of very high resolution space imagery there is no more justification of such a classification, but some governmental organisations like to keep their importance by such restrictions. Space images can be used by private companies for the generation of the different photogrammetric products even if some countries still try to restrict it.

There is a general tendency in the development of high resolution optical space sensors: the resolution is improving and the new systems do have a flexible view direction. By reaction wheels the whole satellites can change the attitudes in a controlled manner very fast and precise enough to generate images also during the rotation. This has advantages against the change of the view direction just across the orbit direction – a stereoscopic coverage can be generated within some seconds, while for the view direction across the orbit, the second image has to be taken from another orbit; that means under optimal conditions at the following day – if this is not possible, problems can be caused for automatic image matching. SPOT Image reacted to this problem with the additional HRS-sensor on SPOT5 viewing with two optics 23° forward and 23° backward, allowing a stereoscopic coverage within approximately 100 seconds. A similar solution is also available for ASTER and Cartosat 1. Based on 3 view directions it has been used by MOMS before.

The very high resolution systems IKONOS, QuickBird, OrbView and EROS A1 are operated by private companies. Without financial support by military contracts they would not survive, so in reality they are belonging to dual use – the use is dominated by military, but the free capacity is commercially available. There are some restrictions – the images from the US companies are not released within 24 hours of its collection and for EROS A1 images the military has the priority of data collection.

The very high resolution systems EROS A1 and TES are not equipped with TDI-sensors, so they have to enlarge the exposure time by continuous change of the view direction (see Fig. 1). This has only a limited influence to the radiometric and geometric image quality, but it is reducing the imaging capacity.

SPOT 5 with the super mode and OrbView are improving the GSD by staggered linear CCDs. An edge analysis of both image types did lead to a GSD identical to nominal resolution. But the analysed images have been edge enhanced like most of the space images and this is leading to too optimistic results.

The access to the images is well organised by commercial companies, but also SPOT Image and India are using a net of commercial distributors. For the FORMOSAT-2 SPOT Image got the exclusive distribution right. The ASTER images are available Web-based for a handling fee over US administration. Also Japan has solved the distribution of the not more active JERS-1 images like Germany for the existing MOMS-images via the DLR. For KOMPSAT and CBERS the distribution is more difficult, but possible.

The required technical knowledge and the access to the required components was limiting the imaging satellites to just few countries, but today the major components and also whole systems can be ordered. So the FORMOSAT-2 satellite has been made by the European EADS ASTRIUM. A similar cooperation exists for the small satellites. The launch is also not a problem – there is a strong competition. Because of the lower price Russia is dominating the launches, followed by the USA, China, Europe, the private Sea Launch and India.

With the reduced size and weight of electronic components, the imaging satellites can be smaller today, leading to small satellites with a weight below 200 kg. These systems are not included in Tab. 1 because of the limited access to the collected images mainly used only by the owning countries. A strong position in this field has the Surrey Satellite Technologies (SSTL), SSTL made the UOSAT12 and a group of satellites belonging to the disaster monitoring constellation (DMC). In the case of natural disasters the DMC satellites are cooperating to generate as fast as possible images from the affected area. The satellite constellation guarantees a daily coverage of the earth by images having the Landsat-ETM bands 2, 3 and 4. SSTL is using off-the-shelf components and so the price for a satellite system including launch and ground station today may be in the range of 10 million US$. The small satellites do have a free view direction. Partially they are equipped with CCD-arrays instead of CCD-line.

Optical images only can be taken under cloud free condition and with sufficient sun light. So all systems listed in Tab. 1 and the

Tab. 2: Announced larger optical space sensors.

System	launch	GSD [m] pan / MS	swath [km]	remarks
IRS Cartosat-2, India	2005	1 pan	10	free view direction
ALOS, Japan	2005	2.5 / 10	35 / 70	−24° nadir +24° in orbit
KOMPSAT 2 South Korea	2005	1 / 4	15	free view direction
Resurs DK1 Russia	2005	1 / 2.5–3.5	28	free view direction
Monitor-E Russia	2005	8 / 20	94 / 160	free view direction
EROS B Israel	2005	0.7 pan	14	free view dir., TDI
EROS C Israel	2009	0.7 / 2.8	11	free view dir., TDI
RazakSat Malaysia	2005	2.5 / 5	20	free view direction, inclin. 7°
CBERS 2B China, Brazil	2005/2006	2.5 / 20		+/−32° across
CBERS-3+4 China, Brazil	2008	5 / 20	60 / 120	+/−32° across
WorldView 1 DigitalGlobe	2006	0.52 /		free view dir., TDI
OrbView 5 OrbImage	2006	0.41 / 1.64	15	free view dir.. TDI
THEOS Thailand	2007	2 / 15		free view dir., TDI
Pleiades 1+2 France	2008/2009	0.7 / 2.8	20	free view dir., TDI
KOMPSAT-3 South Korea	2009	0.7 / 2.8		free view dir., TDI

mentioned small satellites do have sun-synchronous orbits with imaging between 9:30 and 11:00 pm local time – the day time with the best viewing condition. This is different for radar satellites. Radar is an active system, independent upon the sun light. For SAR images the GSD of 10 m and larger, is not sufficient for topographic mapping. So only in tropical rain forest areas SAR-images have been used for this. But in interferometric constellation (InSAR) SAR-image combinations can be used for the generation of height models. So ERS-1 and ERS-1 have been operated for a period of approximately 1 year in the tandem constellation for DEM generation. By the Shuttle Radar Topography Mission (SRTM) a homogenous and qualified DEM covering the earth from 56° southern up to 60.25° northern latitude has been generated.

A higher number of optical satellite systems are announced (Tabs. 2 and 3). The proposed launch time often is delayed and some systems may disappear or the launch may fail. The specification of the systems may change or in some cases they are not fixed or published jet. But today it is not any more so time consuming to assemble qualified reconnaissance satellites, so additional systems may come. There is a general tendency – the GSD is getting smaller, the weight is reducing, TDI will become standard, very high resolution SAR sensors will

Tab. 3: Announced high resolution small optical space sensors.

System	launch	GSD [m] pan/MS	swath [km]	remarks
DMC China	2005	4/32	600	DMC
TopSat UK BNSC	2005	2.5/5	10/15	free view dir., TDI
X-Sat Singapore	2006	10 MS	50	
RapidEye Germany commercial	2007	6.5 MS	78	free view direction, 5 satell.

come and dual use is reducing the expenses and is enabling a commercial use. Nearly all satellites will be equipped with reaction wheels leading to high agility and free view direction. ALOS is designed especially for 3D-mapping based on three cameras having the view in orbit direction for the generation of stereo models with only some second difference in time.

Within the NextView program of the USA contracts have been made with DigitalGlobe and OrbImage for operating satellites with at least 50 cm GSD in the panchromatic range. The GSD for nadir view will be smaller, but the USA is restricting the GSD to at least 50 cm, so the commercial available images will be limited to this. More and more countries are entering the field of commercial very high resolution optical systems. A GSD of at least 1m will be supported by the USA, India, Israel, France, South Korea and Russia. Up to 2.5 m GSD in addition there are Malaysia, China, Brazil, Thailand and the UK. The military systems are not respected here.

Again the small satellites are listed separately because of the often missing distribution systems. Most of the small optical satellites are assembled by SSTL including also Rapid Eye. Rapid Eye will be a system of 5 small satellites, mainly for use by high tech agriculture. It will be the first commercial system outside the area of dual use.

With SAR-X Cosmo-Skymed-1 and Terra SAR-X two radar systems with a GSD of 1m are announced. SAR images with such a resolution can be used for mapping purposes. The information contents of the 1 m SAR-images may be in the range of optical images with 2 m GSD. SAR-images do have the big advantage of being independent upon the cloud coverage – this is important for regions like Germany having only few cloud free days. With RADARSAT-2 and RISAT two systems with a GSD of 3 m will come in addition.

Terra SAR-X will be operated under private public partnership of the German Aerospace Center DLR and EADS ASTRIUM. SAR-X Cosmo-Skymed-1 will be operated by Italy in cooperation with

Tab. 4: Announced SAR space sensors;
ppp = private public partnership.

System	launch	GSD [m]	swath [km]	remarks
SAR-X Cosmo-Skymed-1, Italy	2006	1-several 110th	10-few hundreds	X-band 3.1 cm
RADARSAT-2, Canada	2006	3–100	20–500	C-band 5.6 cm, full polarisation
TerraSAR-X Germany ppp	2006	1/3/16	10/30/100	X-band 3.1 cm
RISAT India	2006	3–50	10–240	C-band
Surveyor SAR, China	2007	10/25	100/250	C-band 5 satellites

France within the dual use ORFEO program. Under this cooperation France will operate two very high resolution optical system Pleiades and Italy four SAR-system.

The Tandem X project is under investigation which shall include a second TerraSAR-X in tandem configuration for the generation of digital elevation models with better than 12 m DEM point spacing and a vertical accuracy of 2 m and better. For the SAR-X Cosmo-Skymed-1 the so called Cartwheel is studied, it could include one active SAR-satellite together with 3 to 4 passive micro satellites for the generation of DEMs with a standard deviation of 1 m.

4 HALE UAV

High altitude long endurance (HALE) unmanned aerial vehicles (UAV) may be in future a completion, on the contrary also a competition to space and aerial images. Up to now UAVs are mainly used for military reconnaissance, but it seems to lead also to civilian application. The Belgian Flemish Institute for Technological Research VITO plans the first test flight of its HALE UAV Pegasus for 2006. The sun powered Pegasus is designed for continuous operation over several month (Biesemann et al. 2005). It shall operate in a height of 20 000 m, over night it will go down to 16 000 m and raise again at the next morning. This altitude is above the aeronautic control, avoiding safety problems. In a partially autonomous flight it can be directed to the area for imaging. It shall carry a digital camera with 4 spectral bands and 12000 pixels having a GSD of 20 cm. This later shall be extended to 10 spectral bands and 30 000 pixels and SAR and LIDAR may be included.

Conclusion

The conditions for mapping with high and very high space images are improved permanently. More and more sensors are entering the field leading to better coverage and the possibility to select the optimal solution. The image data bases are becoming more and more complete, allowing a fast access corresponding to the requirement. The competition between the different distributors has improved the order conditions and partially was leading to reduced prices. On the other hand the high expenses for the large systems cannot be covered by civilian projects. Without dual use the private companies in this field cannot survive. This may change with the raising capacity of small satellites.

Not only the optical images, also SAR has to be taken into account. With the very high resolution of the announced systems, SAR is becoming important for mapping purposes. With InSAR accurate digital surface models can be generated. Only in cities and mountainous areas InSAR and also SAR do have some problems by lay over.

The operation of high resolution satellites is not any more restricted to few countries with advanced technology. More and more components of the shelf can be used and in addition satellites can be ordered from different manufacturers. So in the above listed tables in total 22 countries are mentioned.

With the improving ground sampling distance space images do come into competition with aerial images. Because of classification of aerial photos, in some regions space images became more important than in countries without restrictions. In near future with the HALE UAV there will be a stronger overlap of the applications. Very high resolution space images are not only a supplement or competition to aerial photos; they are also in use for new applications.

References

Baudoin, A., 2004: Beyond SPOT5: Pleiades, Part of the French-Italian Program ORFEO. – ISPRS Istanbul IntArchPhRS, Vol XXXV, B1: 260–267.

Biesemann, J., Everaerts, J. & Lewyckyj, N., 2005: Pegasus: Remoe Sensing from a HALE-UAV, ASPRS annual convention Baltimore, 2005. – on CD.

McDonald (editor), 1997: CORONA Between the Sun & the Earth. – 440 pp., ASPRS, Bethesda, Md, USA.

Internet References

Digital Globe: http://www.digitalglobe.com/

DLR – German Aerospace Center: http://www.dlr.de/

ImageSat Intl.: http://www.imagesatintl.com/

ISRO: http://www.isro.org/index.htm

NASA SpaceWarn Bulletin: http://nssdc.gsfc.nasa.gov/spacewarn/

NSPO: FORMOSAT-2 Spacecraft: http://www.nspo.org.tw/e60/menu0402.html

JAXA EORC: http://www.eorc.jaxa.jp/en/index.html

KARI, Korea Aerospace Research Inst.: http://www.kari.re.kr/

Orbimage: http://www.orbimage.com/

RapidEye: http://www.rapideye.de/

RADARSAT International.: http://www.rsi.ca/

Sovinformsputnik: http://www.sovinformsputnik.com

SpaceImaging: http://www.spaceimaging.com/

SPOT Image: http://www.spotimage.com

SSTL: http://www.sstl.co.uk/

Address of the author:

Dr.-Ing. Karsten Jacobsen
Institut für Photogrammetrie und GeoInformation
Universität Hannover
Nienburger Str. 1, D-30167 Hannover
Tel.: +49 511 762 2485, Fax: +49 511 762 2483
e-mail: jacobsen@ipi.uni-hannover.de

Manuskript eingereicht: Juni 2005
Angenommen: Juli 2005

Photogrammetrie • Fernerkundung • Geoinformation 6/2005, S. 497–510, 6 figs., 2 tabs.

Land Deformation Measurement using SAR Interferometry: State-of-the-Art*

MICHELE CROSETTO, Barcelona, BRUNO CRIPPA, Milano, ERLINDA BIESCAS, ORIOL MONSERRAT, MARTA AGUDO, Barcelona & PAZ FERNANDEZ, Granada

Keywords: remote sensing, satellite, detection, modeling, software

Abstract: In the last fifteen years the differential interferometric SAR, Synthetic Aperture Radar, (DInSAR) techniques have demonstrated their potential as land deformation measurement tools. In the last few years their capability has been considerably improved by using large stacks of SAR images acquired over the same area, instead of the classical two images used in the standard configurations. With these advances the DInSAR techniques are becoming more and more quantitative geodetic tools for deformation monitoring, rather than simple qualitative tools. The goal of the paper is to review the state-of-the-art of the spaceborne DInSAR-based land deformation monitoring. The airborne DInSAR is not considered in this work. The paper begins with a concise description of some basic DInSAR concepts, followed by a discussion of the most important DInSAR applications. Then the state-of-the-art of DInSAR is analysed, by discussing few important technical issues, by addressing the issues of data and software availability, and by describing some relevant DInSAR results.

Zusammenfassung: *Stand der Bestimmung von Oberflächendeformationen mit SAR Interferometrie*. In den letzten fünfzehn Jahren haben die Techniken der differentiellen SAR Interferometrie (DInSAR) ihr Potenzial zur Bestimmung von Oberflächendeformationen gezeigt. In den letzten Jahren haben sich die Möglichkeiten durch die Verwendung einer großer Anzahl von SAR Bildern, die dasselbe Gebiet zeigen, im Gegensatz zu der klassischen Methode, die mit zwei Bildern arbeitet, deutlich verbessert. Durch diese Entwicklungen wird DInSAR zunehmend zu einem geodätischen Werkzeug zur quantitativen, und nicht nur zur qualitativen Deformationsbestimmung. Das Ziel dieses Beitrags ist es, den Stand von DInSAR in Wissenschaft und Technik für die Deformation der Landoberfläche mit weltraumgetragenen Sensoren zu beschreiben. Flugzeuggetragene Sensoren werden in diesem Artikel nicht berücksichtigt. Der Beitrag beginnt mit einer kurzen Beschreibung der Prinzipien von DInSAR, gefolgt von einer Vorstellung der wichtigsten DInSAR Anwendungen. Danach wird der Stand anhand einiger wichtiger technischer Aspekte sowie der Frage der Verfügbarkeit von Daten und Software und durch die Beschreibung einiger relevanter Ergebnisse diskutiert.

* Enhanced version of a paper published in the proceedings of the ISPRS Hannover Workshop 2005 "High Resolution Earth Imaging for Geospatial Information", May 17–20, 2005, Institute of Photogrammetry and GeoInformation, University of Hannover.

1432-8364/05/2005/0497 $ 3.50

1 Introduction

This paper is focused on the land deformation measurement based on the differential interferometric Synthetic Aperture Radar techniques (DInSAR). Its goal is to review the state-of-the-art of the DInSAR techniques that make use of data acquired by spaceborne SAR sensors. The airborne DInSAR, which still plays a minor role in deformation applications, is not considered in this work.

The DInSAR techniques exploit the information contained in the radar phase of at least two complex SAR images acquired in different epochs over the same area, and forming an interferometric pair. Unlike a simple amplitude SAR image, which only contains the amplitude of the SAR signal, a complex SAR image contains two components per pixel, from which the amplitude and phase signal can be derived. The phase is the key observable of all interferometric SAR techniques. The repeated acquisition of images over a given area is usually performed by using the same sensor, e. g. the Envisat ASAR, or sensors with identical system characteristics, as it was the case of ERS-1 and ERS-2. Only in particular cases it is possible to make cross-interferometry by using images acquired with different systems. One example, which is discussed later in this paper, is given by ERS and Envisat ASAR, e. g. see Arnaud et al. (2003). Besides the compatibility of the systems used for the repeat pass DInSAR, the condition of forming interferometric pairs imposes a severe constraint on the acquisition geometry. In order to obtain coherent SAR image pairs, i. e. couples of SAR images whose interferometric phase is useful for digital elevation model (DEM) generation (using interferometric SAR, InSAR, techniques) or deformation monitoring, the images have to share almost the same image geometry. In fact, the image acquisition from different viewpoints in space engenders a loss of coherence, which is called geometric decorrelation (Gatelli et al. 1994). For each SAR system there is a critical perpendicular baseline (the component of the vector that connects the two satellite positions during image acquisition, measured in the direction perpendicular to the SAR line-of-sight) which corresponds to a complete decorrelation of the interferometric phase. For instance, for ERS the critical baseline is about 1100 m: the employed baseline lengths are usually shorter, say of some hundreds of metres. An exception, as discussed in section 4, occurs using the so-called Persistent or Permanent Scatterers techniques that can exploit image pairs with baselines in the interval ± 1200 m (Colesanti et al. 2003a). This is due to the fact that the Persistent Scatterers that are smaller than the resolution cell have good coherence even for interferograms with baselines larger than the critical baseline. Anyways, the constraint on the baseline plays a key role for all DInSAR applications.

In the following, the principle of the DInSAR technique is briefly summarized. A scheme of the image acquisition is shown in Fig. 1, considering a single pixel footprint P:

– The sensor acquires a first SAR image at the time t_0, measuring the phase Φ_M. The

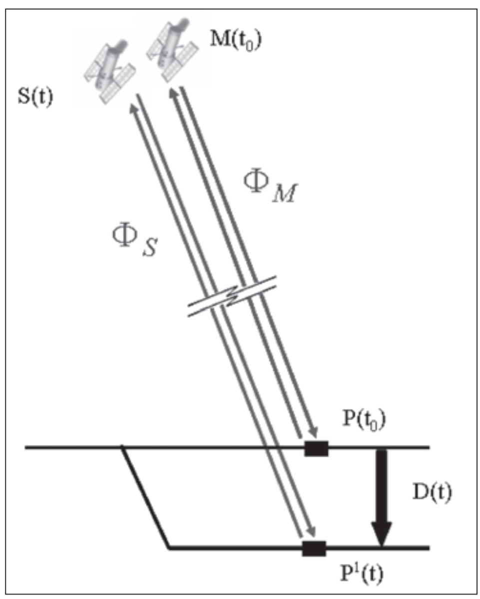

Fig. 1: Principle of DInSAR for deformation measurement.

first satellite and the corresponding image are usually referred as the master, M.

– Assuming that a land deformation D(t) occurs, which has a given evolution in time, the point P moves to P^1.
– The sensor acquires a second image at the time t, measuring the phase Φ_S. The second satellite is usually referred as the slave, S.

The InSAR techniques exploit the phase difference $\Phi_S - \Phi_M$, named interferometric phase $\Delta\Phi_{Int}$. Assuming that D(t) is naught, i. e. the terrain is stable and P^1 coincides with P, this phase is related to the distance difference $SP - MP$, which is the key element for the InSAR DEM generation. When the point moves from P to P^1 between two image acquisitions, besides the topographic phase component Φ_{Topo}, $\Delta\Phi_{Int}$ includes the terrain movement contribution, Φ_{Mov}:

$$\begin{aligned}\Delta\Phi_{Int} &= \Phi_S - \Phi_M \\ &= \frac{SP - MP}{\frac{\lambda}{4\cdot\pi}} + \frac{SP^1 - SP}{\frac{\lambda}{4\cdot\pi}} + \Phi_{Atm} + \Phi_{Noise} \\ &= \Phi_{Topo} + \Phi_{Mov} + \Phi_{Atm} + \Phi_{Noise}\end{aligned}$$

where Φ_{Atm} is the atmospheric contribution; Φ_{Noise} is the phase noise; SP^1 is the slave-to-P^1 distance; and λ is the radar wavelength. As mentioned above, by using the topographic component Φ_{Topo} it is possible to generate a DEM of the observed scene. In the DInSAR techniques the inverse transformation is used: if a DEM of the imaged scene is available, Φ_{Topo} is simulated and subtracted from $\Delta\Phi_{Int}$, obtaining the so-called DInSAR phase $\Delta\Phi_{D-Int}$:

$$\begin{aligned}\Delta\Phi_{D-Int} &= \Delta\Phi_{Int} - \Phi_{Topo\_Sim} = \\ &= \Phi_{Mov} + \Phi_{Atm} + \Phi_{\mathrm{Res}\_Topo} + \Phi_{Noise} \quad (1)\end{aligned}$$

where Φ_{Topo_Sim} is the simulated topographic component, and Φ_{Res_Topo} is the residual component due to errors in the simulation of Φ_{Topo}, e. g. due to errors in the employed DEM. In order to derive information on the terrain movement, Φ_{Mov} has to be separated from the other phase components. The techniques that use an external DEM in order to derive the topographic phase component use the so-called two-pass DInSAR configuration. There is another configuration, the three-pass one, which can work without an a priori known DEM, but which requires at least three images over the same scene (Zebker et al. 1994). For a general review of SAR interferometry, see Rosen et al. (2000) and Bamler & Hartl (1998).

In the following section some of the most important DInSAR applications are discussed. In the remaining part of the paper the state-of-the-art is analysed, by discussing the following topics:

– the number of SAR images used in the DInSAR procedures.
– the criteria used to select the pixels suitable to estimate the land deformation,
– the availability of DInSAR software tools,
– the available DInSAR satellite data,
– the quality and validation of the results.

2 DInSAR applications

Since the first description of the technique, which was based on L-band SEASAT SAR data (Gabriel et al. 1989), the great potential of DInSAR for land deformation applications has been recognized. Of major interest were, in particular, some typical features of the remote sensing systems, like the wide areas covered by the images, the global coverage and the repeat observation capabilities, associated with the intrinsic high metric quality of the DInSAR observations. In fact, since the beginning, it was clear that the spaceborne DInSAR is able to measure small deformations with high sensitivity, which is comparable to a small fraction of the radar wavelengths that are in the order of centimetres to few tens of centimetres. Later on, other important characteristics were recognized. Firstly, the high spatial resolution capability of the SAR systems, which in particular cases allows the deformation monitoring of small features, like buildings or infrastructures, to be performed. Secondly, in the last years another aspect has gained importance: the availability of historical SAR datasets, which in the case of ERS1/2 covers almost 14 years.

In the last fifteen years many deformation-related DInSAR applications have been developed, and the capability of the D-InSAR techniques has been extensively documented. Hundreds of high level journal papers devoted to DInSAR have been published. A great contribution to this success certainly comes from the spectacular results achieved in different fields of geosciences. Some of the most relevant DInSAR application fields are listed below.

Seismology probably represents the field where the major number of scientific achievements have been obtained, including different types of coseismic studies, see e. g. Massonnet et al. (1993); postseismic deformation studies (Peltzer et al. 1996); and the monitoring of aseismic events (Rosen et al. 1998). It is worth emphasising that some of the above applications are characterized by very small deformations, e. g. less than 1 mm/yr for some aseismic and interseismic events. As it is described later in this paper, such deformations can only be achieved by using advanced DInSAR processing and analysis tools.

Vulcanology is another relevant application field, with several studies of volcanic deflation and uplift, e. g. see Amelung et al. (2000). Several examples of DInSAR applications to vulcanology are described in Massonnet & Sigmundsson (2000).
Different researches have been conducted in the field of glaciology, mainly on the ice sheets of Greenland and Antarctica. They included InSAR ice topography measurements (Kwok & Fahnestock 1996), ice velocity measurements (Goldstein et al. 1993), and other glaciological applications.

Landslides is another important application, where less results have been achieved so far, mainly due to the loss of coherence that usually characterises the landslides areas. However, with the Persistent Scatterers techniques for some types of landslide phenomena it seems to be possible to perform deformation measurements, e. g. see Colesanti et al. (2003b), and Hilley et al. (2004).

Ground subsidences and uplifts due to fluid pumping, construction works, geothermal activity, etc. have been described in several papers, see e. g. Amelung et al. (1999); Crosetto et al. (2003). Most of the published results concern urban areas, over which DInSAR data remains coherent over large observation periods. With the advent of the Persistent Scatterers techniques it is expected to get more and more deformation monitoring results outside the urban, suburban and industrial areas.

Finally, comprehensive reviews of different DInSAR geophysical applications are provided by Massonnet & Feigl (1998) and Hanssen (2001). An interesting link, where the latest DInSAR results based on data acquired by the ERS and Envisat satellites are described, is given by eopi.esa.int/esa/esa.

3 DInSAR and advanced DInSAR techniques

A large part of the DInSAR results mentioned above have been achieved by using the standard DInSAR configuration, i. e. by analysing a single differential interferogram derived from a pair of SAR images. This is the simplest DInSAR configuration, which often is the only one that can be implemented, due to the limited SAR data availability. However, as it is discussed later, the standard two-image configuration suffers important limitations. Even if for some types of application it may provide valuable results, e. g. for the estimation of large, say from decimetres to meters, deformation patterns, in general it is necessary to be aware of its limitations. A remarkable improvement in the quality of the DInSAR results is given by the new DInSAR methods that make use of large sets of SAR images acquired over the same deformation phenomenon. These techniques, hereafter called Advanced DInSAR (A-DInSAR) techniques, represent an outstanding advance with respect to the standard ones, both in terms of deformation modelling capabilities and quality of the deformation estimations.

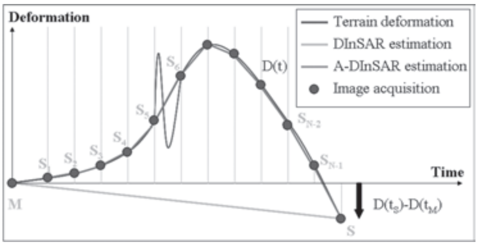

Fig. 2: Temporal sampling of a deformation phenomenon performed with the DInSAR and A-DInSAR techniques.

Temporal deformation modeling. As it is illustrated in Fig. 2, a standard DInSAR technique, which samples temporally a given deformation phenomenon with only two samples, a master image M and a slave one S, is only able to estimate the integrated deformation:

$$D_I(\Delta T) = D(t_S) - D(t_M),$$

or, equivalently, the linear deformation velocity between t_M and t_S. In contrast, the A-DInSAR techniques are in principle able of providing a whole description of the temporal behaviour of the deformation field at hand. This capability is clearly limited by the number N and the temporal distribution of the available SAR images. For instance, the highly non linear deformation that occurs between the acquisitions S_5 and S_6 in the example of Fig. 2 cannot be measured with the available SAR image acquisitions.

Quantitative vs. qualitative DInSAR. There is a second fundamental difference between DInSAR and A-DInSAR techniques. The standard configuration represents a zero-redundancy case, where it is not possible to check the presence of the different error sources that may affect the interferometric observations, or, equivalently, it is impossible to separate the movement component from the other phase components, see formula 1. For this reason the estimations derived with this configuration have, in general, a qualitative character and have to be employed with care. Note that in different applications some external information on the deformation under analysis may be available (e. g. a priori knowledge of stable areas, of the shape of the deformation field, etc.), which can considerably help in interpreting the DInSAR results. In contrast, the A-DInSAR methods may implement suitable data modelling and analysis procedures that associated with appropriate statistical treatments of the available DInSAR observations make possible the estimation of different parameters. The main parameters estimated by the DInSAR are briefly discussed below. In addition to this extended capability, the A-DInSAR techniques take usually advantage of a high data redundancy, which allows quantitative DInSAR results to be achieved, both in terms of precision and reliability.

1) By proper modelling the phase component due to terrain movement Φ_{Mov}, it is possible to estimate the spatial and temporal evolution of the deformation. The modelling strategies are strictly dependent on the type of application at hand. Anyway, the ability to fully describe a deformation phenomenon depends temporally on the number of available images, and spatially on the availability of "good pixels", i. e. pixels which are characterized by a low level of phase noise, Φ_{Noise}. This aspect is discussed in the following section. Often the temporal evolution of the deformation is modelled with linear functions, e. g. see (Ferretti et al. 2000, Ferretti et al. 2001). Crosetto et al. (2005) model the deformation by stepwise linear functions, whose parameters are computed by least squares adjustment. Other approaches allow a more complex description of the temporal behaviour of the deformation, see e. g. Lanari et al. (2004).

The complete estimation of the temporal evolution of deformation represents a remarkable improvement of the A-DInSAR techniques with respect to the standard DInSAR results. Fig. 3 shows an example which concerns the roof of an industrial building located in the metropolitan area of Barcelona. This result was obtained in the frame of an ESA funded Project named "Develop-

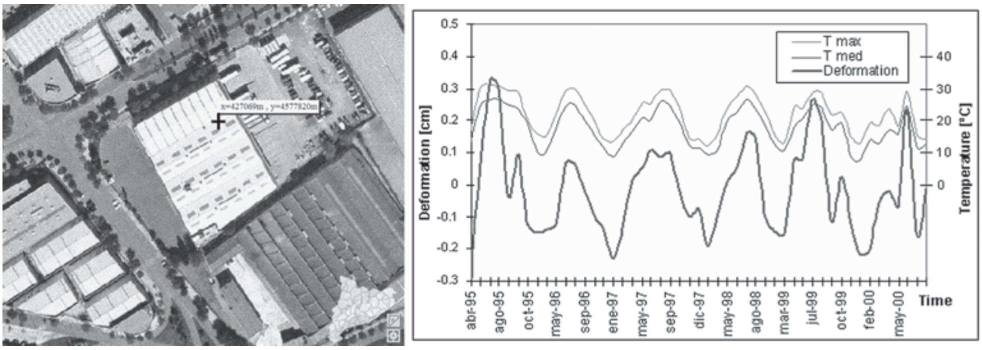

Fig. 3: Estimation of the temporal evolution of deformation of the roof of an industrial building located in the area of Barcelona. Input data: 49 ERS images that cover the period 1995 to 2001. The deformation is probably due to thermal dilation of the portion of the observed roof. Data courtesy of Altamira Information.

ment of algorithms for the exploitation of ERS-Envisat using the SAR permanent scatterers technique", coordinated by Altamira Information (www.altamira-information.com), one of the few commercial companies worldwide that has A-DInSAR capabilities. This result was validated at the Institute of Geomatics. In this case 49, ERS-1 and ERS-2 images were used, which cover the period 1995 to 2001. One may appreciate the highly non-linear behaviour of deformation. The deformation pattern shows a high correlation coefficient (0.84) with the time series of temperatures of Barcelona in the acquisition days of the 49 images. This indicates that the deformation is probably due to thermal dilation of the portion of the observed roof. It is worth noting the magnitude of the deformation oscillation, which ranges in the interval ± 3 mm: this result is useful to get an idea of the sensitivity of the A-DInSAR outcomes.

2) The residual topographic error e_{Topo} represents another interesting type of parameter that can be estimated by the A-DInSAR techniques. e_{Topo} is given by the difference between the true height of the scattering phase centre of a given pixel, and the height given by the employed DEM or digital terrain model (DTM). The information on this parameter is contained in the component Φ_{Res_Topo}, which depends linearly on the residual topographic error (Ferretti et al. 2000) with a magnitude, on a given interferogram, which is modulated by its perpendicular baseline $B_{\perp}$. Therefore, given a set of interferograms, the wider is the spectrum of $B_{\perp}$, the better is the configuration to estimate e_{Topo}. This parameter plays an important role only for two specific goals: for A-DInSAR modelling purposes, and for geocoding purposes. As said above, Φ_{Res_Topo} can be explicitly modelled, i. e. can be explained by estimating one parameter e_{Topo} per each pixel. If this parameter is disregarded, Φ_{Res_Topo} will contribute to the non modelled part of $\Delta\Phi_{Int}$, i. e. it will partially affect the estimation of other parameters of interest. Therefore, the estimation of e_{Topo} results in a net benefit for modelling. The second important use of e_{Topo} is the implementation of advanced geocoding procedures for the A-DInSAR products. The standard methods simply employ the same DEM or DTM used in the simulation of Φ_{Topo_Sim} to geocode the DInSAR products. That is, they use an (often rough) approximate value of the true height of the scattering phase centre of a given pixel, which results in a location error in the geocoding. By using the estimated e_{Topo} this kind of error can be largely reduced, thus achieving a more precise geocoding: this may considerably help the interpreta-

Fig. 4: Advanced geocoding of A-DInSAR results over the San Paolo Stadium of Naples (Italy). Pixel location without (left) and with (right) the correction based on the residual topographic error. An optical image of the area is on the background. This result was achieved by using an A-DInSAR technique described in LANARI et al., (2004), with 55 ERS images. (Images courtesy of Dr. RICCARDO LANARI from IRECE-CNR, Naples, Italy).

tion and the exploitation of the A-DInSAR results. An example of advanced geocoding is shown in Fig. 4. It concerns the area of the Stadium of Naples (Italy). The left image shows the location of the measured DInSAR pixels achieved with a standard DEM-based geocoding, while the right image shows a precise location, which was computed by using e_{Topo}, see for details LANARI et al. (2004).

The formal precision that can be achieved in the estimation of e_{Topo} is a function of the distribution of the $B_{\perp}$. Using large baselines, which range in the interval $\pm$ 1200 m, COLESANTI et al. (2003a) achieve a standard deviation of the estimated e_{Topo} that is less than 1 m. Despite the importance of the above uses of e_{Topo}, it is important to note that this parameter describes a rather specific feature, i. e. the height of the radar scattering phase centre, which depends on several factors that drive the dominant mechanism of scattering, e. g. orientation, size, shape, density and dielectric constant. This means that e_{Topo} cannot in general be used to improve the quality of the DEM used in the A-DInSAR procedure. It can only be used to derive a kind of improved "radar DEM". Furthermore, it is worth noting that e_{Topo} is only estimated over the "good pixels" exploited by the A-DInSAR procedures.

3) The A-DInSAR techniques can estimate the atmospheric phase contribution of each image of the used SAR stack (this contribution is sometimes called Atmospheric Phase Screen, APS), starting from the phase component Φ_{Atm} of the interferograms. Even if this information is usually useless for other applications, it is fundamental to achieve an accurate DInSAR modelling and thus to properly estimate the deformation contribution. In fact, only if APS contributions are properly estimated and removed it is possible to avoid the strong degradation of the DInSAR quality caused by the atmospheric effects. The A-DInSAR strategies used to estimate the APS contributions usually exploit the spatio-temporal correlation characteristics of the APSs, i. e. that the atmospheric effects are usually uncorrelated in time, while they are spatially smooth, e. g. see FERRETTI et al. (2000).

4 Pixel selection: coherence vs. persistent scatterers

Even if SAR sensors perform a regular 2D sampling of the terrain, only the pixels characterized by a low level of Φ_{Noise} are exploited to derive the deformation estimations. This requires adopting a pixel selection criterion. As mentioned above, the loss of coherence results in a noisy interferometric phase. During the interferometric process it is possible to estimate, for each interferogram, the coherence (i. e. the correlation) of the two images that form the given interferogram. The standard DInSAR techniques use this information for the pixel selection, i. e. they perform a coherence-based pixel selection. Note that the same criterion is used by some A-DInSAR techniques (Lanari et al. 2004, Crosetto et al. 2005). Another important class of A-DInSAR techniques use as a pixel selection criterion the stability of the SAR amplitude (Ferretti et al. 2000). The points selected with such a criterion are usually referred to as Permanent or Persistent Scatterers (PS).

The choice of the selection criterion depends on the application at hand. The coherence-based A-DInSAR methods work well over long-term coherent areas: urban, suburban and industrial areas. Their major limitation is that most spaceborne sensors are operated in C-band, see Tab. 2, a frequency in which decorrelation effects are strong in particular over vegetated areas. Furthermore, the repeat cycles of these satellites are rather long: this causes a loss in coherence, and usually prevents the generation of deformation results outside the urban areas. Fig. 5 shows a result derived with a coherence-based A-DInSAR technique. The deformation velocity field is superposed to a SAR amplitude image of the same area. In this case 13 ERS images have been used. In this case different unknown subsidence phenomena have been discovered: this example shows the potential of DInSAR as an "early detection tool" of deformations. Fig. 6 shows a zoom of Fig. 5 over an industrial area. In this second image the geocoded deformation velocities are superposed to an orthoimage. One may notice in Figs. 5 and

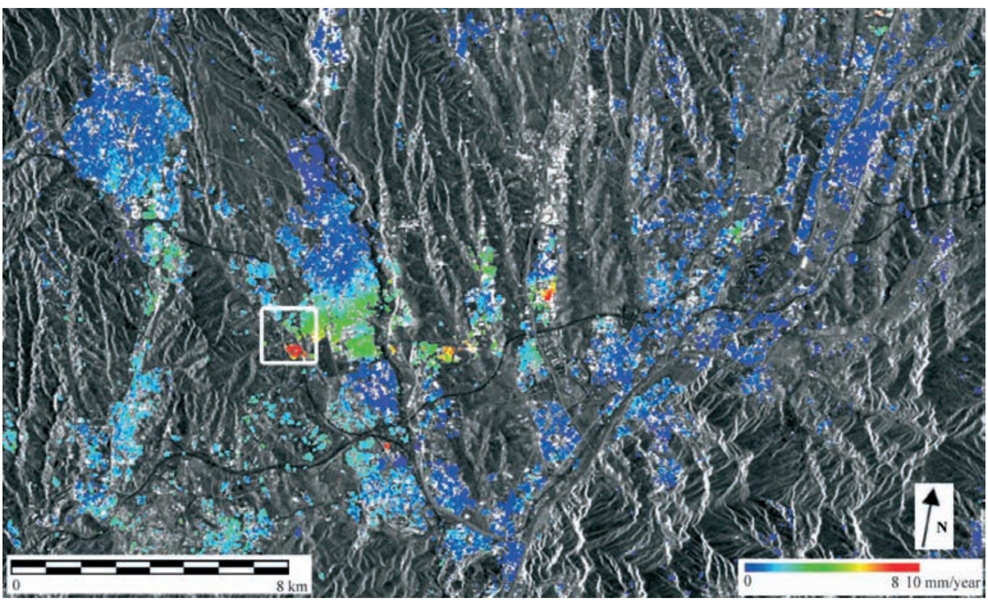

Fig. 5: Coherence-based A-DInSAR analysis over an area of 28 km × 12 km, using 13 ERS images: vertical deformation velocity in the period June 1995 and August 2000. The velocity, in colour, is superposed to a SAR amplitude image of the same area. The areas in grey values are those where no velocity estimation is possible due to coherence loss.

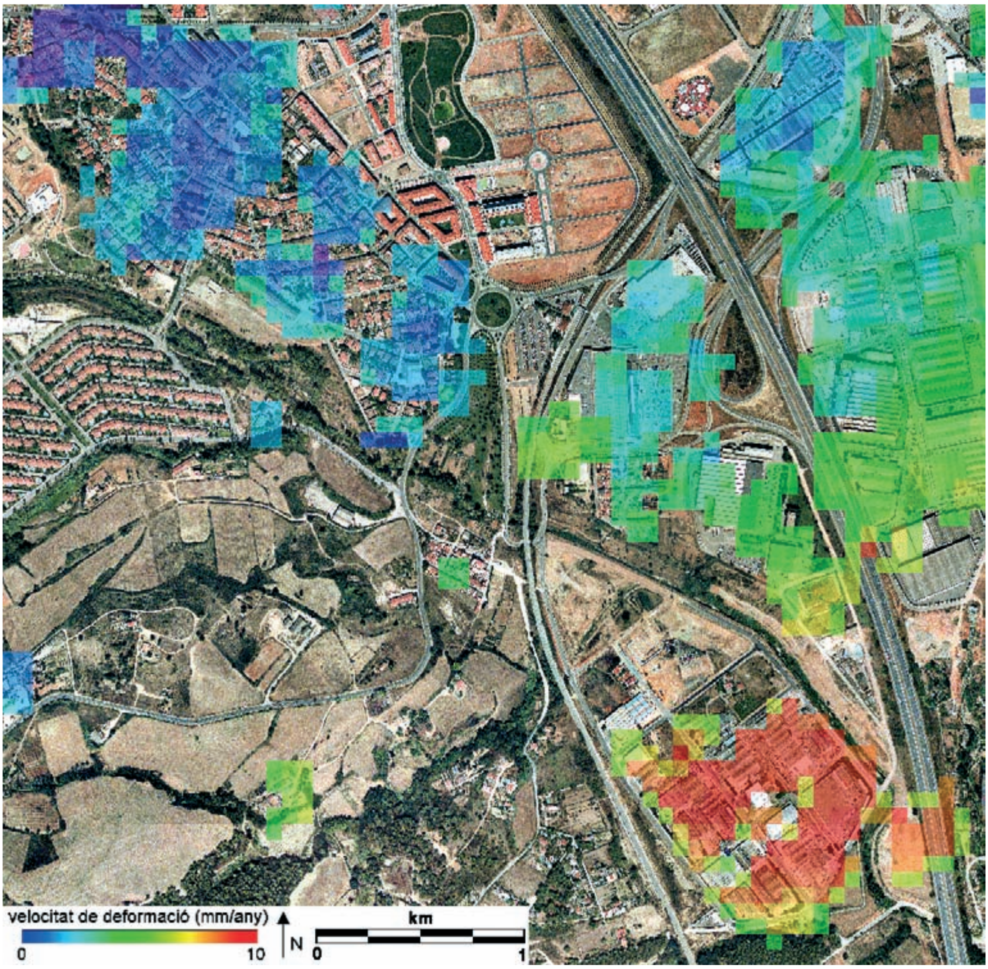

Fig. 6: A-DInSAR analysis over an industrial area, whose location is shown by a white frame in Fig. 5. The vertical deformation velocity field is superposed to a 1:5000 orthoimage of the Cartographic Institute of Catalonia.

6 that over a large part of the analyzed area the deformation cannot be measured, due to a lack of coherence. This result could be probably improved by using PS-based techniques, whose main advantage is to potentially exploit all the coherent targets of the covered scene, even those that are isolated. In fact, the coherence of a given pixel is estimated over a window centred on the same pixel: if a single and very coherent target (e. g. a small man-made object) is located in a very noisy area (e. g. a grass field) it will probably have a low coherence value. This does not occur with the PS techniques, which work at full resolution and which select the pixels without considering the neighbourhood pixels.

5 Available softwares

The importance that DInSAR is gaining as a deformation monitoring tool is reflected in the number of available softwares with DInSAR analysis capabilities. Some of them are listed in Tab. 1. Note that this list is not exhaustive and, more importantly,

Tab. 1: Available software with standard DInSAR or advanced DInSAR capabilities.

Software name	Company/ University	Web site/ type of licence	Platform and software characteristic	DInSAR capabilities
Doris	TU Delft	enterprise.lr.tu-delft.nl/doris free license for non-commercial purposes	Unix/Linux/ WinXP (C++ source code available)	Standard DInSAR with ERS1/2, RADARSAT, ENVISAT, JERS. Additional programs for unwrapping (Snaphu) and orbit processing (Getorb) available
Roi_pac	Berkley University	www.openchannel-foundation.org free license for non-commercial purposes	Unix/Linux (C and F90 source code available)	Standard DInSAR with ERS1/2, JERS
Diapason	Developed by CNES	www.altamira-information.com commercial licence distributed by Altamira Information	Linux/Win 95, 98, NT, 2000	Standard DInSAR with ERS1/2, JERS-1, RADARSAT, ENVISAT
Envi	Research Systems Inc. (RSI)	www.rsinc.com/ envi commercial licence	Unix/Linux/ Win2000 and WinXP	Module of ENVI, SARscape, standard DInSAR with ERS1/2, JERS-1, RADARSAT, ENVISAT
Vexcel 3DSAR	Vexcel Corp.	www.vexcel.com commercial licence	Unix/Linux/Windows	Module of the EV-InSAR, CTM – Coherent Target Monitoring, with advanced DInSAR capabilities with ERS1/2, JERS-1, RADARSAT, ENVISAT
Gamma	Gamma	www.gamma-rs.ch/ commercial licence	UNIX, Linux, Win Modular packages in C code available	Advanced DInSAR with ERS1/2, JERS-1, SIR-C, X-SAR, RADARSAT, ENVISAT

that the reported information comes from publicly available documentation: these softwares have not been tested by the authors. The table does not include the software tools developed by research centres that are not commercialized or freely distributed for non-commercial purposes. Moreover, it does not include the tools developed by those private companies that do not commercialise their software. This, for instance, is the case of TRE, based in Milan, and Altamira Information, located in Barcelona.

The first two softwares listed in Tab. 1 are freely available for non-commercial purposes: DORIS, see a description in Kampes et al. (2003), and ROI—PAC. Both of them have the source code available. The DIAPASON is a command line software developed by a research group at the French CNES, which is suitable for advanced users. Some remote sensing software tools include specific modules for standard DInSAR analysis, i. e. the analysis based on single interferograms. This is the case of ENVI, while other packages e. g. ERDAS, seem to provide only tools for InSAR analysis. Example of A-DInSAR commercial tools are those sold by Vexcel and Gamma. This last company, which is based in Switzerland, besides selling its products, provides A-DInSAR analysis services.

6 Data availability

The availability of data acquired by spaceborne sensors represents a key issue for the successful use of DInSAR and especially A-DInSAR techniques that require large series of SAR images. Furthermore, for these techniques plays a fundamental role the image acquisition continuity over large time periods of the same sensor, or compatible sensors, e. g. ERS-1 and ERS-2. The continuity is needed in particular for all the applications characterized by small deformation rates, for those that require long-term deformation monitoring, and in general for the acceptation of the A-DInSAR techniques as operational land deformation monitoring tools. In Tab. 2 the principal SAR missions and satellites that have demonstrated DInSAR capabilities are reported. For each satellite are given at least two references to studies realized with its data. Besides the Seasat mission, which gave the data used to derive the first DInSAR results (Gabriel et al. 1989) but which however had a very short life, the satellite which has provided the data to fully demonstrate the DInSAR potentiality was ERS-1. This satellite has been operative for 10 years, and, more importantly, with its exact copy, ERS-2, has provided a valuable historical archive of interferometric SAR data, which has global spatial coverage and covers a time period of almost 14 years, with the first images that date back to summer 1991. Besides the four references given in the table, there are hundreds of high level scientific publications that demonstrate the success of the ERS mission.

The satellites that are currently operational are RADARSAT-1 and ENVISAT. Various space agencies are planning new missions for earth observation with microwave SAR sensors, e. g. RADARSAT-2 a mission of the Canadian Space Agency in cooperation with other partners; TERRASAR-X of the German Aerospace Centre; COSMO-SKYMED (Constellation of Small Satellites for Mediterranean basin observation) of the Italian Space Agency; and MAPSAR, a joint Brazilian-German project which is expected to have high spatial resolution L-band capabilities for polarimetry, and interferometry, see Schroeder et al. (2005). A special mention is reserved by the continuity issue between the ERS and Envisat missions of the European Space Agency. It would be very useful to guarantee in the near future the continu-

Tab. 2: Main SAR missions with interferometric SAR capabilities.

Satellite	Frequency [GHz]	Start mission	End mission	Wavelength [cm]	DInSAR works based on these data
SEASAT	1.275	1978	1978	23.5	Gabriel, A. K et al. (1989), Li and Goldstein (1990)
ERS-1	5.300	1991	2000	5.6	Massonnet D. et al. (1993), Goldstein et al. (1993)
ERS-2	5.300	1995	–	5.6	Ferretti A. et al. (2000), Rosen P.A. et al. (2000)
JERS-1	1.275	1992	1998	23.5	Kimura and Yamaguchi (2000), Fujiwara et al. (1998)
RADARSAT-1	5.300	1995	–	5.6	Wegmüller et al. (2000a), Lu et al. (2003)
ENVISAT	5.331	2002	–	5.6	Wegmüller et al. (2000b), Arnaud et al. (2003)
RADARSAT-2	5.300	*2006*	–	5.6	–

ity of the existing 14 year archive of interferometric SAR images. There is a temporal overlap between the ERS-2 and Envisat missions: this new instrument could in principle continue the success of the ERS satellites and increase the value of the archived ERS data. In reality, there is a big problem in mixing Envisat and ERS data: the two systems have slightly different radar frequencies, and this prevents the simple combination of their data (the interferometric phase is strongly dependent on the wavelength, and thus on the radar frequency).

In the last two years a big effort has been devoted to this topic, e. g. see ARNAUD et al. (2003) which describe the generation of the first ERS-Envisat cross-interferogram. Without going into details, it is worth mentioning that combining ERS and Envisat data for A-DInSAR applications, i. e. using mixed image stacks of ERS and Envisat, under given conditions is possible, see some interesting results in DURO et al. (2005). In particular, this is possible by taking advantage of a special feature of the PS: they usually are much smaller than the resolution cell, and thus have a reduced geometric decorrelation due to the fact that the two SAR images are not acquired exactly from the same point.

7 DInSAR quality and validation issues

An important goal of the current A-DInSAR research is to provide deformation observations characterized by high quality standards (accuracy, precision and reliability), which are comparable with those of the observations coming from the geodetic techniques. As mentioned in previous sections, the above goal can only be achieved using a high observation redundancy (i. e. by using several SAR images of the same area), and by implementing appropriate data analysis tools. In the last few years there has been an increasing attention to the A-DInSAR estimation quality, e. g. see COLESANTI et al. (2003a), which provide a comprehensive error budget analysis of the Permanent Scatterers technique. Another topic that is receiving particular attention is the validation of the A-DInSAR results, e. g. see DURO et al. (2005). In general, the validation is difficult, especially for the extension of the measured areas: often there are no reference data are available. An additional complication comes from the relatively high quality of the A-DInSAR and the consequent difficulty to get suitable reference data of higher quality.

8 Conclusions

In this paper the state-of-the-art of DInSAR techniques for land deformation monitoring has been analysed, discussing in particular:

- the main differences between the standard DInSAR techniques, which are based on a single SAR image pair, and the advanced DInSAR techniques, which exploit large sets of images acquired over the same area,
- the importance of the criteria used to select the pixels suitable to deformation measurement,
- the availability of DInSAR software tools, and of data coming from spaceborne SAR sensors,
- and finally some aspects related to the quality and validation of the DInSAR results.

Different other important topics are not considered in this paper, e. g. an analysis of the limitation of the techniques, the discussion of key technical aspects, such as the phase unwrapping, and the possible synergy with data coming from other sources, etc. This aspects are treated in detail in more comprehensive DInSAR reviews, see ROSEN et al. (2000), BAMLER & HARTL (1998), and HANSSEN (2001).

Acknowledgements

This work has been partially supported by the Spanish Ministry of Science and Technology, through the research project REN2003-00742, AURORAE. The authors acknowledge ALAIN ARNAUD and JAVIER DURO from Altamira Information for providing their A-DInSAR results over the city of Barcelona, and Riccardo Lanari from IRECE-CNR, Naples, for providing the advanced geocoding results over the San Paolo Stadium of Naples.

References

Amelung, F., Galloway, D.L., Bell, J.W. et al., 1999: Sensing the ups and downs of Las Vegas: InSAR reveals structural control of land subsidence and aquifer-system deformation. – Geology **27**(6): 483–486.

Amelung, F., Jonson, S., Zebker, H.A. & Segall, P., 2000: Widespread uplift and 'trapdoor' faulting on Galápagos volcanoes observed with radar interferometry. – Nature **407:** 993–996.

Arnaud, A., Adam, N., Hanssen, R. et al., 2003: ASAR ERS interferometric phase continuity. – IGARSS, 21–25 July 2003, Toulouse (France), (CDROM).

Bamler, R. & Hartl, P., 1998: Synthetic aperture radar interferometry. – Inverse Probl. **14:** R1–R54.

Colesanti, C., Ferretti, A., Novali et al., 2003a: SAR monitoring of progressive and seasonal ground deformation using the Permanent Scatterers Technique. – IEEE T Geosci. Remote **41**(7): 1685–1701.

Colesanti, C., Ferretti, A., Prati, C. & Rocca, F., 2003b: Monitoring landslides and tectonic motions with the Permanent Scatterers Technique. – Eng. Geol. **68:** 3–14.

Crosetto, M., Castillo, M. & Arbiol, R., 2003: Urban subsidence monitoring using radar interferometry: Algorithms and validation. – Photogr. Eng. Rem. S. **69**(7): 775–783.

Crosetto, M., Crippa, B. & Biescas, E., 2005: Early detection and in-depth analysis of deformation phenomena by radar interferometry. – Eng. Geol. **79** (1-2): 81–91.

Duro, J., Closa, J., Biescas, E. et al., 2005: High Resolution Differential Interferometry using time series of ERS and ENVISAT SAR data. – Proc. of the 6th. Geomatic Week, February 2005, Barcelona, Spain (CDROM).

Ferretti, A., Prati, C. & Rocca, F., 2000: Nonlinear subsidence rate estimation using permanent scatterers in differential SAR interferometry. – IEEE T Geosci. Remote **38**(5): 2202–2212.

Ferretti, A., Prati, C. & Rocca, F., 2001: Permanent scatterers in SAR interferometry. – IEEE T Geosci. Remote **39** (1): 8–20.

Fujiwara, S., Rosen, P., Tobita, M. & Murakami, M., 1998: Crustal deformation measurements using repeat-pass JERS-1 synthetic aperture radar interferometry near Izu Peninsula. – Japan. J. Geophys. Res. **103:** 2411–2424.

Gabriel, A.K., Goldstein, R.M. & Zebker, H.A., 1989: Mapping small elevation changes over large areas: differential radar interferometry. – J. Geophys. Res. **94** (B7): 9183–9191.

Gatelli, F., Monti Guarnieri, A., Parizzi, F., et al., 1994: The Wavenumber Shift in SAR Interferometry. – IEEE T Geosci. Remote **32**(4): 855–865.

Goldstein, R.M., Englehardt, H., Kamb, B. & Frolich, R.M., 1993: Satellite radar interferometry for monitoring ice sheet motion: application to an Antarctic ice stream. – Science **262:** 1525–1530.

Hanssen, R., 2001: Radar interferometry. – Kluwer Academic Publishers, Dordrecht (The Netherlands).

Hilley, G.E., Bürgmann, R., Ferretti, A. et al., 2004: Dynamics of Slow-Moving Landslides from Permanent Scatterer Analysis. – Science **304:** 1952–1955.

Kampes, B.M., Hanssen, R.F. & Perski, Z., 2003: Radar Interferometry with public Domain Tools. – Proc. of Fringe 2003, SP-550, ESA (CD-ROM).

Kimura, H. & Yamaguchi, Y., 2000: Detection of landslide areas using satellite radar interferometry. – Photogramm. Eng. Rem. S. **66**(3): 337–344.

Kwok, R. & Fahnestock, M.A., 1996: Ice sheet motion and topography from radar interferometry. – IEEE T Geosci. Remote **34**(1): 189–200.

Lanari, R., Mora, O., Manunta, et al., 2004: A small-baseline approach for investigating deformations on full-resolution differential SAR interferograms. – IEEE T Geosci. Remote **42** (7): 1377–1386.

Li, F. & Goldstein, R.M., 1990: Studies of multibaseline spaceborne interferometric synthetic aperture radars. IEEE T Geosci. Remote **28**(1): 88–97.

Lu, Z., Wright, T. & Wicks, C., 2003: Deformation of the 2002 Denali Fault Earthquakes, Mapped by Radarsat-1 Interferometry. – EOS **84**(41):. 430–431.

Massonnet, D., Rossi, M., Carmona, C. et al., 1993: The displacement field of the Landers earthquake mapped by radar interferometry. – Nature **364:** 138–142.

MASSONNET, D. & FEIGL, K. L., 1998: Radar interferometry and its application to changes in the earth's surface. – Reviews of Geophysics **36** (4): 441–500.

MASSONNET, D. & SIGMUNDSSON, F., 2000: Remote sensing of volcano deformation by radar interferometry from various satellites. – In: MOUGINIS-MARK et al. (eds.): Remote sensing of active volcanism. – Geophysical Monographs 116, American Geophysical Union, pp. 207–221.

PELTZER, G., ROSEN, P., ROGEZ, F. & HUDNUT, K, 1996: Postseismic rebound in fault stepovers caused by pore fluid flow. – Science **273:** 1202–1204.

ROSEN, P., WERNER, C., FIELDING, E. et al., 1998: Aseismic creep along the San Andreas fault northwest of Parkfield, CA measured by radar interferometry. – Geophys. Res. Lett. **25**(6): 825–828.

ROSEN, P.A., HENSLEY, S., JOUGHIN et al., 2000: Synthetic Aperture Radar Interferometry. – Proc. of the IEEE **88**(3): 333–382.

SCHROEDER, R., PULS, J., HAJNSEK, I. et al., 2005: MAPSAR: a small L-band SAR mission for land observation. – Acta Astronautica **56**(1-2): 35–43.

WEGMULLER, U., STROZZI, T. & TOSI, L., 2000a: Differential SAR interferometry for land subsidence monitoring: methodology and examples. – Proc. SISOLS 2000, 25–29 September 2000, Ravenna (Italy).

WEGMÜLLER, U., STROZZI, T. & TOSI, L., 2000b: ERS and ENVISAT differential SAR interferometry for subsidence monitoring. – Proc. ERS-ENVISAT Symposium, 16–20 October 2000, Gothenburg (Sweden).

ZEBKER, H.A., ROSEN, P.A., GOLDSTEIN, R.M. et al., 1994: On the derivation of coseismic displacement fields using differential radar interferometry: The Landers Earthquake. – J. Geophys. Res. **99** (B10): 19617–19634.

Addresses of the authors:

Dr. MICHELE CROSETTO
e-mail: michele.crosetto@ideg.es
Ms. ERLINDA BIESCAS
e-mail: erlinda.biescas@ideg.es
Mr. ORIOL MONSERRAT
e-mail: oriol.monserrat@ideg.es
Ms. MARTA AGUDO
e-mail: marta.agudo@ideg.es
Institute of Geomatics, Parc Mediterrani de la Tecnologia, Av. del Canal Olímpic, s/n, Castelldefels (Barcelona), E-08860, Spain
Tel.: +34-93-5569294, Fax: +34-93-5569292

Prof. Dr. BRUNO CRIPPA
e-mail: bruno.crippa@unimi.it
Department of Earth Sciences, University of Milan, Via Cicognara 7, I-20129 Milan, Italy
Tel: +39-02-50318474, Fax: +39-02-50318489

Ms. PAZ FERNÁNDEZ
e-mail: pazferol@ugr.es
Departamento de Ingeniería Civil, Universidad de Granada, ESCCP, Edificio Politécnico, Campus de Fuentenueva s/n, E-18071, Granada, Spain
Tel: +34-958-240486, Fax: +34-958-246138

Manuskript eingereicht: Juni 2005
Angenommen: Juli 2005

Photogrammetrie • Fernerkundung • Geoinformation 6/2005, S. 511–522, 8 figs., 1 tab.

Digital Building Map Refinement from Knowledge-driven active Contours and very High Resolution Optical Imagery*

TIMOTHÉE BAILLOEUL, VÉRONIQUE PRINET, BRUNO SERRA, PHILIPPE MARTHON, PINXIANG CHEN & HAITAO ZHANG

Keywords: photogrammetry, satellite optical imagery, Quickbird, building, accuracy, active contours, GIS, DSM, fusion.

Abstract: We propose a novel approach for digital building map refinement based on the use of knowledge-driven active contours and very high resolution panchromatic optical imagery. This methodology is designed to finely match each building symbolized in an urban Geographical Information System (GIS) database onto its counterpart representation in remote sensing data. This method is GIS map-driven: GIS data globally registered to the image allows to initialize an active contour near the target building in the image to achieve subsequent refinement. Moreover the digital map provides valuable shape information about the object in the image we aim at matching. This geometric and specific prior knowledge is embedded as a shape constraint into the active contour and enables to overcome urban artifacts issues. Besides, we propose to embed a coarse Digital Surface Model (DSM) as well as a spatio-temporal shape prior constraint within the active contour model. Experimental results carried out over Beijing city area and illustrated in this paper show how these latter contributions improve the robustness and speed of the map refinement process. Map refinement addressed in this paper is becoming an essential issue for urban planning, telecommunications, automobile navigation, crisis and pollution management, which all rely on up-to-date and precise digital maps of a city.

Zusammenfassung: *Verfeinerung digitaler Gebäudedaten aus hoch aufgelösten optischen Satellitendaten durch wissensbasiert gesteuerte aktive Konturen.* In diesem Beitrag wird ein neuer Ansatz zur Verfeinerung digitaler Gebäudedaten aus hoch aufgelösten panchromatischen Satellitendaten mithilfe wissensbasiert gesteuerter aktiver Konturen vorgeschlagen. Die Methode ermöglicht eine genaue Zuordnung eines Gebäudes einer GIS Datenbank zu der entsprechenden Repräsentation im Fernerkundungsbild. Die Methode geht von den GIS-Daten aus: global zu den Bildern zugeordnete GIS-Daten erlauben die Initialisierung einer aktiven Kontur in der Nähe des korrespondierenden Gebäudes als Startwert für die Verfeinerung. Daneben bieten die GIS-Daten wertvolle Forminformation für die zuzuordnenden Objekte. Diese Vorinformation wird als zusätzliche Bedingung für die aktive Kontur formuliert und ermöglicht es, Probleme zu lösen, die speziell in städtischen Gebieten entstehen. Daneben wird vorgeschlagen, auch Bedingungen für ein DGM und eine raumzeitliche Komponente in das Konturmodell aufzunehmen. Tests mit Bildern aus Beijing zeigen, wie die zuletzt genannten Verbesserungen die Zuverlässigkeit und die Geschwindigkeit der Gebäudedatenverfeinerung verbessern. Die in diesem Beitrag beschriebene GIS-Datenverfeinerung stellt sich zunehmend als eine wichtige Thematik für Stadtplanung, Telekommunikation, Fahrzeugnavigation, Management von Krisen und Luftverschmutzung heraus, die allesamt auf aktuelle und geometrisch genaue Daten angewiesen sind.

* Enhanced version of a paper published in the proceedings of the ISPRS Hannover Workshop 2005 "High Resolution Earth Imaging for Geospatial Information", May 17–20, 2005, Institute of Photogrammetry and GeoInformation, University of Hannover.

1432-8364/05/2005/0511 $ 3.00

1 Introduction

1.1 *Context and focus*

The era of sub-meter resolution satellite imagery presents new opportunities for users of spatial data. Indeed high resolution satellite imagery is becoming an affordable solution to add large-scale and high level of geographic knowledge and detail to geospatial databases. The more regular revisit capabilities of satellites also enable a higher frequency of map revision and monitoring. However the maintenance of such Geographical Information System (GIS) data is time and cost consuming when achieved manually. Efforts have been undertaken for more than thirty years by the Computer Vision and Image Processing communities to assist and automate the photogrammetric processing chain in order to shorten revision cycles and therefore improve the currency of information. Image interpretation from very high resolution images raises difficulties and challenges that do not appear with low and mid-resolution data: profusion of details makes automatic analysis of images arduous, and causes traditional bottom-up approaches to fail. This is particularly critical for urban environments where shadows, occlusions and apparent perspective distortion of high buildings are common *artifacts* to cope with. In order to ensure a reliable automatic image understanding of dense urban environments, a recent trend is to use multiple sources of information, which complementarity may disambiguate the analysis. Multiple sources of information can embody collateral imagery data of the same scene or prior knowledge towards the target object to be extracted from the data, the input data to be used as well as the processing methods to be applied (Baltsavias 2002). Map revision comprehends three main aspects. The first one deals with the detection of new objects to be incorporated into the map from more recent imagery data. The second applies to the issue of removing from the map any object that is no longer present in imagery data. The last one focuses on improving the spatial quality of the map from imagery as well as enhancing its level of information (such as adding 3D information to a 2D map). In this paper we address the latter aspect of map revision by proposing a novel method based on the use of active contours and very high resolution panchromatic optical remote sensing imagery in order to improve the spatial location of cartographic buildings objects included in a 2D digital map. This methodology is designed to automatically improve the accuracy of urban GIS databases while overcoming the difficulties of analyzing urban scenes sensed at a high resolution. We take advantage of the geometric prior knowledge derived from the map and adapt region-based and shape constrained active contours models exposed in (Paragios & Deriche 2002, Chan & Zhu) in order to accurately match each building symbolized in the map to its counterpart representation in the satellite image. Besides, we propose two approaches to increase the robustness of the active contours matching. The first deals with adding an exogenous source of information in the active contour model. In our application, additional data is a coarse orthoscopic Digital Surface Model (DSM) encoding the altitude of the same scene as the satellite image. The second approach consists in allowing a spatio-temporal change of the prior shape constraint during the active contours convergence, which may robustly accelerate the refinement process. In the next subsection we briefly outline former works using active contours for roads or buildings extraction from remote sensing data. In section 2, we review the prerequisite background towards knowledge-based active contours and how we adapt them to building map refinement. We detail the contributions of our scheme as well as its domain of application. In section 3, we present some results achieved with 1:10,000 scale cartographic data and Quickbird imagery over Beijing city area. We finally conclude in section 4 with a discussion about future improvements of the proposed scheme.

1.2 *Related works*

Recently active contours or deformable models have raised the interest of the Photogrammetric and Image Processing communities for the purpose of object extraction from remote sensing imagery (Agouris et al. 2001, Vinson et al. 2001, Guo & Yasuoka 2002, Péteri & Ranchin 2003, Rochery et al. 2003, Oriot 2003). Active contours are attractive since they are flexible, can be easily interfaced with the user in a semi-automatic fashion, and can readily embed high level information, which may be useful to ease the extraction process and to make it more reliable. High level information and *a priori* knowledge embrace multiple aspects which are comprehensively reviewed in (Baltsavias 2002). In this paper we focus on the incorporation of geometric prior knowledge within active contours based frameworks. Geometric prior knowledge has two aspects: it can be *generic* or *specific*. Generic information is derived from common sense knowledge and empirical learning. Statements like "buildings roof outlines often have ninety degrees angles" or "roads have parallel borders" are examples of generic knowledge and are already extensively used to enable object extraction. In (Péteri & Ranchin 2003) double snakes are used to extract both sides of roads from high resolution images of a dense urban environment. The snakes (Kass et al. 1987) are initialized from an existing road network graph which may be derived from a map or manually. The snakes evolve according to parallelism inner constraints as well as gradient-based external image forces in order to drive the active contour close to the road borders. In (Rochery et al. 2003) active contours derived from a variational approach are used for road extraction from mid-resolution images. The authors propose a novel quadratic energy to model non local interactions between contour points. This enables to incorporate generic knowledge towards road parallelism and the minimum width of the roads to be extracted. Unlike the previously cited method, this scheme is not sensitive to initialization and it naturally embeds roads geometrical properties and intrinsically incorporates the concept of network. The authors of (Agouris et al. 2001) use existing GIS data, aerial imagery and snakes active contours to update and revise road digital maps. The map accuracy is first quantified by the input of an image acquired at the same time as the GIS data: snakes initialized on the GIS road objects move to the actual road track of the image. According to the snake motion, and for each of its node, an accuracy score is computed using fuzzy logic. This last score is the input of an additional energy which is part of the total energy functional of the active contour. This energy will constrain the motion of the snake in a more recent image of the same scene. The final segmented road revises the map from erroneous digitization and updates it from changes. In (Guo & Yasuoka 2002) an Ikonos image and a laser scanning DSM are jointly used for snake-based building extraction. The snake is initialized from a multiple height bins thresholding of the DSM and evolves according to edge information derived from the image and the DSM. In (Oriot 2003) some statistical snakes are used for building extraction from aerial images. They embed a correlation cost function from stereoscopic images, which favours the inclusion within the active contour of higher disparity measures than the background. Building extraction is simultaneously refined by edge information derived from the images and by generic shape constraint favouring ninety degrees corners. Initialization is achieved by human interaction while the optimization process is based on insertion/updating/deletion of vertices. Good results are demonstrated even if mistakes arise with vegetation closely surrounding buildings. In (Vinson et al. 2001) deformable templates are used to finely extract rectangular buildings from the output of an above-ground structures detection. Optimal rectangular model parameters are later found from the edge information derived from an orthoimage.

Generic geometric knowledge includes social and cultural aspects which augment its variability across geographical locations and therefore decrease the robustness of this information (roads widths and buildings shapes may vary at a regional/national level and even more at a worldwide scale). Unlike the aforementioned works we propose to make use of *specific* geometric information, which is derived from symbolized buildings contained in a digital 2D map. Specific shape information is highly discriminative, object and scene dependent and may enable better recognition and matching performances. This specific geometric prior information derived from the map will be embedded as a shape constraint within an active contours framework. Shape constrained active contours have been extensively studied since the early nineties, especially by the Medical Imaging community which has to deal with data corrupted by noise, occlusions or low contrast. Their use has been recently extended to natural scenes or manufactured objects images and object tracking from video sequences (Chen et al. 2001, Rousson 2002, Chan & Zhu 2003, Cremers et al. 2004). However, the already proposed shape constrained models are not robust enough to deal with complex dense urban scenes. The next section describes how prior shape knowledge has been incorporated within region-based active contours as well as our contributions to increase their robustness.

2 Methodology

2.1 *Active contour model*

We propose to adapt knowledge-driven active contours to digital building map refinement from very high resolution optical satellite imagery. Our goal is to finely match each building symbolized in a map to its counterpart representation in a panchromatic high resolution image. This image is assumed to be the ground truth and has higher geocoding accuracy than the map. Cartographic objects are initially and coarsely registered to the satellite image (this could be the result of rough registration process). Their accuracy is later improved by our proposed fine matching technique. The information provided by the map is used to initialize active contours: initial location is provided by the global map-to-image registration, and the initial shape is similar to the considered cartographic object. Since region based active contours are known to be less sensitive to initialization than their gradient-based counterparts, we make use of the region-based formulation of the Bayesian MAP (Maximum a Posteriori) deformable model formerly proposed in (Paragios & Deriche 2002) in order to drive the active contour to the target building in the image. This approach best befits segmentation of piecewise smooth components of an image. Since we deal with buildings that exibits shape singularities (such as corners) we choose to implicitly represent active contours by their level set functions which naturally model sharp corners (Osher & Sethian 1988). Derived from a variational approach, such active contours minimize the following energy functional:

$$\begin{aligned} J^s(\phi) = & \int \left\{ \frac{\left(I^s(\mathbf{x}) - \overline{I}^s_{in}(t)\right)^2}{2\,\sigma^s_{in}(t)^2} + \ln\sqrt{2\,\pi\,\sigma^s_{in}(t)^2} \right\} \\ & \cdot H\big(\phi(\mathbf{x})\big)\,d\mathbf{x} \\ & + \int \left\{ \frac{\left(I^s(\mathbf{x}) - \overline{I}^s_{out}(t)\right)^2}{2\,\sigma^s_{out}(t)^2} + \ln\sqrt{2\,\pi\,\sigma^s_{out}(t)^2} \right\} \\ & \cdot \big(1 - H\big(\phi(\mathbf{x})\big)\big)\,d\mathbf{x} \end{aligned} \tag{1}$$

where $\overline{I}^s$ and σ^{s^2} respectively denote the image mean and variance grey level. Subscripts *in* and *out* refer to the computation of these statistical quantities inside and outside the evolving active contour. The active contour is embedded in a level set function ϕ which is assumed to be positive inside the contour. The superscript s refers to the satellite image to be analyzed. H represents the Heaviside function. Edge-based and contour regularization terms have been deliberately omitted in equation (1) since we only investigate region-based active contours. Besides, the shape constraint introduced in the next step will act as a contour regularizer. Shape knowledge directly derived from the map is incorporated as a shape constraint in the active contour to make it akin the considered cartographic reference template. The gain of shape constraint is twofold: i) it enables to match the right building in the image according to shape information. ii) it overcomes common urban artifacts such as occlusions or low contrast of the target building. We propose to use the shape constraint energy proposed in (Chan & Zhu 2003), which compares the area within the active contour and the reference template:

$$J_{shape}(\phi, \psi) = \int \left\{ H\big(\phi(\mathbf{x})\big) - H\big(\psi(\mathbf{x})\big) \right\}^2 d\mathbf{x} \tag{2}$$

ψ is the level set function embedding the prior shape. This term is made invariant from any similarity transformation: $\psi(\mathbf{x}) = \psi_0\big(T_{sim}(\mathbf{x})\big)$ where ψ_0 is the level set function embedding the static prior shape derived from the map. In addition to the active contour evolution process, invariance from similarity transformation requires an additional optimization scheme to estimate the best parameters (rotation, translation, scale), which minimize (2). Shape prior incorporated into region based active contours yields the functional J_{SC}:

$$J_{SC}(\phi, \psi) = J^s(\phi) + \lambda J_{shape}(\phi, \psi) \tag{3}$$

The constant weight λ balances the influence of the shape prior regarding to image information. To perform the gradient descent method and retrieve ϕ that minimizes equation (3), we need to calculate the derivative of J_{SC} with respect to ϕ, which yields the following evolution equation of the active contour:

$$\phi_t(\mathbf{x}, t) = \left\{ -\frac{\big(I^s(\mathbf{x}) - \bar{I}^s_{in}(t)\big)^2}{2\,\sigma^s_{in}(t)^2} + \frac{\big(I^s(\mathbf{x}) - \bar{I}^s_{out}(t)\big)^2}{2\,\sigma^s_{out}(t)^2} + \ln\left(\frac{\sigma^s_{out}(t)^2}{\sigma^s_{in}(t)^2}\right) + 2\,\lambda\big[H_a\big(\phi(\mathbf{x})\big) - H_a\big(\psi(\mathbf{x})\big)\big] \right\} \cdot \delta_a\big(\phi(\mathbf{x})\big) \tag{4}$$

where H_a and δ_a are regularized approximations of the Heaviside and Dirac functions. The matching algorithm for map refinement is as follows for each building:

1. Build the shape template level set ψ_0 from the map and initialize the active contour level set function: $\phi(t = 0, \mathbf{x}) = \psi_0(\mathbf{x})$.
2. Compute the mean and variance $\bar{I}^s_{in}(t)$, $\bar{I}^s_{out}(t)$, $\sigma^s_{in}(t)^2$, $\sigma^s_{out}(t)^2$.
3. Evolve the constrained active contour according to (4).
4. Optimize the parameters of T_{sim}.
5. Loop steps 2 to 4 until convergence. The convergence is reached when evaluations of the overall energy functional at two consecutive iterations is below a given threshold ε. In other words, the active contour minimizing the energy functional J_{SC} has converged at time $t_c = n_c \Delta t$ when the following condition is fulfilled:

$$|J_{SC}\big(\phi(\mathbf{x}, n_c \Delta t)\big) - J_{SC}\big(\phi(\mathbf{x}, (n_c - 1)\,\Delta t)\big)| < \varepsilon$$

where $n_c \in \mathbb{N}^+$ and Δt is the time step discretizing the continuous temporal variable t.

From experiments, we found that a threshold ε ranging from 10^{-6} to 10^{-3} is a good compromise between computational time and matching accuracy. It is however important to notice that a too high threshold would make the active contour sensitive to local minima of the functional. We propose two contributions to address the latter issue in order to improve the robustness of the active contours matching:

Exogenous DSM fusion: First we propose to support building map refinement with the input of an exogenous DSM. The DSM data encoding the altitude of the scene components is not redundant with the satellite image. Therefore we could make them cooperatively drive the active contour to the building target to achieve fine matching. Unlike the satellite image, the DSM enables a good contrast of buildings from the rest of the scene, which is a desirable property for the piecewise smooth segmentation model that we use. The joint use of DSM and optical imagery data has already been achieved in (Guo & Yasuoka 2002). Unlike the former method, we do not need a high quality DSM since we do not use gradient-based active contours, which are sensitive to noise and artifacts. Moreover the embedded shape constraint and the implicit active contours representation of our scheme enable to overcome occlusions and manage complex buildings shapes, which is not the case in (GUO & YASUOKA 2002).

Flexible shape prior incorporation: The tuning of the shape constraint weight that balances the influence of the shape prior with respect to the image information is not trivial. Indeed, a too low weight prevents from accurate matching and from overcoming image corruption. Conversely a too high weight will weaken the intrinsic property of flexibility of active contours. Besides, a remote initialization of an active contour embodying a strong shape constraint may be sensitive to local minima of the functional: far from the target building, the image-based information, which drives the active contour, may be penalized by the predominant shape constraint. The active contour may converge to an undesired solution, preventing from carrying out map-to-image matching. We address this issue in turning the constant weight λ into a monotonically increasing function of the iteration time t. The weight is low at the beginning of the iterative process, allowing more shape freedom to the active contour. As a result, the active contour will converge more surely to the desired target in the image. As time goes by, the shape prior is enforced to recover contour regularization and to overcome image alterations. Additionally, λ is also a function of the shape prior ψ to confine the active contour freedom within a restricted space: λ is lower close to the reference template, and asymptotically tends to a higher constant far away from the reference template. This freedom space is gradually reduced as the amplitude of λ increases. Such spatio-temporal shape constraint weight conveys more freedom to the active contour in a restricted space in order to overcome the problem of local minima leading to unsuccessful map-to-image matching.

In summary, the two proposed contributions are formalized as additional terms in the original energy functional:

$$J_{flux,flex}(\phi, \psi) = J^s + \lambda_{DSM} J^d + \lambda_{flex}(\psi, t)\, J_{shape} \tag{5}$$

Superscript d refers to the DSM data, which influence is balanced by the constant weight λ_{DSM}. Details of the formulation of λ_{flex} and the optimization scheme to retrieve T_{sim} can be found in BAILLOEUL et al. 2005.

2.2 *Application scope*

Implicit assumptions have been made for the design of the newly proposed methodology. We intend to detail them in this section in order to define the application scope of our scheme. First the image-based terms of equation (5) partition image data into piecewise smooth components, which may limit our study to buildings with a quite smooth and homogeneous roof reflectance. Second, exogenous data to be merged must fulfill two consistency criteria:

a. Data must be superimposable. This raises the issue of data geometry and registration accuracy. Ideally both satellite image and DSM might be projected into the same geometry and may have a high registration precision in order to ensure that a given pixel in both data represents the same part of the considered building.

b. Data must depict the same scene. This raises the issue of data acquisition time. Since the DSM is made from different acquisition means then the image ones, it may be possible that some changes (building removal) happened between the acquisition times of the satellite image and the DSM. This will constrain DSM data fusion to be solely applicable to unchanged areas.

Cartographic data projection is orthoscopic. As a result, the initial active contour derived from the map will be closer to the target building footprint than its roof that we aim at matching. Matching the building roof is the most tractable solution since it is the most visible part of a building, which is moreover the part represented in the map. A too high footprint-to-roof discrepancy may be problematic since active contours techniques are intrinsically local and may not be able to match a too remote target building roof. This effect is non-existent in case we deal with orthoscopic remote sensing data. Otherwise it is significant for high buildings which exhibit sharp perspective distortion but negligible for low buildings. As a consequence, our scheme is applicable to nearly orthoscopic data or low buildings areas.

Last but not least, we assume that the map is free from shape errors and from generalization effect. A mistaken prior shape derived from the map may bias the matching process since the shape is not consistent with its representation in the image data (Fig. 8). Generalization effect embodies two aspects. The first one deals with the simplification in the map of a single building outline. This may have the same side effect as a mistaken cartographic object. The second is the inclusion of a group of buildings within the same cartographic object. In that case the entity to be matched in the image might not be homogeneous, which violates our first assumption toward piecewise smooth buildings roofs.

3 Results

3.1 *Data and preprocessing*

In our application, additional exogenous data is an orthoscopic DSM encoding the altitude of the same scene as a panchromatic Quickbird satellite image of Beijing city (0.6 m/pixel). Both data depict a dense urban area. This DSM was computed by edge preserving correlation of digitized stereoscopic aerial images couples (Paparoditis et al. 1998). The subsequent DSM was next orthorectified and reached 1 m planimetric and altimetric geocoding accuracy. The satellite image was rectified from terrain variations by the Beijing Institute of Surveying and Mapping (BISM) to reach 0.4 m geocoding accuracy. Since both data are geocoded in the same cartographic system, overlay is straight-forward, satisfying the first exogenous consistency requirement. However we may stress that the satellite image is not in orthoscopic geometry, which obliges us to carry out experiments over low buildings areas. The second data fusion requisite dictates data to represent the same object, and therefore raises the issue of data acquisition time. Indeed, the DSM we used in experiments was generated from 1999 aerial images whereas the satellite image is from year 2002. This anachronism constrained us to carry out experiments on areas where no change is noticeable between these dates. GIS data were manually generated from aerial imagery of the same area by the BISM. Buildings represented in the 2D map are vectorized polygons. The satellite image is pre-processed by anisotropic diffusion to enhance piecewise homogeneity.

3.2 *Experimental results*

Shape and location information from the GIS map enables a good global initial superimposition between the initial active contour and its counterpart representation in the image. However, we intentionally corrupted it in order to examine how well our method could manage inaccurate initial overlay of the data and to illustrate fine map-to-image matching. To do so, any original cartographic vectorized polygon is subject to a global similarity transformation before being overlaid onto the image to initialize the refinement process. This transformation is to be retrieved by the estimation of T_{sim} during the optimization step 4 exposed in the pseudo-code of section 2.1, which will in the end enable a successful matching. The first experiment illustrated in Fig. 2 shows

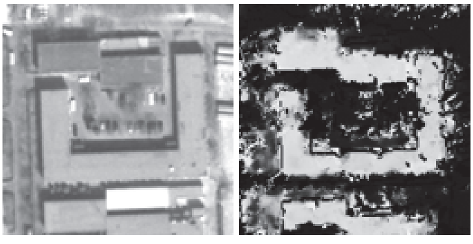

Fig. 1: U-shaped building represented in a satellite image (left) and a DSM which contrast has been enhanced by nonlinear clipping (right).

Fig. 2: Matching without shape prior. Left: initial state close to the desired solution. Right: result without shape prior, "leak" of the active contour.

the need for prior shape knowledge in the matching process. We deliberately initialize the active contour very close to the matching solution of a U-shaped building. The matching task performs poorly without shape prior derived from the map, even though the initialization is close to the desired solution: lack of contrast at the building borders makes the active contour "leak" all over the image, segmenting areas having similar statistical features. This problem is solved in incorporating shape prior (Fig. 3). A more remote initialization than Fig. 2 is possible since shape constraint incorporation is invariant from similarity transformation in order to achieve building fine matching. Figs. 4 to 6 illustrate experiments results carried out with two kinds of buildings and a remote initialization. The figures compare the constrained active contours model of equation (3) with our improved scheme (5). We notice that our scheme outperforms the model without exogenous data fusion or flexible shape prior constraint, enabling in both cases a satisfying matching (Figs. 5–6).

Fig. 3: Matching with shape prior and remote initialization ($\lambda = 10$). Left: initial state. Right: successful matching result even with remote initialisation.

The active contour driven by the model of equation (3) fails in matching the target building in the image (Fig. 4). Lack of discrimination of the building in the image as well as a predominant shape constraint are the two main reasons which may trap the energy functional minimization in a local minimum. The input of a soften shape constraint (Fig. 5) conveys more flexibility to the active contour while globally preserving the reference template shape in order to reach the target building. As we can see on the convergence sequence, the active contour topology may change at the beginning of the iterative process due to a low shape constraint. At the end of the matching action, extra blobs are naturally erased by a stronger shape constraint. Fig. 1 shows the DSM integrated into our model. This DSM looks rough, which is inherent to the method that generated it as well as the complexity of urban scenes. We may notice that some parts of the buildings are not well reconstructed, especially at the boundaries. However this representation of the building is not corrupted by shadows or peripheral objects located on the ground and allows a better discrimination of the building from the background. On the other hand, the representation from the satellite image yields quite clear building boundaries but with lack of discrimination and presence of artifacts. Fig. 6 shows how the complementarity of both satellite and DSM representations overcomes far initialization to carry out a successful matching. Since the DSM has a lower geocoding accuracy than the satellite image and exhibits reconstruction artifacts, we choose to drastically lower its contribution at the end of the convergence process ($\lambda_{DSM} \ll 1$) to favour the satellite image where the building outline is better defined. The use of our full model incorporating both flexible shape constraint and DSM data fusion would yield the same results as Figs. 5–6. The only difference arises in the convergence time (this issue will be investigated in the next sub-section).

The result of Fig. 3 showed there is no restriction towards the shape convexity of the target building to be matched in imagery data. The Fig. 7 illustrates this aspect further with a more complex topology of the building which contains an inner courtyard. As a consequence the cartographic object includes a hole, which is naturally handled by the flexible topology of the active contour implicitly represented by its level set function.

3.3 *Convergence time*

The Tab. 1 displays the computational convergence time ratio of the method in equation (3) with respect to our scheme performance (5). We investigate computational time distinction with the U-shaped and rectangular buildings and two different initializations. Time comparisons are shown with the sole fusion of DSM data, with the sole flexible shape constraint and finally our full model. The results demonstrate that DSM data fusion enables a faster convergence than the model of equation (3). The DSM represents more obviously the target building and drives more surely the active contour, which may explain the convergence time gain. The input of a flexible shape constraint increases even more the convergence efficiency. A lower shape constraint allows increasing the active contour evolution speed while globally keeping the prior shape information. This enables to quickly reach a rough and close solution to the target before the prior shape is gradually enforced. The flexible shape constraint always performs faster results, however while coupled with the DSM data it makes the active contour more sensitive to the DSM reconstruction artifacts and drives it away from the final solution before the DSM weight is relaxed and the prior shape enforced. As a result we obtain a slower convergence with the full model than the sole input of a flexible shape constraint. It is important to stress that the convergence time gain is image and initialization dependent and can not be stated theoretically from algorithmic considerations. However the results of Tab. 1 empirically show an obvious trend of computational cost decrease compared to the model of equation (3). Statistics over a high number of cases would be needed to indubitably confirm this inclination.

Tab. 1: Convergence time comparison.

Time ratio	DSM data fusion	Flexible shape constraint	DSM + flexible shape
U-shaped,1	1.4	1.8	1.6
Rect,1	1.3	3.1	1.8
U-shaped,2	2.5	4.3	2.1
Rect,2	1.3	2.0	2.0

3.4 *Discussion*

From experiments illustrated in Figs. 2 to 7 we showed how the input of an exogenous DSM and a flexible shape constraint could alleviate the sensitivity of the proposed refinement method with respect to incorrect GIS data position. It is worth noticing that a too low registration accuracy would not yield successful matching results as active contour techniques strongly rely on a good initialization, close to the desired solution. Since we address the issue of map refinement, we assume that the initial overlapping area between the map object and its counterpart representation in the image is quite

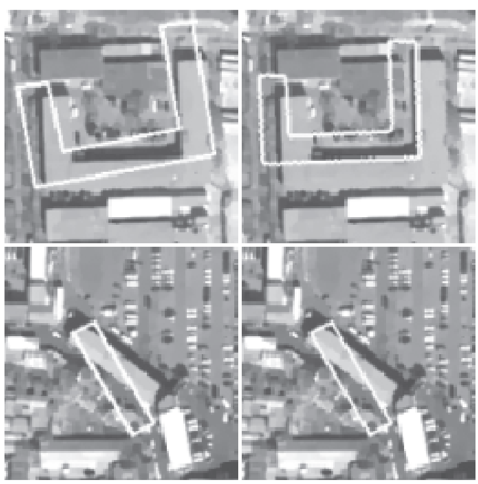

Fig. 4: U-shaped and rectangular buildings: failed matching with the model of equation (3) and $\lambda = 10$. Left: initial state. Right: result.

Fig. 5: Convergence sequence (from top to bottom and left to right) illustrating the matching process with a flexible shape constraint ($5 < \lambda_{flex} < 30$, $\lambda_{DSM} = 0$).

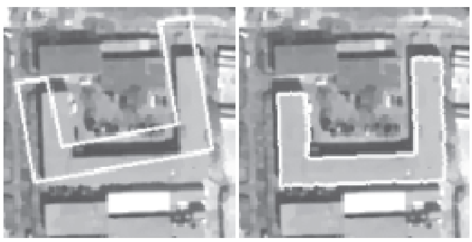

Fig. 6: Matching with DSM fusion ($\lambda_{flex} = cst$, $\lambda_{DSM} = 0.75$). Left: initial state. Right: successful matching with DSM fusion.

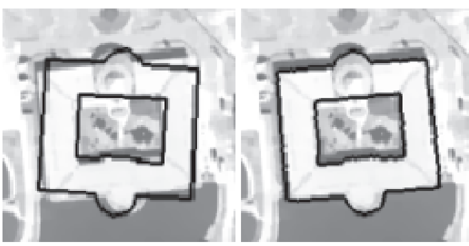

Fig. 7: Matching with flexible shape prior ($5 < \lambda_{flex} < 30$, $\lambda_{DSM} = 0$) and complex topology. Left: initial state. Right: successful matching result with complex topology.

high, which would guarantee a satisfying subsequent refinement. The quantification of such initial overlapping rate allowing a

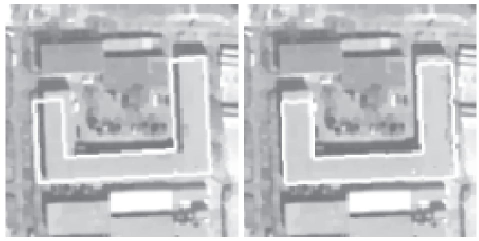

Fig. 8: Matching with flexible shape prior and DSM fusion and a locally mistaken cartographic object ($5 < \lambda_{flex} < 30$, $\lambda_{DSM} = 0.75$). Left: initial state derived from the map. Right: unsuccessful complete matching result.

successful matching is not an easy task as it may be image and object dependent. However, we can qualitatively state that the more the buildings are discriminated from the image background, the more successful the matching with a remote initialization.

Experiments were carried out while assuming that map objects are free from shape errors or generalization effects and that the pose inaccuracy can be modelled by a simple global transformation (similarity transform). The invariance of the algorithm from more complex global transformations (affine or perspective projections) is however possible to handle an extended class of form inaccuracies which may arise in the GIS data. Nevertheless, shape incorrectness from the map is usually local and cannot be modelled by a global transform. We illustrate this aspect with the experiment carried out with the U-shaped building which cartographic representation is locally mistaken at the top of the U branches (Fig. 8). The matching result is then a compromise between the image and the erroneous shape information contained in the map. The similarity invariance of the scheme enables a global refinement of the cartographic data, but local discrepancies between the target building and the reference template are too large at the top of the U branches to be recovered. This is inherent to the fact that no transformation input in J_{shape} is able to model such kind of local discrepancies and because the active contour shape is compelled to be akin to the mistaken shape information. Such hard incorporation of the shape constraint prevents from a completely successful matching. An intuitive solution consisting in relaxing locally the shape constraint to correct local discrepancies would face two difficulties. First it is not trivial to decide where the constraint has to be weakened. Second, the active contour may be subject to image corruptions and urban artifacts at locations where the prior shape information is relaxed. An alternative to handle the problem would be to reformulate the shape energy functional in order to allow a restricted class of displacement or discrepancies of the active contour from the prior shape template. Such restricted motion would allow the active contour to deviate from the cartographic shape prior while preserving its geometric properties at a local level. The formulation of such shape energy and its implementation is still an ongoing work.

4 Conclusions

We have introduced a novel scheme based on the use of active contours to refine digital building map using a high resolution satellite image. Our method is supported by data fusion: active contours are initialized and constrained by a GIS map and make use of an exogenous DSM to achieve successful matching. We demonstrated how the input of the DSM and a flexible spatio-temporal shape constraint could outperform traditional knowledge-based active contours while decreasing the computational cost. Future works will attempt to get rid of the limitations of the presented approach. Extension of our methodology to non-homogeneous or clustered buildings will be tackled with the incorporation in the active contours functional of edge information derived from the remote sensing image. Presence of mistakes or simplifications in the map is still an open and challenging question that we may consider by incorporating a new class of flexible shape constraint allowing larger discrepancies from the reference template. Finally, the proposed method is a preliminary step to building map-to-image change detection as it increases the consistency and comparability of both representations. The map refinement would alleviate the problem of exogenous discrepancies between the map and the image (inaccurate registration, mistakes and generalization effects in the map), enabling more robust subsequent change detection to state what cartographic buildings are no longer present in a more recent remote sensing image.

Acknowledgements

This project is supported by the Chinese Ministry of Science and Technology 863 programme and Alcatel Alenia Space. We thank the editors of the ISPRS Hannover Workshop 2005 and PFG for their invitation to publish the present article in a special issue of the journal.

References

Agouris, P., Stefanidis, A. & Gyftakis, S., 2001: Differential snakes for change detection in road segments. – Photogrammetric Engineering and Remote Sensing **67**(12): 1391–1399.

Bailloeul, T., Prinet, V., Serra, B. & Marthon, P., 2005: Spatio-temporal shape constraint for level set segmentation. – Proc. EMMCVPR, LNCS 3757, Springer-Verlag, Berlin–Heidelberg, pp. 503–519.

Baltsavias, E., 2002. Object extraction and revision by image analysis using existing geospatial data and knowledge: State-of-the-art and steps towards operational systems. – Commission VI Mid-Term Symposium, Xian, China, International Archives of Photogrammetry and Remote Sensing, XXXIV (2): 13–22.

Chan, T. & Zhu, W., 2003: Level set based shape prior segmentation. – Computational and Applied Mathematics technical report no 03–66 of the University of California, Los Angeles.

Chen, Y., Thiruvenkadam, S., Tagare, H., Huang, F., Wilson, D. & Geiser, E. A., 2001: On the incorporation of shape priors into geometric active contours. – Proc. of the IEEE 1st Workshop on Vatiational Framework and Level Sets methods, pp. 145–152.

Cremers, D., Osher, S. & Soatto, S., 2004: Kernel density estimation and intrinsic alignment for knowledge-driven segmentation: teaching level sets to walk. – Pattern Recognition, Proc. of DAGM 2004, Springer Verlag LNCS Vol. 3157, pp. 36–44.

Guo, T. & Yasuoka, Y., 2002: Snake-based approach for building extraction from high-resolution satellite images and height data in urban areas. – Proc. of the 23rd Asian Conference on Remote Sensing.

Kass, M., Witkin, A. & Terzopoulos, D., 1987: Snakes: active contour models. – 1st International Journal of Computer Vision **1**(4): 321–331.

Oriot, H., 2003: Statistical snakes for building extraction from stereoscopic aerial images. – International archives of photogrammetry, remote sensing and spatial information sciences, vol XXXIV-3/W8.

Osher, S. & Sethian, J., 1988: Fronts propagating with curvature-dependent speed: algorithms based on Hamilton-Jacobi formulations. – Journal of Computational Physics **79:** 12–49.

Paparoditis, N., Cord, M., Jordan, M. & Cocquerez, J.-P., 1998: Building detection and reconstruction from mid- and high-resolution aerial imagery. – Computer Vision and Image Understanding **72**(2): 122–142.

Paragios, N. & Deriche, R., 2002: Geodesic active regions: A new paradigm to deal with frame partition problems in computer vision. – Journal of Visual Communication and Image Representation **13**(1/2): 249–268.

Péteri, R. & Ranchin, T., 2003: Multiresolution Snakes for urban road extraction from IKONOS and Quickbird images. – In: Benes, T. (ed.): 23nd EARSeL Annual Symposium "Remote Sensing in Transition". – Mill-press, Rotterdam, Netherlands, Ghent, Belgium.

Rochery, M., Jermyn, I. & Zerubia, J., 2003: Higher order active contours and their application to the detection of line networks in satellite imagery. – IEEE Workshop on Variational, Geometrical, and Level Set Methods in Computer Vision, VLSM'03 at ICCV, Nice, France.

Vinson, S., Cohen, L. & Perlant, F., 2001: Extraction of rectangular buildings using DEM and orthoimage. – Proc. of Scandinavian Conference on Image Analysis (SCIA'01).

Addresses of the authors:

Timothée Bailloeul, PhD student
Dr. Véronique Prinet
LIAMA, Institute of Automation, Chinese Academy of Sciences, P. O Box 2728, Beijing 100080, China
Tel.: (+86 10) 82 61 44 62
Fax: (+86 10) 62 64 74 58
e-mail: tbailloeul@liama.ia.ac.cn
prinet@nlpr.ia.ac.cn

Dr.-Ing. Bruno Serra
Alcatel Alenia Space, 100 bd du Midi
06156 Cannes La Bocca, France
Tel.: (+33) 4 92 92 67 26
Fax: (+33) 4 92 92 76 60
e-mail: bruno.serra@alcatelaleniaspace.com

Prof. Dr. Philippe Marthon
LIMA (IRIT), 2 rue Camichel, 31071 Toulouse France – Tel.:/ Fax: (+33) 5 61 58 83 53
e-mail: Marthon@enseeiht.fr

Pinxiang Chen, Haitao Zhang
Beijing Institute of Surveying and Mapping
15 Yangfangdianlu, Haidian District
Beijing 100038, China
Tel.:(+86 10) 63951326, Fax:(+86 10) 63963144
e-mail: cpx@bism.cn
Tel.:(+86 10) 63953948, Fax:(+86 10) 63971019
e-mail: zhanght@bism.cn

Manuskript eingereicht: Juni 2005
Angenommen: Juli 2005

Berichte

International Workshop »High Resolution Earth Imaging for Geospatial Information«

ISPRS Working Groups I/5 and IV/3

17. bis 20. Mai 2005 in Hannover

Der fünfte Workshop seiner Art, wieder hervorragend organisiert vom Institut für Photogrammetrie und GeoInformation (IPI) in Hannover, war diesmal Prof. Dr.-Ing. Dr. h.c. GOTTFRIED KONECNY zu seinem 75. Geburtstag gewidmet. Veranstalter war neben der ISPRS Working Group I/5: *Geometric Modeling of Optical Spaceborne Sensors and DEM Generation* die WG IV/3: *Automated Geo-Spatial Data Acquisition and Mapping*, die eine starke Anwendungsorientierung in den Gesamtworkshop einbrachte. Insgesamt war eine deutlich höhere Beteiligung als in den letzten Jahren zu verzeichnen. In den vier Tagen wurden 52 hoch qualitative Vorträge gehalten und 25 Poster vorgestellt, und dies vor 134 Teilnehmern aus 30 Ländern (alle Kontinente). Außerdem gab es diesmal eine Intergraph Z/I Imaging Masterclass zum Thema: Technologietransfer in Photogrammetrie und Fernerkundung.

Überblick

Die Veranstaltung war ein äußerst informativer und nützlicher Workshop mit vielen hochwertigen Beiträgen. Die zentralen Themen waren diesmal: Neue Sensorsysteme auf Satelliten (auch Klein- und Mikro-Satelliten) vor allem auch im Radarbereich sowie neue flugzeuggetragene Kamerasysteme. Die Themen im Softwarebereich waren: Extraktionsalgorithmen für Gebäude, Straßen und Landnutzungsarten sowie neue Anwendungen, wie z. B. die Erkennung des Materials von Dächern und Verkehrsmonitoring mit Serienbildern oder durch Radarinterferometrie. Neben den sehr anregenden Diskussionen in den gut organisierten Kaffee- und Mittagspausen konnten die Teilnehmer – von denen sich viele aus der „ISPRS community“ bereits kannten – diesmal sogar bei zwei Abendveranstaltungen Erfahrungen austauschen. Zum einen war das obligatorische „Get together“ auf dem Messdach des IPI mit ausgezeichneten Speisen ein voller Erfolg und zum zweiten lud die Firma Intergraph Z/I Imaging zu einem Abendessen in einem sehr schönen Wirtshaus am Zoologischen Garten von Hannover ein, inklusive „Schlangenbeschwörung“ zur allgemeinen Belustigung.

Plenarsitzung

Der erste Tag des Workshops startete mit einer Einleitung von Prof. CHRISTIAN HEIPKE, der vier der sechs Mitglieder des Councils der ISPRS begrüßen konnte: Prof. IAN DOWMAN, Prof. ORHAN ALTAN, Prof. CHEN JUN und Dr. EMMANUEL BALTSAVIAS. Anschließend gab es Willkommensadressen von Prof. L. SCHÄTZL, dem Präsidenten der Universität Hannover, und von Prof. IAN DOWMAN, University College London, dem Präsidenten der ISPRS, der mit einem historischen Abriss über die Stereoskopie aus dem Weltraum begann und darauf hinwies, dass es immer noch nötig ist Regierungsstellen davon zu überzeugen, wie wichtig Satellitendaten bzw. die daraus abgeleiteten Produkte sind und welcher gesellschaftliche Nutzen daraus gezogen werden kann.

Bei den eingeladenen Vorträgen am Vormittag startete Sir M. SWEETING vom Surrey Space Center, U.K., mit einem Vortrag *Small Satellites – A Technical & Business Challenge,* in dem er auf die vielfältigen Möglichkeiten des Einsatzes von Klein- und Kleinstsatelliten hinwies. Der Vorteil der „Kleinheit“ besteht natürlich nicht nur im Gewicht sondern auch in den Kosten sowie in der wesentlich kürzeren Planungszeit. Auch der Betrieb ist so organisiert, dass z. B. bei Surrey nur eine Person für insgesamt 14 Satelliten im Orbit zuständig ist. Die Disaster Monitoring Constellation (DMC) Satelliten, die von Ländern wie Algerien, China, Nigeria, Türkei und Vietnam betrieben werden, wurden genauer beschrieben. M. CRAMER (Universität Stuttgart) hielt einen ausgezeichneten Überblicksvortrag zum Thema *Digital Airborne Cameras – Status and Future*. In diesem Bereich sind zwei Tendenzen zu sehen, einmal die hoch entwickelten Kamerasysteme wie DMC von ZEISS, ADS40 von Leica und UltraCam von Vexcel, die in Konkurrenz zu klassischen Luftbildkameras stehen und andererseits die „klein und billig" Lösungen (mit geringerer Pixelanzahl) die sich auf konventionelle Produkte wie Kodak- oder Canon-Kameras stützen und meist für nicht-photogrammetrische Anwendungen genutzt werden. Zurzeit liegt der Anteil von digitalen Kameras (aus dem ersten Bereich) für die Luftbildaufzeichnung bei ca. 80 verkauften Exemplaren weltweit und hält daher einen Marktanteil von ca. 10%. Bei einer weiteren Entwicklung im bisherigen Rahmen wird der Anteil bis 2010 auf 25% steigen. Die Notwendigkeit von detaillierten Qualitätsuntersuchungen wurde betont, wie sie z. B. im Rahmen von EuroSDR durchgeführt werden. Schließlich fasste „Lokalmatador" KARSTEN JACOBSEN (Universität Hannover), die momentanen und geplanten *High Resolution Satellite Imaging Systems* sehr schön zusammen. Wichtig ist hier zu erwähnen, dass innerhalb der nächsten 3 Jahre voraussichtlich insgesamt 6 Länder Kameras mit 1 Meter Bodenauflösung (ground sampling distance, GSD) haben werden, weitere 5 Länder planen Kameras mit 2,5 Meter GSD. Das bedeutet natürlich eine wesentlich höhere Verfügbarkeit dieses Datentyps sowohl räumlich als auch zeitlich. Es wurde auch auf die Unterschiede der Systeme hingewiesen, die zum Teil erheblich sind. Auch der zukünftige Einsatz von HALE (High Altitude Long Endurance)-Systemen auf unbemannten Stratosphärenflugkörpern wurde diskutiert, ebenso die neuen SAR-Systeme im Weltraum wie z. B. TerraSAR-X, der auch in den Auflösungsbereich von einem Meter vordringen wird.

Am ersten Abend hielt M. SCHROEDER (DLR) einen Vortrag: *25 Years Space Photogrammetry in Germany – A Research Field Initiated by* GOTTFRIED KONECNY, in dem er die Leistungen von Prof. KONECNY anlässlich seines 75. Geburtstag, gewürzt mit vielen interessanten Begebenheiten, würdigte.

Bildgeometrie und DEM

Eine ganze Reihe von Vorträgen gab es wieder zur geometrischen Modellierung von optischen Daten und hier insbesondere zum Thema Genauigkeit von Orthobildern und DEM. Für eine hohe Absolutgenauigkeit kommt es sehr auf die Auswahl und Qualität der Passpunkte (GCP) an. Auch mit sehr wenigen aber guten(!) GCP werden RMSE Werte aus z. B. IKONOS Daten im Bereich von 1 Meter und besser erreicht. E. BALTSAVIAS (ETH Zürich) unterscheidet zwischen den Sensoren IKONOS, bei dem meist Translationen für eine Korrektur nach RPC Anwendungen reichen und Quickbird, bei dem affine Transformationen nötig sind. In diesem Vortrag wurde auch ein aus IKONOS Stereo-Daten abgeleitetes DEM mit einem Referenz DEM verglichen, wobei RMSE-Werte für die Höhe im Bereich von 1 bis 4 Meter in Abhängigkeit von der Oberflächenklasse erhalten wurden. T. TOUTIN (CCRS, Kanada) stellte ein Verfahren zur *Spatiotriangulation of combined HR stereo sensors* vor, bei dem mehrere Sensoren (SPOT HRS, SPOT HRG, IKONOS und Quickbird) in einem gemeinsamen Modell ausgewertet wurden. Durch die Verwendung von Verknüpfungspunkten konnten hier mit ganz wenigen GCP sehr genaue Ergebnisse erzielt werden.

Grundsätzlich ist der Tenor, dass bei allen Datensätzen – allerdings mit unterschiedlichem Aufwand – eine Genauigkeit im Bereich der Pixelgröße und sogar teilweise darunter für die Georeferenzierung erreicht werden kann. Bei der Erstellung von DEM aus Stereoweltraumdaten kommt es stark auf den Konvergenzwinkel zwischen den beiden Aufnahmen an: bei einem kleineren Basis/Höhen-Verhältnis (B/H) ist durch eine leichtere Bildzuordnung eine höherer Relativgenauigkeit zu erreichen, während bei einem größeren B/H die absolute Genauigkeit höher ist, jedoch Probleme bei der Punktzuordnung entstehen. Mithilfe von drei oder mehr Blickrichtungen (auch möglich bei IKONOS innerhalb eines Orbits, allerdings sehr teuer!) lassen sich die Ergebnisse deutlich verbessern, wie z. B. F. STOLLE (University of Massachusetts) nachwies. Auch 3D-Modelle von Städten können auf diese Weise verbessert erstellt werden, wobei die Qualität ohne manuelle Interaktionen nicht sehr hoch ist. T. KRAUSS (DLR) stellte in seinem Poster neuartige Verfahren zur Extraktion eines Stadtmodells unter Benutzung von Routinen aus der Spracherkennung mittels dynamischer Programmierung dar, ein sehr viel versprechender Ansatz.

SAR

Bei diesem Workshop spielte das Thema SAR eine größere Rolle als in den vorangegangenen. Dies lässt sich sicher teilweise darauf zurückführen, dass mit dem TerraSAR-X Satelliten, der im Frühjahr 2006 starten soll, erstmalig SAR-Daten mit einer GSD von bis zu einem Meter aufgezeichnet werden und damit viele neue Anwendungen möglich sind. In der SAR-Sitzung wurde ein breites Spektrum der Nutzung von SAR-Daten vorgestellt. M. CROSETTO (Institute of Geomatics, Barcelona) hielt einen sehr schönen Einführungsvortrag über differerentielle SAR-Interferometrie, während M. EINEDER (DLR) über mögliche Verbesserungen bei der Erstellung von DEM in steilem Gelände aus InSAR-Daten von mehreren Orbits berichtete. Weitere Vorträge beschäftigten sich mit den Möglichkeiten von sehr hoch aufgelösten SAR-Daten im urbanen Bereich, mit Genauigkeiten von Deformationsanalysen durch „persistent scatterer“ und mit der Messung von bewegten Fahrzeugen aus InSAR Daten. Letztere Untersuchungen wurden vor allem im Hinblick auf eine weitere TerraSAR-X Anwendung durchgeführt, bei der ein Verkehrsmonitoring von Hauptverkehrsadern durchgeführt werden soll. Bei den geplanten Missionen wurde auch über den TanDEM-X Satelliten referiert, der zusammen mit TerraSAR-X durch sehr eng gekoppelte Orbits viele weitere Interferometrie Anwendungen ermöglichen würde. Z.B. könnten weltweit DEM mit einer Höhengenauigkeit von ca. 1–2 Meter erstellt werden. Die Entscheidung über die Durchführung fällt voraussichtlich im Herbst 2005.

Digitale flugzeuggetragene Kamera-Systeme

Ebenfalls einen sehr wichtigen Anteil an diesem Workshop nahmen die digitalen Luftbildkameras ein, die zurzeit, gleichzeitig zu einem operationellen Einsatz, in ihren radiometrischen und geometrischen Eigenschaften sozusagen auf Herz und Nieren überprüft werden. Diese Untersuchungen werden häufig im Vergleich zu klassischen Luftbildkameras durchgeführt. Einigkeit herrschte über das deutlich bessere radiometrische Verhalten gegenüber den analogen Bilddaten. Beispielsweise sind im hochreflektiven Bereich die Kontraste in den digitalen Bildern wesentlich höher. So wurde ein Siemensstern bei gleicher GSD im digitalen Bild besser aufgelöst, wie R. ALAMUS (ICC, Barcelona) berichtete. A. ROHRBACH (Leica Geosystems) sprach davon, dass eine GSD von 10 cm im analogen Bild einer GSD von 20 cm im digitalen Bild der ADS40 entspricht. Für Stereo-Aufnahmen ist das Basis/Höhen Verhältnis bei der Zeilenkamera ADS40 und den Analogkameras doppelt so hoch wie bei den Flächen-CCDs. Die abgeleiteten Höhenmodelle sind jedoch auf Grund der höheren Punktgenauigkeit der flächenhaft abbildenden Digitalkameras trotz des geringeren B/H-Verhältnisses vergleichbar mit denen der Analogkameras, dies gilt vor allem auch im steileren Gelände. H. WEICHELT (ILV Fernerkundung GmbH) berichtete über den operationellen Einsatz der DMC, auch in Entwicklungsländern und betonte die Wichtigkeit von Kalibrierung und Beobachtung der Langzeitstabilität für multitemporale Analysen. Das Poster zur Bestimmung und Verbesserung der räumlichen Auflösung von Bilddaten digitaler Luftbildkameras von S. BECKER (Universität Stuttgart) wurde als bestes Poster ausgewählt.

Insgesamt lässt sich sagen, dass der Übergang von Analog- zu Digitaltechnik im photogrammetrischen Bereich in Gang kommt und der operationelle Einsatz der neuen Technik immer häufiger wird.

Die letzte Aussage wurde auch im Rahmen der Intergraph Z/I Masterclass getroffen. Nach einer kurzweiligen Einführung von H. Rosengarten, in der er über die „kinderleichte" Bedienung der DMC und den „oh shit"- Knopf berichtete, wurden historische, technische und Marketingaspekte aus dem gesamten Intergraph Programm dargeboten. M. Madani (Intergraph USA) sprach über Trends in der Anwendung wie z. B. Real-Time Notwendigkeiten im Falle von Katastrophen, Veränderungsanalysen, verteilter Produktion u. a., sowie die vielfältigen Vorzüge der Image Station incl. TerraShare Software. C. Dörstel (Intergraph Deutschland) berichtete anschließend über das ausgefeilte Missionsplanungstool und das äußerst anwenderfreundliche Post-Processing-System (PPS) – ein insgesamt gelungener Überblick über die Qualitäten der DMC von der Einsatzplanung bis zum Produkt.

Informationsextraktion und Monitoring

Zu diesem Themenkomplex gab es insgesamt fünf Sitzungen, die von der Gebäudeextraktion über Kartierung und Datenfusion bis zu Straßen- und Verkehrserfassung aus optischen Bilddaten reichten. Zum Thema Gebäudeextraktion präsentierte J. Hyyppä (Finnisches Geodätisches Institut) eine sehr übersichtliche Zusammenfassung einer EuroSDR Studie zum Vergleich der Möglichkeiten mittels Laser-Scanner, Luftbild oder einer Kombination aus beiden. 11 teilnehmende Institutionen arbeiteten mit den gleichen Datensätzen in 4 Testgebieten. Ein Ergebnis: automatisches Laser-Scanning ergibt einen vierfach höheren Fehler, bei jedoch nur 5% des Arbeitsaufwandes. Es lohnt sich diese Studie im Detail anzusehen. Die Frage bleibt immer: wie genau muss es sein und wie viel manueller Aufwand ist noch vertretbar? Sicher sind in den nächsten Jahren noch verbesserte Automatisierungsverfahren zu erwarten.

Eher exotisch aber interessant war die Anwendung von H.-P. Bähr (Universität Karlsruhe), mit Hilfe einer Kombination von Hyperspektraldaten (DAIS) und Laser-Scanner-Daten Dachmaterialien zu unterscheiden und das mit sehr hoher Genauigkeit. Zum Thema Laser-Scanning waren noch weitere Vorträge aus dem Küstenbereich von A. Brzank (IPI, Hannover) und zur Wellenform Analyse von B. Jutzi (FGAN-FOM) zu hören.

Zwei Vorträge zur Analyse von Serienbildern bzw. Lidardaten aus dem Flugzeug bezeugten das Potential einer detaillierten Verkehrsbeobachtung aus der Luft als Input für Verkehrsmodelle und Simulationen. Auch wurde die Möglichkeit einer Verifikation bzw. der Aktualisierung von Straßendatenbanken (ATKIS) mit VHR Satellitendaten erörtert mit dem Ergebnis, dass die Möglichkeiten an die Resultate mit Luftbildern herankommen, vor allem unter Benutzung des NDVI aus IKONOS-Daten.

Zusammenfassung

Alles in allem war der „ISPRS Hannover" Workshop wieder einmal ein voller Erfolg. Dies lässt sich sowohl inhaltlich – jeder konnte neues Wissen und neue Ideen mit nach Hause nehmen – wie organisatorisch – ein herzlicher Dank an die Organisatoren für die ausgezeichnete Durchführung und Gastfreundschaft – als auch persönlich – man hat wieder mal viele alte Bekannte getroffen – sagen. Das Schöne an diesem alle zwei Jahre stattfindenden Workshop ist einfach seine persönliche Note, die zu den fachlich hochqualitativen Beiträgen hinzukommt.

Peter Reinartz, DLR, Oberpfaffenhofen

European Association of Remote Sensing Laboratories

Während des 25th EARSeL – Symposiums vom 6. bis 8. Juni 2005 in Porto, Portugal hat das Council beschlossen, den Sitz des EARSeL – Sekretariats zu verlegen von Paris nach Hannover. Nachfolgerin von Mme. Madeleine Godefroy wurde:

Frau Gesine Böttcher
EARSeL Secretariat
University of Hannover, Institute of Photogrammetry and GeoInformation (IPI)
Nienburger Strasse 1, D-30167 Hannover,
Tel.: +49-511-762 2482, Fax: +49–511-762 2483, e-mail: boettcher@ipi.uni-hannover.de, www.earsel.org

EARSeL ist 1977 unter der Schirmherrschaft von ESA, Europarat und Europäischer Kommission gegründet worden. EARSeL ist ein wissenschaftliches Netzwerk von europäischen Instituten für Fernerkundung aus dem akademischen und dem kommerziellen/industriellen Bereich. Auch Einzelpersonen können Mitglied werden. Die Zahl der Mitglieder beträgt gegenwärtig rund 250.

EARSeL wird von einem *Council* geführt, das sich aus gewählten nationalen Vertretern der beteiligten Länder zusammensetzt. Das Council wählt seinerseits das *executive Bureau*. Gegenwärtig besteht das Büro aus folgenden Mitgliedern:

Prof. Rudi Goossens, Chairman
Universität Gent, B
Dr. Rainer Reuter, Vice Chairman
Universität Oldenburg, D
Dr. André Marçal, Secretary General
Universität Porto, P
Dr. Lena Halounova, Schatzmeisterin
Czech Technical University, CZ
Dr. Mario Hernandez, External Relationships
UNESCO/Natural Sciences Sector, F

Die Hauptaktivitäten von EARSeL:
– Stimulierung und Förderung von Ausbildung und Training in Fernerkundung und Erdbeobachtung,
– Organisation und Koordinierung von anwendungsorientierter Forschung,
– Verbindung von Technologie und Anwendung für die breite Nutzergemeinschaft,
– Unterstützung von Behörden und Institutionen bei der Entwicklung neuer Sensoren und Systeme sowie allen anderen relevanten technischen Fragen,
– Schaffung eines Netzwerks von Experten für die europäischen Behörden,
– Förderung der Kooperation zwischen Fernerkundungsexperten, Managern und Entscheidungsträgern aus dem Bereich der Umwelttechnik, sowie der Zusammenarbeit europäischer Institutionen.

Die wissenschaftliche Arbeit von EARSeL wird konzentriert in *Special Interest Groups (SIG)*. Gegenwärtig bestehen folgende SIG:

- *Data Fusion*. Leitung: Dr. Lucien Wald, Ecole des Mines de Paris, lucien.wald@ensmp.fr
- *Developing Countries*. Leitung: Prof. Rudi Goossens, Universität Gent, Belgien, rudi.goossens@ugent.be
- *Forest Fire*. Kontakt: Dr. Emilio Chuvieco, Alcalá University, oder Dra. Maria Pilar Martin, Instituto de Economía y Geografia (C.S.I.C), Spanien, emilio.chuvieco@uah.es
- *Forestry*. Leitung: Håkan Olsson, Swedish University of Agricultural Sciences Umea, hakan.olsson@resgeom.slu.se
- *Geological Applications*. Leitung: Prof. Freek van der Meer, Technische Universität Delft and ITC, Niederlande, vdmeer@itc.nl
- *Imaging Spectroscopy*. Leitung: Andreas Müller, DLR Oberpfaffenhofen, Andreas.Mueller@dlr.de
- *Land Ice and Snow*. Kontakt: Thomas Nagler, Universität Innsbruck, Österreich, thomas.nagler@uibk.ac.at
- *Land Use/ Land Cover*. Leitung: Matthias Braun, Universität Bonn, earsel@uni-bonn.de

- *Multilateral Environmental Agreements* (MEA). Leitung: Gérard Begni, MEDIAS France, Toulouse, Gerard.Begni@medias.cnes.fr
- *Remote Sensing of the Coastal Zone*. Leitung: Dr. Rainer Reuter, Universität Oldenburg, rainer.reuter@uni-oldenburg.de
- *Urban Remote Sensing*. Leitung: Prof. Carsten Jürgens, Ruhr Universität Bochum, carsten.juergen@rub.de
- *3D Remote Sensing*. Leitung: Dr. Karsten Jacobsen, Universität Hannover, jacobsen@ipi.uni-hannover.de
- *Temporal Analysis of Image Data*. Kontakt: Keith McCloy, Danish Institute of Agricultural Sciences, Tjele, Dänemark, keith.mccloy@agrsci.dk

EARSeL-Publikationen:

- EARSeL Newsletter, 4 × pro Jahr,
- Symposium Proceedings, bisher sind 24 Proceedings erschienen,
- EARSeL eProceedings, das Open Access Remote Sensing Journal. Bisher sind drei Ausgaben online erschienen, Vol. 4 ist in Vorbereitung,
- Workshop Proceedings.

EARSeL kooperiert bei der Veranstaltung von Fachtagungen wo immer das möglich ist mit ISPRS, EUROGI, EuroSDR, Eurogeographics und EARSC.
Das 26. EARSeL Symposium unter dem Motto „New Developments and Challenges in Remote Sensing" wird vom 29.5. bis 2. 6. 2006 in Warschau stattfinden.

Quellen: www.earsel.org, PFG, 5/2001, S. 382

GeoUnion Alfred-Wegener-Stiftung

Ziele und Aufgaben der 1980 gegründeten Alfred-Wegener-Stiftung zur Förderung der Geowissenschaften (AWS) sind:

Einheit der Geowissenschaften
- fachübergreifende Förderung der Zusammenarbeit zwischen den geowissenschaftlichen Disziplinen,
- Förderung der Kooperation mit den anderen naturwissenschaftlichen Disziplinen und den Ingenieurwissenschaften,
- Initiierung größerer interdisziplinärer Gemeinschaftsprojekte, Ausrichtung und Förderung gemeinschaftlicher geowissenschaftlicher Veranstaltungen, wie AWS-Konferenzen, AWS-Arbeitskreise und Teilnahme an geowissenschaftlich ausgerichteten Messen,
- Verleihung von Preisen und Ehrungen für herausragende Leistungen auf dem Gebiet der Geowissenschaften.

Außendarstellung der Geowissenschaften
- Darstellung geowissenschaftlicher Themen für Öffentlichkeit, Politik und Verwaltung,
- Förderung der geowissenschaftlichen Ausbildung an Schulen und Hochschulen,
- Hochschulpolitische Vertretung der Geowissenschaften,
- Vermittlung von geowissenschaftlichen Forschungsergebnissen und Sachverhalten an Schüler, Lehrer, die breitere Öffentlichkeit und Medien,
- Förderung des Dialogs zwischen Geowissenschaften und Bevölkerung,
- Organisation von Ausstellungen und Informationsveranstaltungen.

Brücke zur Praxis
- Ausbau der Kontakte zu Wirtschaft und Industrie,
- Darstellung des Geowissenschaftlichen Leistungsspektrums.

Die *GeoUnion – Alfred-Wegener-Stiftung* wird von 33 geowissenschaftlich orientierten Organisationen (Trägereinrichtungen) getragen, dazu gehört auch die Deutsche Gesellschaft für Photogrammetrie, Fernerkundung und Geoinformation (DGPF) e.V. Die GeoUnion repräsentiert ca. 50 000 Mitglieder.

Im Jahre 2004 erfolgte die Umbenennung. Die GeoUnion ist eine Stiftung Bürgerlichen Rechts und verfolgt ausschließlich gemeinnützige Belange. Finanziert wird sie aus Erträgen des Stiftungsvermögens, über Projekte des Vereins zur Förderung der AWS e.V. und aus Zuwendungen von Mitgliedern und Dritten.

Sitz der Redaktion:
GeoUnion Alfred-Wegener-Stiftung
Arno-Holz-Str. 14, Alexander von Humboldt-Haus, 12165 Berlin
Tel.: 030-790 1374-0, Fax:030-790 1374-1
e-mail: infos@geo-union.de
Frau Dr. Nicole Schmidt

Quelle: www.geo-union.de/

DAGM e.V.

Die Deutsche Arbeitsgemeinschaft für Mustererkennung

Zweck des Vereins ist die Forschung und Förderung der wissenschaftlichen Arbeiten auf dem Gebiet der Mustererkennung, der gegenseitige Erfahrungsaustausch und die gemeinsame Behandlung wissenschaftlicher und technischer Fragen aus dem gesamten Gebiet der Mustererkennung im In- und Ausland.

Die Aufgabe ist gemäß §3 der Satzung wie folgt formuliert:

1. Die Aufgabe der DAGM ist die Förderung der Arbeit auf dem Gebiet der Mustererkennung, der gegenseitige Erfahrungsaustausch und die gemeinsame Behandlung wissenschaftlicher und technischer Fragen aus dem gesamten Gebiet der Mustererkennung. Diese Aufgabe soll im Geist der Zusammenarbeit und des gegenseitigen Einvernehmens zwischen den Trägern durchgeführt werden.
2. Die DAGM vertritt als „Nationales Komitee“ die Träger auf dem Gebiet der Mustererkennung in entsprechenden internationalen Organisationen und leitet dabei die erhaltenen Informationen an die Mitglieder ihrer Trägergesellschaften weiter.
3. Die DAGM organisiert im Einvernehmen mit den Trägern und auf Kosten eines oder mehrerer ihrer Träger Tagungen oder beteiligt sich an Tagungen der Träger oder anderer Veranstalter.
4. Die DAGM sorgt für weitgehende Verbreitung ihrer Arbeitsergebnisse und für eine möglichst umfassende Unterrichtung aller Interessenten über die in- und ausländische Entwicklung der Mustererkennung durch Veröffentlichungen in einschlägigen Fachzeitschriften, durch Berichte und Rundschreiben sowie durch Herausgabe von Arbeitsblättern und Richtlinien.

Wichtigstes Instrument ist das jährlich stattfindende DAGM – Symposium Mustererkennung.

Die DAGM vertritt die deutschen Interessen auf dem Gebiet der Mustererkennung auf internationaler Ebene, insbesondere gegenüber der *International Association for Pattern Recognition (IAPR)*.

Vorsitzender der DAGM:
Prof. Dr. Hans Burkhardt, Universität Freiburg
Stellvertreter: Prof. Dr. G. Sommer, Universität Kiel
Vorsitzender (Sprecher) des Technischen Komitees (TK): Prof. Dr. H. Ney, RWTH Aachen
Stellvertretender Sprecher des TK: Prof. Dr. W. Förstner, Universität Bonn

Gründungs-/Trägergesellschaften sind:
- Deutsche Gesellschaft für angewandte Optik (DGaO)
- Deutsche Gesellschaft für Medizinische Informatik, Biometrie und Epidemologie (GMDS)
- Gesellschaft für Informatik
- Informationstechnische Gesellschaft (ITG)
- Deutsche Gesellschaft für Nuklearmedizin (DGN)
- Deutsche Sektion des IEEE
- Deutsche Gesellschaft für Photogrammetrie, Fernerkundung und Geoinformation (DGPF)
- VDMA Fachabteilung Industrielle Bildverarbeitung/Machine Vision
- German Chapter of European Neural Network Society (GNNS)
- Deutsche Gesellschaft für Robotik DGR

Die *DAGM-Symposien Mustererkennung* der letzten fünf Jahre:

22. Symposium: 2000 in Kiel
23. Symposium: 2001 in München
24. Symposium: 2002 in Zürich
25. Symposium: 2003 in Magdeburg
26. Symposium: 2004 in Tübingen
27. Symposium: 30.8.–2. 9. 2005 in Wien

Die Ergebnisse dieser Veranstaltungen und auch aller vorangegangenen Symposien sind in Form von Proceedings publiziert worden.

Quelle: www.dagm.de/

Hochschulnachrichten

Technische Universität Wien

Dipl.-Ing. Georg Vozikis promovierte im Juni 2005 am Institut für Photogrammetrie und Fernerkundung der TU Wien mit der Arbeit „*Automatisierte Erstellung und Aktualisierung von Digitalen Stadtmodellen mittels hoch auflösender Zeilenscanner*“ zum Dr. techn.
1. Begutachter: a.o. Prof. Dr. Josef Jansa, TU Wien
2. Begutachter: Prof. Andreas Georgopoulos, Athens National Technical University

Kurzfassung:
Digitale Stadtmodelle zählen zu den begehrtesten Produkten der Photogrammetrie und Fernerkundung. Die Erstellung und Aktualisierung dieser Modelle gehört zu den zeitaufwendigsten und teuersten Aufgaben, die in der Regel manuell durchgeführt werden. Ziel dieser Arbeit ist es eine automatisierte Methode zu entwickeln, die möglichst selbständig digitale Stadtmodelle erzeugt und aktualisiert. Als Grundlage sollen panchromatische Stereo-Bilder von hoch auflösenden flugzeug- und satellitengetragenen Zeilenscannern dienen.

Die vorgeschlagene Vorgehensweise kann in 3 wesentliche Schritte eingeteilt werden: Datenvorbearbeitung, Gebäudeextraktion (entspricht der Erstellung des Stadtmodells) und Feststellung von Veränderungen sowie Aktualisierung alter Datenbestände. Der erste Schritt beinhaltet die Akquisition und Orientierung der Bilddaten, sowie die Erstellung von Oberflächenmodellen und den daraus abgeleiteten normalisierten Geländemodellen. Bei der Gebäudeextraktion werden vorerst Regionen gesucht, in denen potentielle Gebäudekandidaten existieren könnten.

Dies geschieht durch eine Grauwertanalyse im Bild und einer Höheneinschränkung im normalisierten Geländemodell. In Folge werden die geometrischen Eigenschaften der gefundenen Gebäude mit Hilfe eines adaptiven *Region Growings* und einer darauf folgenden *Hough-Transformation* extrahiert. Die errechneten Gebäudeecken werden in einer Datenbank abgelegt und können zur Auffindung von Veränderungen verwendet werden.

Da diese Methode auf Gebäude, die eine Mindestgröße von ca. 25 Pixeln haben eingeschränkt ist, wurden weiter zwei alternative Ansätze untersucht: Gebäudeextraktion mittels *Bildmatchings* oder mittels *Texturanalyse*.

Die Qualitätsanalyse der Ergebnisse zeigt, dass die untersuchte Methode des *adaptiven Region Growings* mit der darauf folgenden *Hough-Transformation*, sehr erfolgreich ist. Das *Bildmatching* liefert in kleinmaßtäbigem Bildmaterial gute Resultate. Die Methodik basierend auf der vorgeschlagenen Texturanalyse ist hingegen nicht empfehlenswert, um einzelne Gebäude zu detektieren und extrahieren.

Vorankündigungen

2005

30. November – 2. Dezember: 2nd International **Conference "Earth from Space – the Most Effective Solutions"** in **Moskau**. Auskünfte durch: Polina Glazyrina, e-mail: polina@scanex2.ss.msu.ru und Conference Secretary, Tel./Fax: +7-095-939-4284, e-mail: conference@scanex.ru, www.transparentworld.ru/conference/

8.–10. Dezember: ISPRS WG II/4 **Workshop on Spatial Planning & Decision Support Systems** in **Macres**, Malaysia. Auskünfte durch: Prof. Ali Sharifi, Chair WG II/4, Tel.: +31-53-4874261, Fax: +31-53-4874575, e-mail: alisharifi@itc.nl, www.itma.upm.edu.my/isprs

9./10. Dezember: **Geokosmos** 4th International **Conference and Exhibition in Moskau**. Auskünfte unter: inna_bartchan@geokosmos.ru

15./16. Dezember: 5th International **Workshop on Web & Wireless Geographical Information Systems (W2GIS2005)** in Lausanne. Auskünfte durch: Dr. Christelle Vangenot, Tel.: +41-21-6935 255, Fax: +41-21-6935195, e-mail: christelle.vangenot@epfl.ch, www.lbd.epfl.ch/e/conferences/w2gis05/

2006

23.–25. Januar: Internationales Symposium Ostrava 2006 **"Informatics for Geoinformatics"** in **Ostrava**, Tschechische Republik. Auskünfte durch: Jan Ruzicka, Tel.: +420-597-325 472, Fax: +420-596-918 589, e-mail: jan.ruzicka@vsb.cz, http://gis.vsb.cz/

25.–27. Januar: **Workshop „Multi-platform Sensing and Sensor Networks – EuroCOW 2006"**, organisiert vom Institute of Geomatics, Spanien für EuroSDR, Kommission I und ISPRS, WG I/3 in **Castelldefels**, Spanien. Auskünfte durch: Dr. Vincent Tao, York University Kanada (Chair), Dr. Ismael Colomina, Institut of Geomatics, Spanien, (Co-Chair) und Dr. Raad A. Saleh, University of Visconsin-Madison, USA (Co-Chair). www.eurosdr.org, www.eurocow.org/presentation.htm

1./2. Februar: **5. Oldenburger 3D-Tage**. Auskünfte durch: Prof. Thomas Luhmann, Institut für Angewandte Photogrammetrie und Geoinformatik und Institut für Mess- und Auswertetechnik der FH Oldenburg. http://www.fh-oow.de/3dtage

13.–15. Februar: **ISPRS** WG VIII/11 & **EARSeL joint Conference "3D Remote Sensing in Forestry"** in **Wien**. Auskünfte durch: Prof. Werner Schneider, Tel.: +43-1-47654-5100, e-mail: werner.schneider@boku.ac.at, http://ivfl.boku.ac.at/3DRSFForestry

14.–16. Februar: **ISPRS** WG I/5 & I/6 Workshop on **Topographic Mapping from Space** in **Ankara**. Auskünfte durch: Ugur Murat Leloglu, Tel.: +90-312-210-1310, Fax: +90-312-210-1315, e-mail: leloglu@bilten.metu.edu.tr, http://www.commission1.isprs.org/wg5

22.–24. Februar: **ISPRS** WG II/3 & II/6 Workshop on **Multiple Representation & Interoperability of Spatial Data** in **Hannover**. Auskünfte durch: Prof. Monika Sester (Chair WG II/3), Tel.: +49-511-762 3588, Fax: +49-511-762 2780, e-mail: Monika.Sester@ikg.uni-hannover.de

1.–3. März: 11. **Münchner Fortbildungsseminar „Geoinformationssysteme"** in **München**. Leitung: Prof. M. Schilcher. Auskünfte durch: Runder Tisch GIS e.V. und TU München, FG Geoinformationssysteme, Arcisstr. 21, 80290 München. http://www.runder-tisch-gis.de, Tel.: +49-89-2892 28 49, Fax: +49-89-28 92 28 78; e-mail: roland.dietrich@bv.tum.de

2./3. März: 1^{th} Workshop of the **EARSeL** Special Interest Group **Urban Remote Sensing – Challenges & Solutions** in **Berlin**-Adlers hof. Auskünfte durch: Prof. Patrick Hostert, Workshop Chairman und Prof. Carsten Jürgens, Chairman EARSeL SIG URS. www.hurs.de

29.–31. März: 5^{th} Inernational Symposium **Turkish-German Joint Geodetic Days** in **Berlin**. Auskünfte durch: Prof. Lothar Gründig, Tel.: +49-30-3142 2375, e-mail: gruendig@inge3.bv.TU-Berlin.de

1.–5. Mai: **ASPRS Annual Conference** in **Reno** Hilton Hotel, Nevada, USA. Auskünfte durch: ASPRS, Tel.: +1-301-493-0290, Fax: +1-30 1-493-0208, e-mail: asprs@asprs.org, www.asprs.org/asprs/meetings/calendar.html

8.–11. Mai: 5^{th} International **Symposium on Mobile Mapping Technology (MMT 2006)** in **Padua**, Italien. Auskünfte durch: Prof. A. Vettore, e-mail: antonio.vettore@unipd.it oder Prof. N. El-Sheimy, e-mail: elsheimy@ucalgary.ca, www.cirgeo.unipd.it/sito-CIRGEO/mmt_frst.html

8.–12. Mai: **ISPRS Mid-term Symposium Commission VII** in **Enschede**, Niederlande. Auskünfte durch: Prof. John van Genderen, Pres. Com. VII, e-mail: genderen@itc.nl; http://www.commission7.isprs.org

29. Mai–2. Juni: 26. **EARSeL-Symposium** in **Warschau**. Auskünfte durch: Frau Gesine Böttcher, EARSeL-Sekretariat Hannover, e-mail: boettcher@ipi.uni-hannover.de und www.earsel.org

8.–10. Juni: **Geomatiktage 2006** in **Luzern**. Auskünfte durch: SGPBF, www.igs-gfsvvk.ch/d/oeffentlichkeit/veranstaltungen/findex.html

27.–30. Juni: **ISPRS Mid-term Symposium Commission VI** in **Tokyo**/Japan. Auskünfte durch: Prof. Kohei Cho, Pres. Com. VI., Department of Network and Computer Engineering, Tokai University, 2-28-4, Tomigaya, Shibuya-ku, Tokyo, 151-0063, Japan, Tel.: +813-3481-0611, Fax: +813-3481-0610, e-mail: kcho@key aki.cc.u-tokai.ac.jp oder: cho@yoyogi.ycc.u-tokai.ac.jp, www.commission6.isprs.org

3.–6. Juli: **ISPRS Mid-term Symposium Commission I "From Sensors to Imagery"** in **Marne-la-Vallée**/ Paris. Auskünfte durch: Alain Baudoin, Pres. Com.I, CNES, 2, place Maurice Quentin, F-75039 Paris Cedex 01, Tel.: +33-144767810, Fax: +33-14 4767867 e-mail: alain.baudoin@cnes.fr, www.cnes.fr, www.commission1.isprs.org

4./5. Juli: 9^{th} Symposium on the **3-D Analysis of Human Movement** in **Valenciennes**, Frankreich. Auskünfte durch: Franck Barbier, e-mail: franck.barbier@univ-valenciennes.fr, www.univ-valenciennes.fr/congres/3D2006/

12.–14. Juli: **ISPRS Mid-term Symposium Commission II "GICON 2006-Geoinformation Connecting Societies"** in **Wien**. Auskünfte durch: Prof. Wolfgang Kainz, Pres. Com.II., Department of Geography and Regional Research, University of Vienna, Universitätsstr. 7, A-1010 Wien. Tel.: +43-1-4277-48640, Fax: +43-1-427 7-9486, e-mail: wolfgang.kainz@univie.ac.at, http://www.gicon2006.at/www.commission2.isprs.org

31. Juli–4. August: **IEEE/IGARSS 2006** in **Denver**, CO, USA. Auskünfte durch: Ms. Lisa A. Ostendorf, Tel.: +1-540-658-1676, Fax: +1-540-658-1686, e-mail: ieeegrss@adelphia.net, http://www.igarss06.org

1.–3. September: **ISPRS** 7th Joint **ICA/EuroGeographic International Workshop on Incremental Updating & Versioning** in **Haifa**, Israel. Auskünfte durch: Ammatzia Peled, Tel.: +972-48-34 3591, Fax: +972-48-34 3763, e-mail: peled@geo.haifa.ac.il, http://ge o.haifa.ac.il/~icaupdt/

4.–7. September: **ISPRS Mid-term Symposium Commission VIII "Remote Sensing Applications and Policies"** in **Haifa**, Israel. Auskünfte durch: Ammatzia Peled, Pres. Comm. VIII, Tel.: +972-48-34 3591, Fax: +972-48-34 3763, e-mail: peled@geo.haifa.ac.il, www.commission8.isprs.org

20.–22. September: **ISPRS Mid-term Symposium Commission III "Photogrammetric Computer Vision 2006"** in **Bonn**. Auskünfte durch: Prof. Wolfgang Förstner, Pres. Comm. III, Tel.: +49-228-732 2713, Fax: +49-228-732 2712, e-mail: wf@ipb.uni-bonn.de, www.commission3.isprs.org

25.–27. September: **ISPRS Mid-term Symposium Commission V "Image Engineering and Vision Metrology"** in **Dresden**. Auskünfte durch: Prof. Hans-Gerd Maas, Pres. Comm. V, Tel.: +49-351-463-33680, Fax: +49-351-463-37266, e-mail: hmaas@rcs.urz.tu-dresden.de, www.commission5.isprs.org

27.–30. September: **ISPRS Mid-term Symposium Commission IV "Geospatial Databases for Sustainable Development"** in **Goa**/Indien. Auskünfte durch: Shailesh Nayak, Pres. Comm.IV, Tel.: +91-79-2691 4141, Fax: +91-79-26915, e-mail: snaykad1@sancharnet.in oder: shailesh@sac.isro.org, www.commission4.isprs.org

8.–13. Oktober: XXIII. Internationaler **FIG – Kongress** in **München**. Auskünfte durch: FIG Office, Tel.: +45-38-861 081, Fax: +45-38-86 0252, e-mail: fig@fig.net und Thomas Gollwitzer, Kongressdirektor, Tel.: 49-9-414022-200, Fax: +49-9-414022-101, e-mail: congress.dirctor@fig2006.de, www.fig2006.de/

9.–13. Oktober: **IX Global Spatial Data Infrastructure Conference** in **Santiago**, Chile. Auskünfte durch: Instituto Geografico Militar (IGM), e-mail: gsdi9@igm.cl, www.igm.cl

10.–12. Oktober: **INTERGEO 2006** in **München**, Messegelände. Kongressdirektor: Dipl.-Ing. Walter Henninger. Auskünfte durch: e-mail: www.dvw.de, www.intergeo2006.de und www.hinte-messe.de

6.–10. November: **ASPRS Fall Meeting** in **San Antonio** Crowne Plaza Hotel, Texas, USA. Auskünfte durch: ASPRS, Tel.: +1-301-493-0290, Fax: +1-301-493-0208, e-mail: asprs@asprs.org, www.asprs.org/asprs/meetings/calendar.html

2008

14.–25. Juli: 21. **ISPRS Kongress** in **Beijing**, China. Auskünfte durch: CSGPC, Tel.: +86-10-6833 9005, Fax: +86-10-6831 15 64, e-mail: fanbsm@public.bta.net.cn, http://www.isprs2008-beijing.com

Buchbesprechung

ALFRED NISCHWITZ & PETER HABERÄCKER, 2005: Masterkurs Computergrafik und Bildverarbeitung. 860 S. Vieweg Verlag, Wiesbaden, ISBN 3-528-05874-9

Wer kennt es nicht, das Standardwerk *Digitale Bildverarbeitung* von PETER HABERÄCKER, seit dem ersten Erscheinen 1985 eine unentbehrliche Hilfe für Einsteiger und Fachleute der digitalen Bildverarbeitung. Nach einigen Folgeauflagen liegt nun ein neues Werk vor, das die beiden Autoren ALFRED NISCHWITZ und PETER HABERÄCKER als *Masterkurs Computergrafik und Bildver-*

arbeitung genannt haben. Auf 860 Seiten machen sie deutlich, dass diese beiden Fachgebiete eng zusammengehören und dokumentieren, wie umfangreich und komplex das Thema ist.

Das Buch ist in zwei große Hauptteile aufgeteilt. In einer Einleitung wird zunächst der Zusammenhang zwischen Computergrafik und Bildverarbeitung erläutert mit Schwerpunkten in Bildcodierung und Rendering. Der erste Hauptteil *Computergrafik* beginnt nicht, wie vielleicht erwartet, mit theoretischen Grundlagen der Computergrafik, sondern die Autoren stellen zunächst den Anwendungsbezug des Themas her. Im Kapitel *Interaktive 3D-Computergrafik* werden Echtzeitaspekte diskutiert. Es folgt eine detaillierte Darstellung wichtiger Anwendungsgebiete der Computergrafik, die von Simulatoren bis zum Thema Augmented Reality reichen. Im folgenden Abschnitt wird dann eine Einführung in das OpenGL-Konzept gegeben, auf dem wesentliche Teile des Lehrbuches und zahlreiche Programmbeispiele basieren.

Es folgen theoretische Grundlagen mit Kapiteln über *Geometrische Grundobjekte*, *Koordinatensysteme und Transformationen*, *Verdeckung* sowie *Farbe, Transparenz und Farbmischung*. Die Abschnitte geben auf fast 90 Seiten einen vollständigen Einstieg in die theoretische Computergrafik, von einfachen Basistransformationen bis hin zu Open GL-basierten Programmbeispielen. In den nachfolgenden Kapiteln werden im Wesentlichen Techniken zur realitätsnahen Visualisierung besprochen. Im Einzelnen widmen sich die Autoren den Abschnitten *Anti-Aliasing*, *Nebel und atmosphärische Effekte*, *Beleuchtung und Schattierung* sowie *Texturen*. Zeitabhängige Fragestellungen werden schließlich noch in den Kapiteln über *Animationen* und *Beschleunigungsverfahren* diskutiert. Der erste Hauptteil gibt somit auf über 300 Seiten einen umfassenden Überblick zur Computergrafik, der sich dem Leser dank anschaulicher Abbildungen leicht erschließt. Eine vertiefte Auseinandersetzung mit der Materie wird durch die vielen OpenGL-Beispiele ermöglicht, die der Rezensent allerdings nicht selbst ausprobiert hat. Dazu stellen die Autoren auf ihren Internet-Seiten entsprechende Arbeitsumgebungen zur Verfügung.

Der zweite Hauptteil *Bildverarbeitung* kommt dem erfahrenen Leser natürlich in weiten Teilen bekannt vor. Hier haben die Autoren vieles aus Haberäcker's „Digitale Bildverarbeitung“ übernommen, einschließlich der kleinen Programmbeispiele und Bildbeispiele. Das erste Kapitel widmet sich Herkunft und Eigenschaften digitaler Bilddaten. Grundlegende Konzepte der Bilddigitalisierung werden besprochen, wobei moderne Entwicklungen im Bereich von Digital- und Videokameras ausgespart werden. Der Abschnitt über Farbbilder und Farbmodelle zeigt einige Überschneidungen mit dem entsprechenden Kapitel in Teil 1, hier wäre eine engere Abstimmung der beiden Hauptteile des Buches wünschenswert gewesen. Im Kapitel *Modifikation der Grauwerte* werden Verfahren zur punktweisen Bildverarbeitung (Grauwert-Transformationen) vorgestellt. Die nachfolgenden Kapitel beschäftigen sich mit den unterschiedlichen Möglichkeiten zur Filterung, von *Operationen im Ortsbereich* über *Mathematische Morphologie*, *Kanten und Linien* bis zu *Operationen im Frequenzbereich*. Es folgt ein Abschnitt über *Modifikation der Ortskoordinaten* (Entzerrungsverfahren), in dem wiederum der Zusammenhang mit entsprechenden Verfahren der Computergrafik (z. B. Texture Mapping) hätte aufgezeigt werden können.

Die folgenden Kapitel sind im Wesentlichen den Bereichen Szenenanalyse und Mustererkennung zuzuordnen. Besprochen werden Verfahren zur Merkmalsextraktion aus *Grauwerten und Farbe*, aus *mehrkanaligen Bildern* und *Bildfolgen* und aus *Texturen*. Die dazu ebenfalls erforderlich Werkzeuge *Gauß- und Laplace-Pyramiden*, *Scale Space Filtering* und *Baumstrukturen* folgen anschließend.

Das Thema Segmentierung ist den weiteren Kapiteln gewidmet. *Segmentierung und numerische Klassifikation*, *Klassifikation mit neuronalen Netzen* und mit *Fuzzy Logic* geben einen umfassenden Überblick über das Gebiet. Die Datenorganisation und Analyse von Segmenten wird in den Abschnitten *Run-Length-Coding*, *Einfache segmentbeschreibende Parameter*, *Strahlenverfahren* sowie *Neuronale Netze und Segmentbeschreibung* diskutiert. Ein ausführliches Kapitel über Kalman-Filter widmet sich der dynamischen Szenenanalyse. Der Hauptteil über Bildverarbeitung endet mit einem Abschnitt über das *Zusammenfassen von Segmenten zu Objekten*.

Auf den Internet-Seiten der Autoren finden sich zahlreiche Beispiele und ein umfangreiches Bildverarbeitungspaket, das sich kostenlos herunterladen lässt (92 MB). Leider ist die Installation auf einem beliebigen Windows-Rechner nicht ganz zeitgemäß, dafür bekommt der Anwender aber eine Vielzahl von Bildverarbeitungsmodulen geliefert, um die Beispiele im Bild nachvollziehen zu können.

Zusammenfassend ist folgendes zu bemerken: Computergrafik und Bildverarbeitung wachsen immer weiter zusammen. Diesem aktuellen Trend folgend, legen Nischwitz und Haberäcker ein Werk vor, das die grundlegenden Verfahren dazu vorstellt und den Lesern, die „sich in dieses Gebiet einarbeiten und praktische Erfahrungen sammeln wollen“, damit gleichzeitig ein sehr nützliches Nachschlagewerk sowie eine Anleitung zum Nachprogrammieren bietet. Gut geeignet ist das Buch für Studierende, so deutet es ja auch der Titel „Masterkurs…“ an. Besondere Vorkenntnisse sind nicht erforderlich, das Buch ist jedoch von zwei Mathematikern geschrieben und somit ist eine Kenntnis wichtiger mathematischer Grundlagen unerlässlich.

Der beträchtliche Umfang des Werkes ist gleichzeitig auch eine Schwäche. An einigen Stellen wäre eine engere Verzahnung der beiden Hauptteile wünschenswert gewesen. Während der Teil über Computergrafik speziell an OpenGL gekoppelt ist, werden im Teil Bildverarbeitung auszugsweise Programmcodes (Pascal) dargestellt. Der relativ günstige Preis des Buches erlaubt jedoch eine weite Verbreitung, besonders auch unter Studierenden. Vielleicht sollte der Verlag über eine „Luxus-Ausgabe“ nachdenken, in der alle wichtigen Abbildungen in Farbe dargestellt werden. Dafür würde es sicher einen interessierten Leserkreis geben.

Thomas Luhmann, Oldenburg

Zum Titelbild

Künstlich erzeugte perspektivische Ansicht des Nanga Parbat

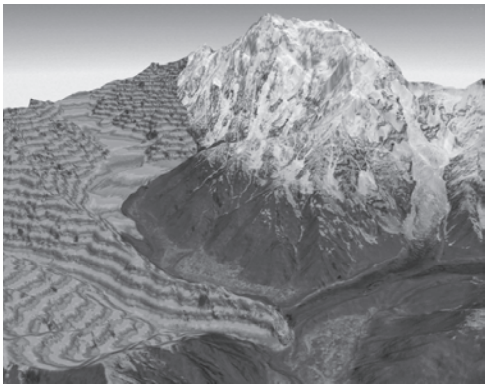

Das Bild zeigt eine künstlich erzeugte – rein aus Daten aus dem Weltraum erstellte – perspektivische Ansicht des 8125 Meter hohen Berges Nanga Parbat in Pakistan, von Westen aus gesehen.

Die für das zu Grunde liegende Geländemodell aufgezeichneten Daten wurden mit dem X-Band Synthetik-Apertur-Radar der Shuttle-Radar-Topografie-Mission (SRTM) im Jahr 2000 aufgenommen. Das aus diesen Daten mittels Radarinterferometrie erstellte Geländemodell hat eine laterale Auflösung von etwa 30 Metern und eine Höhengenauigkeit von etwa 6 Metern. In der linken Bildhälfte wurde die interferometrische Radarphase als Textur über das Geländemodell gelegt, in der rechten Bildhälfte ein räumlich hoch aufgelöstes SPOT-Bild vom 7. Juni 2003, das vorher in eine nahe Echtfarbendarstellung transformiert wurde.

Wegen der starken Abschattungen in diesem Gebiet konnte das Höhenmodell aus den Radardaten nicht mit den Standardverfahren erzeugt werden. Deshalb wurde ein neues Verfahren eingesetzt, welches den Schattenwurf aktiv für die Höhenrekonstruktion nutzt. Dieses Verfahren verbessert die Geländerekonstruktion gerade in steilen Bereichen entscheidend. Der Schattenwurf selbst ist in dieser Darstellung kaum zu erkennen.

Michael Eineder & Peter Reinartz, DLR